UNIVERSITÀ DEL PIEMONTE ORIENTALE
Department of Health Sciences

Ph.D. Program in Medical Science and Biotechnology

XXV cycle

Myeloid Derived Suppressor Cells (MDSCs), Heme-oxygenase-1 (HO-1) and CD88 expression in circulating monocytes: a study of impact on outcome in advanced cancer patients treated with Immune checkpoint inhibitors (ICIs).

Supervisor: Prof. Alessandra Gennari

Co-Ordinator: Prof. Marisa Gariglio

Ph.D. candidate: Vachanaram Ajay Ram

Matricola:009537

UNIVERSITÀ DEL PIEMONTE ORIENTALE

SCUOLA DI MEDICINA

Ph.D. Programme in Medical Sciences and Biotechnology
Dottorato di Ricerca in Scienze e Biotecnologie mediche

Referee (Title, Name): Dr. Carmen Criscitiello

EVALUATION REPORT FOR THE PHD THESIS IN MEDICAL SCIENCES AND BIOTECHNOLOGY

Myeloid Derived Suppressor Cells (MDSCs), Heme-oxygenase-1 (HO-1) and CD88 expression in circulating monocytes: a study of impact on outcome in advanced cancer patients treated with Immune checkpoint inhibitors (ICIs).

submitted by

Vachanaram Ajay Ram

	Yes	No
1. Does the thesis represent an original work making significant contribution to knowledge in or understanding of the field of study.....	x	
2. Does the thesis contain materials worthy of publication in addition to those already published.....	x	
3. Does the work show an adequate knowledge of the field of study and relevant literature	x	
4. Does the thesis contain material that presents a unified body of work, such as could reasonably be achieved on the basis of three years' postgraduate study and research.....	x	

	High	Medium	Low
5. How do you evaluate the overall quality of the content of the thesis.....	x		
6. How do you evaluate the quality of the experimental approach	x		
7. What is the degree of originality.....	x		
8. How do you evaluate the thesis with respect to the further development of the field.....	x		

Evaluation Summary

very good	good	satisfactory	sufficient	poor
■	☐	☐	☐	☐

Milano, 02/02/2023

(place and date) (Signature of referee)

Further Remarks

This thesis is well-written, with a logical structure. This study was conducted in patients with advanced-stage cancers who were candidates to ICIs, where the prognostic role of HO-1, CD88, blood-based biomarkers, and MDSCs was investigated as well as its expression in monocyte subpopulations.

All chapters are adequately addressed. The study design and methodology have been carefully considered and are being used. The patient cohort for lung cancer appears to be adequate to confirm the clinical importance of the gathered data; nevertheless, the patient cohorts for other cancer types need to be expanded in the future in order to reinforce the findings. The thesis's subject is intriguing and deserves more research.

I recommend revising the entire thesis for typos.

The topic and the data are both well-presented, and the thesis overall has a very high quality.

UNIVERSITÀ DEL PIEMONTE ORIENTALE

SCUOLA DI MEDICINA

Ph.D. Programme in Medical Sciences and Biotechnology
Dottorato di Ricerca in Scienze e Biotecnologie mediche

Referee (Title, Name): Prof. Massimo Di Maio, Department of Oncology, University of Turin

EVALUATION REPORT FOR THE PHD THESIS IN MEDICAL SCIENCES AND BIOTECHNOLOGY

Myeloid Derived Suppressor Cells (MDSCs), Heme-oxygenase-1 (HO-1) and CD88 expression in circulating monocytes: a study of impact on outcome in advanced cancer patients treated with Immune checkpoint inhibitors (ICIs).

submitted by

Vachanaram Ajay Ram

	Yes	No
1. Does the thesis represent an original work making significant contribution to knowledge in or understanding of the field of study.....	X	
2. Does the thesis contain materials worthy of publication in addition to those already published.....	X	
3. Does the work show an adequate knowledge of the field of study and relevant literature	X	
4. Does the thesis contain material that presents a unified body of work, such as could reasonably be achieved on the basis of three years' postgraduate study and research.....	X	

	High	Medium	Low
5. How do you evaluate the overall quality of the content of the thesis.....	X		
6. How do you evaluate the quality of the experimental approach	X		
7. What is the degree of originality.....		X	
8. How do you evaluate the thesis with respect to the further development of the field.....		X	

Evaluation Summary

very good	good	satisfactory	sufficient	poor
x				

Turin, February 6th, 2023
(place and date)

_____
(Signature of referee)

Further Remarks

I read with great interest the thesis. Of course the number of patients included in the subgroup analysis of different types of primary tumors is somewhat small to draw definitive conclusions, but the methods are good and the presentation is clear.

ACKNOWLEDGEMENTS

I would like to thank my mentor Professor Alessandra Gennari and my course coordinator Professor Marisa Gariglio for providing me the opportunity and funding for my PhD program and research activity. I would like to thank Dott.ssa Veronica Martini for her support during the period of this course. I would like to thank the clinical trial office and the whole team at Division of Oncology, University of Eastern Piedmont. I extend my acknowledgement to my lab team at Center for Translational Research on Autoimmune & Allergic Diseases – CAAD.

Finally, I would like to thank my mother Santosh Devi, my father Vachanaram, my sisters, Priyanka and Ranjitha, and my friends who always believed in me and supported me throughout my education and career.

Table of Contents

Summary:

Long-term remission induced by immune checkpoint inhibitors (ICIs) in various types of cancers has opened the possibility of broader use of immunotherapy. Although the advantage of ICIs is in their inherent capacity to achieve long-term or even complete responses, the reality is that the majority of patients do not benefit from these treatments. Our hope for the next decade is that biomarkers for predicting ICI efficacy and toxicity will be identified, together with clinical parameters, to optimize ICI regimens and new combinations. By now we enrolled in this study 121 patients with advanced Lung Cancer (LC; n=84), Head and Neck Cancer (HNC, n=14), Melanoma (M; n=13), and Renal Cell Carcinoma (RCC; n=10) who were candidates for ICI therapy. The aim of this study is to identify predict and prognostic biomarkers in response to ICIs. Several clinical biomarkers, including baseline clinical characteristics of patients, nine blood-based clinical biomarkers were identified, and their prognostic potential was analyzed. We demonstrated that in LC patients higher levels of Absolute Neutrophil count (ANC), Neutrophil to Lymphocyte ratio (NLR), systemic inflammation index (SII) and derived Neutrophil to Lymphocyte ratio (dNLR) were associated with poor outcome, instead Lymphocyte to monocyte ratio (LMR) was found to be associated with better outcomes. In M higher Neutrophil to White blood cells ratio (NWR), NLR, dNLR, and Platelet to Lymphocyte ratio (PLR) showed an association with poor outcome. In HNC, Absolute Lymphocyte count (ALC) and NWR were associated with poor outcomes. It has been reported that higher percentage of Myeloid-derived suppressor cells (MDSCs) are positively correlated with poor prognosis in patients with cancer, owing to their immunosuppressive functions. For these reasons, we also phenotyped and identified the MDSCs subpopulations in peripheral blood of our patients, demonstrating that in LC and HNC, the frequency of Mo- was higher than PNM-MDSCs and was associated with poor PFS and OS, respectively. Moreover, tumor-associated macrophages (TAMs), with high levels of heme oxygenase-1 ($HO\text{-}1^{+}$), seem to play a crucial role in defense mechanisms through antioxidant, anti-inflammatory, and anti-apoptotic properties. Based on these premises, we evaluated the prognostic role of HEME catabolism by assessing HO-1 expression levels in monocyte subpopulations in peripheral blood samples of patients with advanced cancer, candidates for ICIs. We showed that HO-1 expression seems to be related to patients outcome, particularly in LC patients higher expression of HO-1 in intermediate monocytes subset was associated with poor outcomes in terms of both OS and PFS. Finally, existing and

accumulating new evidence suggest that the complement system plays a major role in the regulation of TME. Cancer cells along with the optimization of complement-mediated functions remodel the TME and facilitate the tumor progression, metastasis, and evasion of the immune system. Thus, we evaluated C5aR1 (CD88) on monocyte subset as a potential biomarker for therapeutic outcomes, demonstrated that in a patient with LC, higher expression of CD88 on classical monocyte subset was associated with relatively lower risk of in terms of overall survival.

Aim and objectives:

It is now clear that the tumor-host interplay and tumor microenvironment represents a key component in the response to immune checkpoint inhibitors (ICIs) treatment. Thus, patient's immune status, as well as the dynamic changes in the tumor microenvironment, needs to be deeply investigated. In this context there is a need to identify different clinical and immunological biomarkers to establish the understanding of therapeutic outcomes in advanced cancer patients under ICI treatment. The aims of this work are:

- To investigate the basic clinical characteristics, blood based clinical biomarkers and their association with progression and overall survival of advanced cancer patients treated with ICI's.
- To identify and phenotype MDSCs in peripheral blood samples and understand their association with therapeutic outcomes in advanced cancer patients treated with ICI's.
- To identify different monocyte subsets in peripheral blood samples and study the Heme catabolism in context of Heme-oxygenase-1 and establish their association with therapeutic outcomes advanced cancer patients treated with ICI's.
- To study the expression of C5aR1 (CD88) on the identified monocyte subsets and understanding their association with therapeutic outcomes advanced cancer patients treated with ICI's.

1. INTRODUCTION

1.1. Cancer

Cancer is one of the major public concerns in the continent of Europe accounting for almost one-quarter of all cancer globally where only one-tenth of the population lives. According to estimates, there will be 4 million new instances of cancer (excluding non-melanoma skin cancer) and 1.9 million cancer-related deaths. The most prevalent malignancies are prostate (580,000 cases), colorectal (520,000), lung (480,000), and breast (530,000 cases) in women (470,000). In Europe, these four tumors account for half of all cancer cases. Lung (380,000), colorectal (250,000), breast (140,000), and pancreatic cancers are the most prevalent tumors to cause mortality. In the EU-27, there are an estimated 1.4 million new cancer cases in males and 1.2 million in females, with around 710,000 estimated cancer deaths in males and 560,000 in females. (Dyba et al., 2021). The year 2018, EU's budget for the year 2018 was €97 million in terms of economics (Hofmarcher et al., 2020). **(FIGURE 1A)**.

Cancer as a disease is highly complex, and systemic which depends highly on the crosstalk between the tumor and its microenvironment where prolonged inflammation is one of the hallmarks of cancer. The past two decades can be hailed as the renaissance of tumor immunology **(FIGURE 2)** , especially with the emergence of key concepts that put forth the role of pre-existing adaptive immunity within tumors: immunosurveillance and immunoediting (Schreiber et al., 2011, Shankaran et al., 2001) and the importance of immune contexture (Galon et al., 2006, Mascaux et al., 2019) (Galon and Bruni, 2020). Paul Ehrlich, in 1909 predicted that the growth of carcinomas was repressed by the immune system and that he envisioned otherwise would occur with great frequency (Ehrlich 1909), becoming the seed of vehement debate for the century over immunologic control of neoplasia. Decades later, two ideologies converged from different perspectives, one from immune tolerance proposing that neo-antigens that are tumor cell-specific provoke effective immunologic response (Burnet 1957) and the other from an evolutionary point of view (Thomas 1959) theorizing long-lived complex organisms must possess protective mechanisms against neoplastic diseases. With the advent of technological advances, the hypothesis gained traction, and mouse models revealed sentinel cells surveyed host for nascent transformed cells (Old and Boyse 1964). George Köhler and Cesar Milstein's discovery of monoclonal

antibodies (mAbs) produced via "hybridoma technology" in 1975 had a significant impact on clinical medicine and validated the concept of cancer immunosurveillance. On the other side of the coin is the immunoediting hypothesis. According to recent research, the immune system may also encourage the development of primary tumors with decreased immunogenicity that can avoid immune detection and elimination (Shankaran et al 2001). Elimination, equilibrium, and escape are the three dynamic stages of the cancer immunoediting process. Elimination stands for the traditional idea of cancer immunosurveillance, equilibrium is the time following incomplete tumor death in the elimination phase, and escape is the final outgrowth of cancers that have outgrown immunological restrictions of the equilibrium phase (Dunn et al. 2002, Dunn et al. 2004). The immunotherapy has improved the overall survival and progression free survival for cancer patients. **(FIGURE 1B)**

1.1.1. Lung Cancer.

At the start of 20th century lung cancer was a rare disease and by the end of century it had become the world's leading cause of death. In Europe lung cancer is the leading cause of cancer death. It is estimated that in 27 countries under EU, 11.9% of all new cancer diagnosis was lung cancer (excluding non-melanoma) and lung cancer accounted for 20.4% of all deaths related to cancer on the year 2020 (eurostat) yet on the contrary it is the most curable form of cancer but is often diagnosed at advanced or incurable stage.(Siddiqui et al., 2022).

1.1.2. Melanoma

According to estimates, skin melanoma represented 1.3% of cancer-related deaths and 4% of all new cancer diagnoses in the EU-27 nations in 2020 (all cancers, excluding non-melanoma skin cancers)(Forsea, 2020). This made it one of the 20 most frequent causes of cancer death and the sixth most common cancer (after breast, colorectal, prostate, lung, and bladder cancers). (Curti and Faries, 2021)

In addition to Targeted therapy and conventional chemotherapies, novel immunotherapies such the CTLA-4 antibody ipilimumab are available. A Phase 2b Study of Immune Checkpoint Inhibition (Nivolumab, Pembrolizumab and Ipilimumab) With or Without Dorgenmeltucel-L (HyperAcute Melanoma) Immunotherapy for Stage IV Melanoma Patients is currently running (2018-2033) a randomized trial with 47 participants. (Atkins et al., 2021)

1.1.3. Head And Neck Cancer

Despite the fact that head and neck cancer is linked with pain, disfigurement, dysfunction, emotional suffering, and death, recent discoveries have resulted in significant improvement in outcomes. More than 150 000 new patients are diagnosed with head and neck cancer each year (Boscolo-Rizzo et al., 2018), making it one of the most prevalent cancer forms in Europe. Despite being the seventh most prevalent cancer in the world, and each individual tumor being categorized as a rare cancer, there is little knowledge of this, and patient outcomes remain poor for those diagnosed later in the disease's progression (Johnson et al., 2020). However, for those diagnosed early, the survival probability is 80-90%. Some patients had a notable improvement as a result of the introduction of immune-checkpoint inhibitors for the treatment of recurrent or metastatic head and neck cancer. Unfortunately, the requirement for weekly cetuximab treatment, which led to infusion responses and skin reactions, made the quality of life less desirable. Pembrolizumab and Nivolumab, two anti-PD-1 antibodies, were approved by the Food and Drug Administration (FDA) in 2016 after platinum-treated patients with recurrent or metastatic head and neck cancer demonstrated persistent responses and improved survival. Unquestionably, PD-1-directed immune-checkpoint inhibitor medication has enhanced survival, disease remission, or both in a tiny subset of patients. Regrettably, between 85 and 95 percent of patients with advanced or metastatic head and neck cancer do not respond. (Cramer et al., 2019).

1.1.4. Renal Carcinoma

Over 90% of all renal malignancies are renal cell carcinomas (RCC), the most prevalent malignant tumor of the kidney. RCC is a complex set of illnesses that can be sporadic (96%) or familial (4%) and is subclassified into several unique subtypes linked to certain genetic abnormalities. RCC is an insidious malignancy which accounts for approximately 2.4% of diagnosis, approximately more than 400,000 are newly diagnosed and 180,000 mortalities worldwide on the tear 2020 according to GLOBOCON data (WHO – 2020). With early RCC diagnosis, the 5-year survival rate is as high as 93%. For RCC patients with metastases, the 5-year survival rate is only 12%, and at least half of them need systemic medication therapy (Bukavina et al., 2022). RCC is typically regarded as an immunogenic tumor because to its overall resistance to cytotoxic chemotherapy and radiation therapy, and earlier immunotherapies have had some effectiveness, albeit insufficiently (Bukavina et al., 2022) .

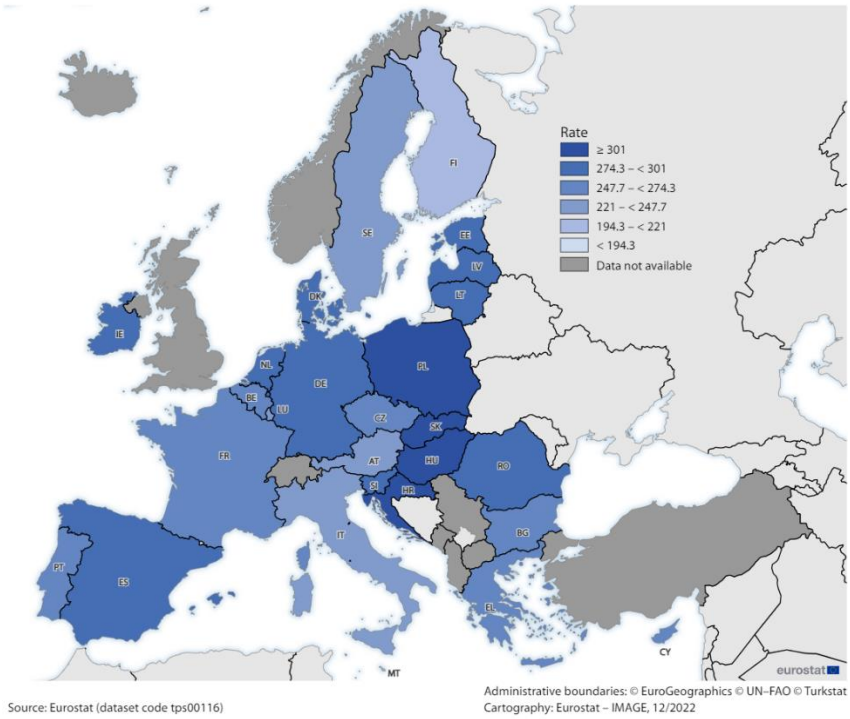

Figure 1 (A) Geographical Distribution of Cancer Related mortality rate estimate for 2020 in EU-27

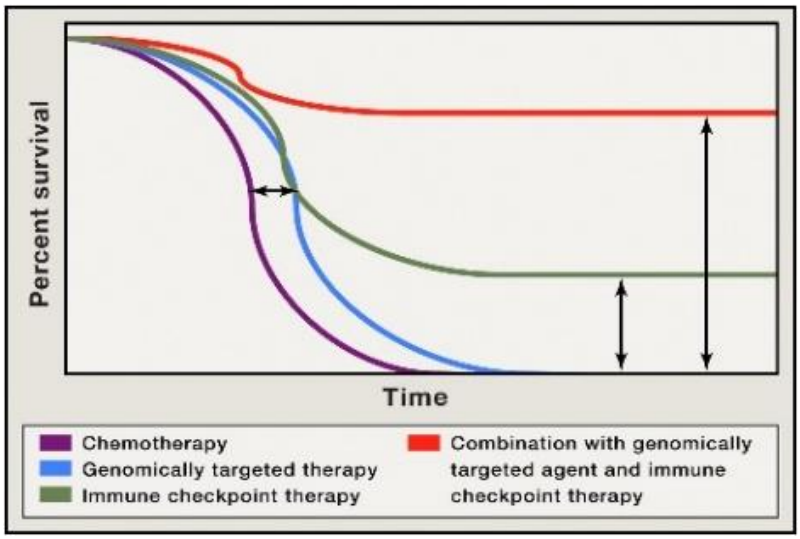

Figure 1 (B) Improved Overall Survival as a Result of Combination Therapy Depiction of Kaplan-Meier survival curve with genomically targeted agents (blue line) as compared to standard therapies (purple line), indicating an improvement in median overall survival but lack of durable responses; improved median overall survival and durable responses in a fraction of patients treated with immune checkpoint therapy (green line); possibility for improved median overall survival with durable responses for the majority of patients in the setting of combination treatment with genomically targeted agents and immune checkpoint therapy (red line).

A

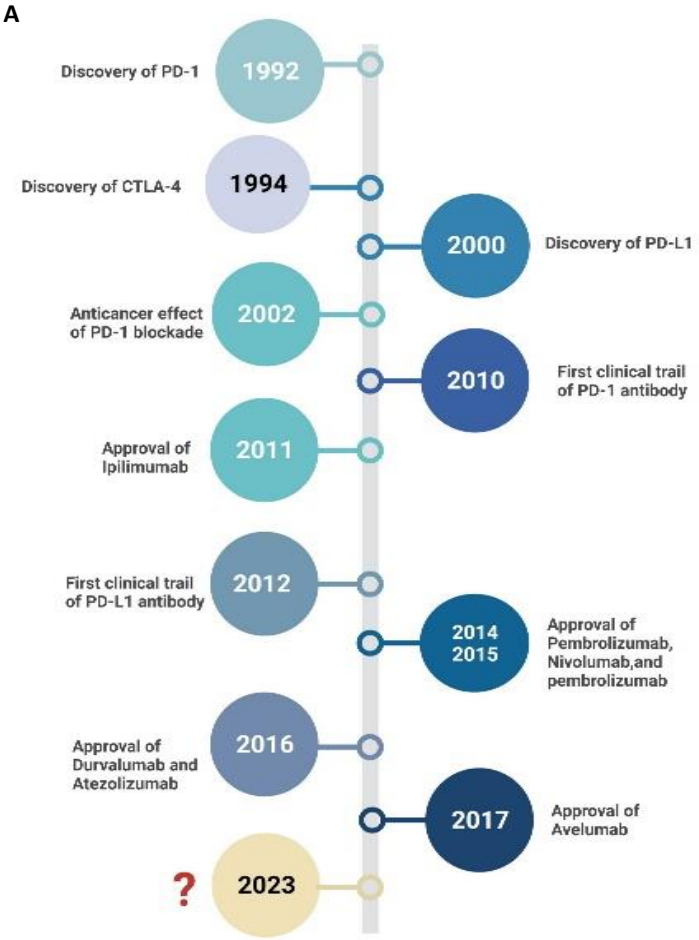

B

PD-1 antibody	Approved
Nivolumab	Melanoma, Lung cancer, Renal cell carcinoma, Hodgkin Lymphoma, ***Urothelial cancer,** Squamous cell carcinoma of the head and neck, **Hepatocellular carcinoma, MSI-H/dMMR colorectal cancer**
Pembrolizumab	Melanoma, Lung cancer, Hodgkin Lymphoma, Urothelial cancer, **Renal cell carcinoma, Squamous cell carcinoma of the head and neck, Hepatocellular carcinoma,** MSI-H or dMMR solid tumor, **Primary mediastinal large B-cell lymphoma, Cervical cancer, Merkel cell carcinoma, Gastric or gastroesophageal junction cancer Squamous cell carcinoma of the esophagus, Endometrial carcinoma**
PD-L1 antibody	**Approved**
Atezolizumab	Lung cancer, **Urotherial cancer,** Breast Cancer
Durvalumab	Lung cancer, **Urotherial cancer**
Avelumab	**Renal cell carcinoma, Urotherial cancer,** Merkel Cell Carcinoma

Figure 2 (A)Timeline of Anti-PD-1/PD-L1 and Anti CTLA-4 Immunotherapy (B) List of Approved PD-1/PD-L antibodies

1.2. Tumor Immunology

Tumor immunology, as a field focuses heavily on local immune responses in the tumor microenvironment (TME), but immunity is coordinated across tissues where the localized antitumor response cannot be achieved without communicating continuously with the periphery(Hiam-Galvez et al., 2021). Increase in immature and immunosuppressive myeloid populations are highlights of peripheral immune perturbations in the context of cancer however this discrepancy also often co-occurs with a many other peripheral immune lineages. In brief, many human and mouse models of cancer drive extensive disruption of haematopoiesis manifesting in expansion of immature neutrophils and monocytes in the periphery later traffics to the TME and contribute to the local immunosuppression (Gabrilovich et al., 2012). As a result of the mobilization of hematopoietic stem and progenitor cells for proliferation and differentiation into the monocytic and granulocytic lineages, immature immunosuppressive neutrophils (also known as polymorphonuclear myeloid-derived suppressor cells, or PMN-MDSCs), monocytes (also referred to as M-MDSCs), and macrophages are accumulated in the periphery and within tumours (Wu et al., 2014). An extensive meta-analysis of more than 40,000 patients indicated that elevated neutrophil frequencies in the blood, as determined by the neutrophil to lymphocyte ratio, were linked to a worse prognosis in patients with mesothelioma, pancreatic cancer, renal cell carcinoma, colorectal carcinoma, gastroesophageal cancer, non-small-cell lung cancer (NSCLC), cholangiocarcinoma, and hepatocellular carcinoma19. G-CSF12,20, GM-CSF17,21,22, IL-17, oxysterol23, IL-8, CCL2 , TNF25, tumour-derived exosomes26, and IL-1 have all been linked to the acceleration of this process (Coffelt et al., 2015; Dominguez et al., n.d.; Wellenstein et al., 2019).

1.3. Immune Checkpoint Blockade

The predominant modalities employed across nearly all cancer types are chemotherapy, radiation, surgery, and molecularly targeted agents, which were often effective in early-stage of cancers but not curative in advanced stage disease.(Van der Mude, 2022) (Sharma and Allison, 2015) In a clinical research point of view the shift in this approach happened with success of immune checkpoint blockade (ICB) in multiple tumor types, nearly half of all patients with metastatic cancer in economically developed countries are eligible to receive ICB therapy(Debela et al., 2021). As of December 2021, there were eight approved agents available for 17 different malignancies, the increasing use and protocols are developed in

several (neo) adjuvant and maintenance settings(Esfahani et al., 2020). The combination regimens are adapted and developed along, including those involving other classes of ICB, cytotoxic chemotherapy, and biological and/or targeted therapies.(Yap et al., 2021) These therapies and combination regimens have become durable in terms of response, even in advanced stages and metastatic setting. Given this growing importance, characterizing the long-term physiological implications of treatment with ICB has gained momentum. (Yu et al., 2022)

The chemotherapy, radiation and especially molecularly targeted cancer therapies has a mode of action which is limited and focused on cell-intrinsic factors such as mutations and/or other genetic influences which often gets altered and tumors develops resistance to these therapies asking for finding a new target. This approach often leads to failure to treatment or relapse, metastasis etc., it ignores tumor-extrinsic factors like the immune system and its components which are indeed contextually exploited by tumors(Yap et al., 2021).

Among the approaches which targets tumor-extrinsic factors like immune system, antibodies that block "immune checkpoints", negative regulators of T cell -function (Topalian et al., 2015), and chimeric antigen receptors have been studied in recent times. The therapeutic antibody ipilimumab, targeting cytotoxic T lymphocyte antigen 4 (CTLA-4), was the first checkpoint inhibitor to be approved for clinical use in cancer. CTLA-4 competes with the co-stimulatory receptor CD28 for binding to B7 ligands. A second immune checkpoint receptor, programmed cell death protein 1 (PD-1), is expressed by activated T cells, while its ligands PD-L1 and PD-L2 are expressed by tumor and immune cells.(Iranzo et al., 2022) The PD-1 pathway is important for driving T cells into a dysfunctional state known as T cell exhaustion (Pauken and Wherry, 2015) **(FIGURE 3)**. Blocking either CTLA-4 or PD-1 has led to unprecedented durable responses with a generally favorable toxicity profile. However, it is clear from clinical trials that only a fraction of patients responds to these therapies, and many will relapse. There are several known tumor-cell extrinsic factors that influence the outcome of ICB, undoubtedly somatic mutation burden, cancer genetics, and epigenetics (Wellenstein and de Visser (2018)) , is important in response to these therapies , however the expression of PD-L1 on tumor and immune cells (Herbst et al., 2014; Tumeh et al., 2014) , and developmental fate of T-cells (Pauken and Wherry, 2015) , are other tumor cell-extrinsic factors that influence response . On the other hand, evidence have emerged that conventional genotoxic therapies (e.g., chemotherapy, radiation), and molecularly targeted therapies can have immunomodulatory effects. A rational combination of strategies requires

the understanding of relevant determinants of response and resistance beyond cell-intrinsic and genetic mechanisms. (Yu et al., 2022).

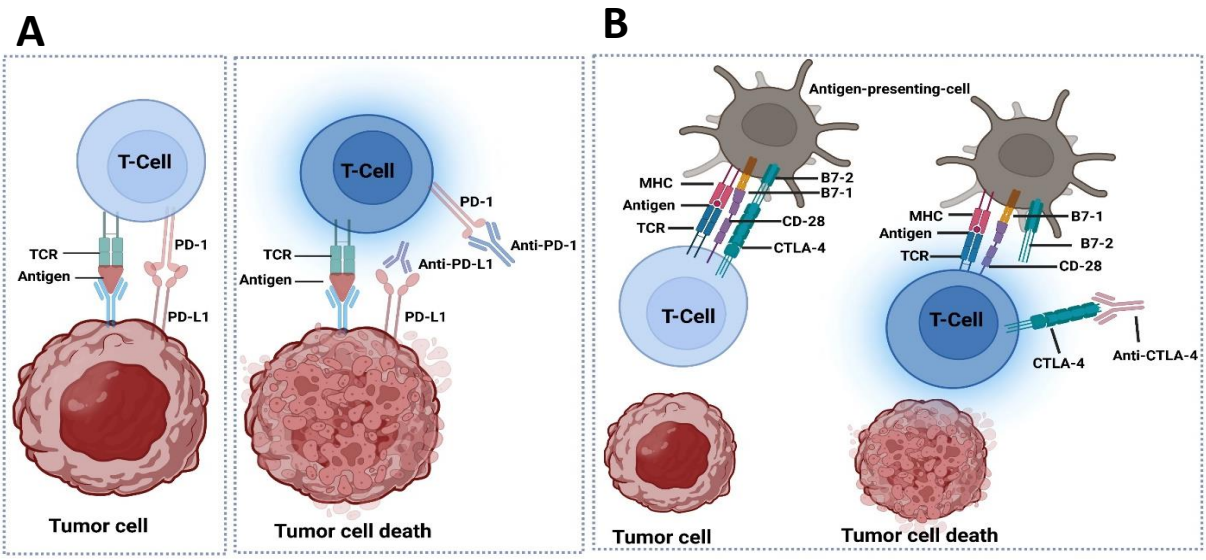

Figure 3 (A) PD-1/PD-L1 axis and its inhibitors' role in regulation of T-cell functions. During prolonged antigenic stimulation, e.g., carcinogenesis, PD-1 overexpression results in the inhibition of T-cell proliferative and cytotoxic activity, PD-1/PD-L1 inhibitors promotes proliferation and activation of T-cells. **(B).** T-cell activation requires 2 signals: the first, binding MCH with TCR; the second, interaction of CD28 on the T-cell with B7 (CD 80, CD 86) on APC. After T-cell activation, CTLA-4 is displaced to the plasma membrane and functions as a T-cell activation inhibitor. Anti-CTLA-4 antibody binds with CTLA-4 which results in T-cell reactivation. PD-1 programmed cell death protein 1; PD-L1, programmed death-ligand 1; MHC, major histocompatibility complex, TCR, T-Cell receptor, CTLA-4, Cytotoxic T-Lymphocyte Associated antigen 4, APC, antigen-presenting cell.

1.4. Myelopoiesis in cancer and implications on immunotherapy - A twist in the PD-1 tale

One of the distinguishing characteristics of most immune cells is their ongoing replenishment from precursors that are eventually descended from bone-marrow-derived-hematopoietic stem cells (HSCs) in adults. Myelopoiesis is the process by which the major myeloid cell types of the immune system, such as granulocytes, monocytes, and dendritic cells, grow and differentiate within the hematopoietic system. Cancers encourage immunological stressors that result in emergency myelopoiesis, which alters the myelopoietic output and produces a variety of myeloid populations with tumor-promoting properties.(Sica et al.,) (Mallick and Duttaroy, 2021).

Terminally differentiated myeloid cells are essential innate immune cells and are required for the activation of adaptive immunity. Strong activation signals mediated by pathogen-associated molecular pattern or danger associated molecular pattern molecules lead to a transient expansion and subsequent differentiation of myeloid progenitors to mature monocytes and granulocytes to protect the host in cancer and infections, In contrast, during emergency myelopoiesis mediated by continuous low-level stimulation mediated by cancer-derived factors and cytokines, bone marrow common myeloid progenitors (CMPs) but, predominantly, granulocyte/macrophage progenitors (GMPs) undergo modest expansion with hindered differentiation, and a fraction of myeloid cells with immunosuppressive and tumor-promoting properties, named myeloid-derived suppressor cells (MDSCs), accumulates. MDSCs suppress CD8+ T cell responses by various mechanisms. (Alvarez et al., 2018) (Wildes et al., 2021)

The consensus is that ICB therapies intrinsically targets the T-cell, triggering the immune response of the adaptive immune system against the tumor. (Sharma and Allison, 2015) However mounting evidence indicate that much of efficacy of checkpoint therapies may attribute to innate immune system. This checkpoint blockade has both a direct and an indirect impact on innate immune lineages.(Morad et al., 2021) (Liu et al., 2021)

In the indirect pathway, anti-PD-1/PD-L1 or anti-CTLA-4 boosts T cell immunity, which phenotypically polarizes innate immune cell reactions in the tumor microenvironment (TME). Due to the subsets of myeloid cells and innate lymphocytes expressing PD-1 and/or PD-L1, immune checkpoint inhibition directly targets innate immune cells in the direct pathway (Waldman et al., 2020) .This extremely complex interplay of cell types following checkpoint therapy emphasizes the significance of understanding how checkpoint biology influences innate immune populations. (Liu et al., 2021)

Direct pathway- Detectable quantities of PD-1 are present on myeloid cells, it has been demonstrated that PD-1-expressing TAMs accelerate tumor growth in several malignancies, including lung cancer, colorectal cancer, and gastric cancer (Li et al., 2022). As the receptor may be activated by inflammatory conditions, the development of PD-1 in myeloid progenitors is an early event in tumor growth. Myeloid cell infiltration, differentiation, effector function, and cellular metabolism are all impacted by PD-1 engagement. Human monocyte metabolism is shifted toward oxidative phosphorylation by PD-1 activation.

Glycolysis can be restored by PD-1/PD-L1 inhibition, which is associated with improved antibody-dependent phagocytosis (Liu et al., 2021) **(FIGURE 4)**.

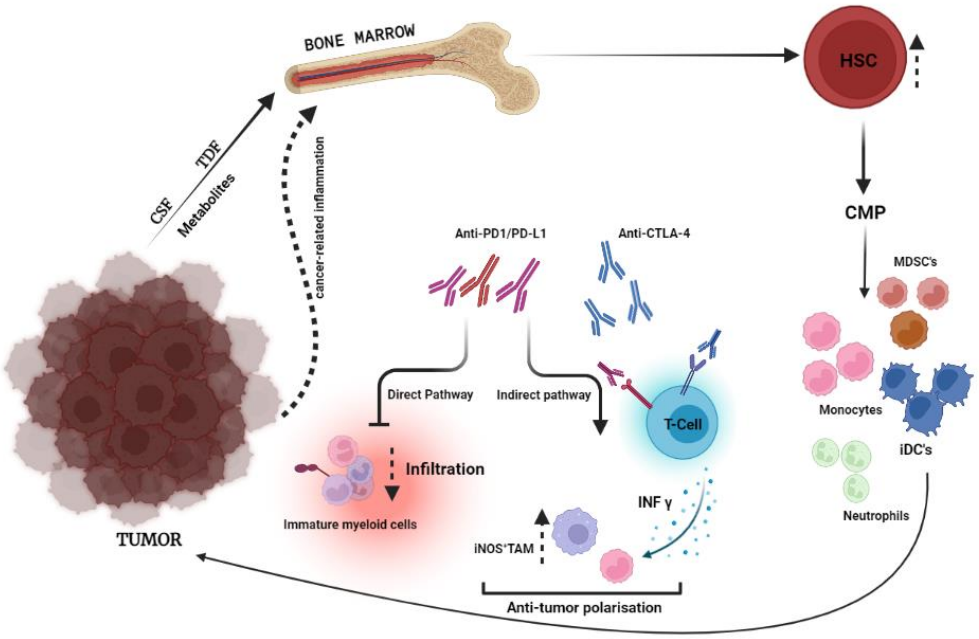

Figure 4 Emergency Myelopoiesis, generation of immature myeloid cells in solid Tumors and role of Immunotherapy. The regulation of innate immune cells by PD-1 blockade is divided into direct and indirect pathways. In the direct pathway, PD-1 blockade reshapes the phenotypes and functions of innate immune subsets, such as TAMs, DCs, MDSCs, NK cells. In the indirect pathway, T cells activated by anti-PD-1 secrete IFN-y, which in turn phenotypically polarizes myeloid cells within the TME. MDSCs, myeloid-derived suppressor cells: NK, natural killer cells; PD-1, programmed cell death protein 1; TAMs, tumor-associated macrophages; TEM, tumor microenvironment, HSC, Hematopoietic stem cells, CMP, common myeloid progenitor, CSF, Colony-stimulating factor, TDF, Tumor-Derived factor.

1.5. Monocytes, its subsets, and immature suppressive cells in myeloid lineage – in context of cancer and emergency myelopoiesis.

1.5.1. Monocyte heterogeneity

The term monocytes are used for mono-nuclear phagocytic cells originating from myeloid lineage, monocytes are mostly precursors of some macrophages and dendritic cell population (Merah-Mourah et al., 2020). Monocytes originate in the bone marrow from pluripotent stem cells, monoblast and promonocytes are the precursor cells for the formation of monocytes, after formation of monocytes from the division of promonocytes, they are short survived (less than a day) in bone marrow compartment, rather they enter the circulation and divide, in the division they maintain a circulating pool and a marginating pool, in circulation they stay for a

long period of time (Ożańska et al., 2020). These monocytes in a random fashion leave the circulation and migrate to tissues and body cavities where they differentiate into macrophages (Cormican and Griffin, 2020).

Human blood monocytes and its subset over the years are proposed and redefined to be classified based on the expression of cell surface receptors CD14 and CD16 (Kapellos et al., 2019). Initially it was considered as two populations described as "classical" monocytes which express CD14 but not CD16 and "non-classical" monocytes with low CD14 and high CD16 expression. Apart from these two subsets a third subset of cells were identified and confirmed, with the expression of receptors divergently expressed in other two subsets (CD14 and CD16) (Sakakura et al., 2021). Despite the phenotypic characterization of monocytes subsets their immune functions in the steady state and also in pathology remains ill defined (Robinson et al., 2021). **(FIGURE 5)**

There are some marked functions and the differences between these subsets were found, nonetheless there are also contradicting results in literature, which adds to the puzzle and increase the difficulties in assigning specific function for the specific populations.

1.5.2. Classical-Monocytes: - $CD14^+$ $CD16^-$

Also defined as inflammatory monocytes classical monocytes can infiltrate tissues, produce inflammatory cytokines, and differentiate into inflammatory macrophages, these are synthesized in the bone marrow and, from there, enter the bloodstream (Kwiecień et al., 2020a). classical- monocytes can enter non-inflamed tissues, where they express major histocompatibility complex MHC II. During infection, Mon1 monocytes are deployed at sites of inflammation, where they recognize and phagocytize pathogens and secrete high levels of pro-inflammatory cytokines (IL-1β, IL-6) and low levels of anti-inflammatory cytokines (IL-10) by secreting monocyte chemotactic protein-1 (MCP1) and CCL2 (Kwiecień et al., 2020b). Classical monocytes attract other immune cells to regulate the inflammatory response. It is known that classical monocytes have higher peroxidase activity, higher ROS production, and are also linked to a more pronounced expression of macrophage antigen-1 (Mac-1) and scavenger receptors SR-A1 (CD204) and SR-A2 (macrophage receptor with collagenous structure, MARCO), as well as stronger binding to plasma low-density lipoprotein (LDL) compared to the non-classical monocyte subset. Consequently, classical monocytes are phagocytically more active than non-classical monocytes and actively occur at

the initiation, development, and resolution stages of inflammation in tissues (Boyette et al., 2017).

1.5.3. Non-Classical-Monocytes: - $CD16^{+}CD14^{-}$

Non-classical or relatively smaller anti-inflammatory monocytes accounts for nearly 10% of all monocytes circulate in vasculature and patrol for the Damage Associated Molecular Patterns (DAMPs) via a mechanism that requires the fractalkine receptor CX3CR1, engulfing apoptotic endothelial cells and sensing danger signals coming from the tissue and differentiate into tissue-resident macrophage in steady stage (Robinson et al., 2021). During inflammation non-classical monocytes differentiate into anti-inflammatory macrophages to repair damaged tissues. These monocytes also occur in complement and Fc γ receptor-mediated phagocytosis and neutrophil adhesion at the endothelial interface (Wolf et al., 2019).

1.5.4. Intermediate Monocytes: - $CD16^{+}$ $CD14^{+}$

Intermediate monocytes are involved in inflammatory processes through antigen presentation, cytokine secretion, the regulation of apoptosis, and angiogenic activity (Schauer et al., 2012). These monocytes express a stronger pro-inflammatory capacity than the non-classical monocyte subset since the cells produce higher levels of ROS, TNF-α, IL-1β and IL-6, and CCL3 and express the highest levels of antigen-presentation-related molecules to restore the damaged tissue (Wildgruber et al., 2016). Thus, it seems that the prolonged activity of Intermediate monocytes becomes harmful. For instance, the intermediate subset was associated with chronic vascular and endothelial damage and atherosclerosis. Suggesting that intermediate monocytes may be involved in the maintenance of chronic inflammation, leading to harmful remodeling of cardiac tissue. However, the reasons for the persistent activity of intermediate monocytes and, consequently, for their involvement in chronic inflammation, remain unclear (Kapellos et al., 2019).

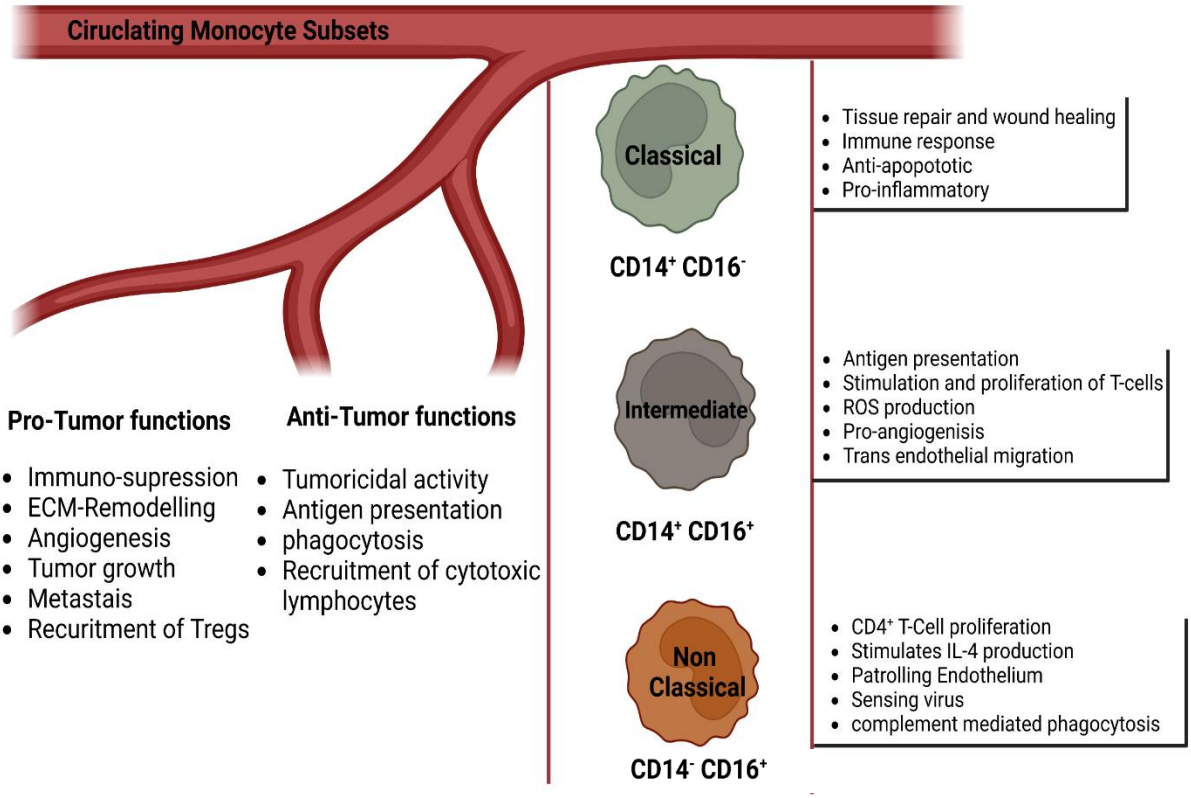

Figure 5 Human monocytes mature in the bone marrow and are subsequently released into the circulation as CD14+ classical monocytes. Progressively, classical monocytes (CD14+CD16−) give rise to non-classical monocytes (CD14dimCD16+) through an intermediate step of CD14+CD16+ monocytes.

1.5.5. Role of different monocyte subsets in cancer.

Both in humans and mice, elevated peripheral blood monocyte numbers have been linked to cancer. In certain cancer forms, patients with higher blood monocyte numbers apparently have a worse prognosis. Blood monocyte counts and the number of macrophages invading tumors are correlated, supporting the idea that classical monocytes can generate tumor-associated macrophages (Olingy et al., 2019). These elevated monocyte levels can be caused either by enhanced mobilization from the bone marrow or increased monopoiesis, both of which have been observed in cancer (Kwiecień et al., 2020a). CCL2, the central regulator of monocyte mobilization from the bone marrow, often shows higher serum levels in both mouse and human cancer (Sakakura et al., 2021).

Monocytes can display diverse functions at different stages of tumor growth and progression (Olingy et al., 2019). Phenotypically similar monocytes can even appear to perform opposing. roles due to differences in cancer type/tissue of origin, subtle differences in tumor microenvironment, stage of tumor growth, and even during therapy (Li et al., 2022). In

multiple models, CCL2 has emerged as the primary mediator of monocyte recruitment. CCL2 expression increases with neoplastic progression in both human and mouse models of colitis-associated colorectal cancer.53 In PyMT mice bearing mammary tumors, classical Ly6Chi monocytes are recruited in a CCL2-dependent manner to both primary tumors and pulmonary metastases (Jin et al., 2021). A similar pattern of recruitment occurred for CD14+CD16– monocytes adoptively transferred into nude mice, suggesting that classical monocyte recruitment is a feature of both mouse and human tumors (Olingy et al., 2019).

Monocytes appear to have the cellular machinery to directly kill malignant cells by cytokine-mediated induction of cell death and phagocytosis (Mantovani et al., 2022). Most tumoricidal activity has been demonstrated in vitro, thus whether monocyte-mediated killing is part of the in vivo antitumoral response during cancer progression needs further exploration (Reis-Sobreiro et al., 2021).

Classical "inflammatory" monocytes are recruited to tumor sites where they contribute to tumor macrophage content and promote tumor growth and metastasis (Hanna et al., 2015).

Non-classical monocytes can act as "intravascular housekeepers" that scavenge microparticles and remove cellular debris from the microvasculature, this characteristic function can be relevant since extracellular vesicles from tumors are important mediators of tumor metastasis, progression, and immune suppression, and targeting their removal is an emerging strategy for cancer therapy (Cassetta and Pollard, 2016).

R.Wang et.al , demonstrated that Intermediate monocytes expand when induced with IFN- γ, this induced expansion inhibited lung cancer metastasis by inducing NK(Natural Killer) cell expansion through IL-27 . Another evidence from Koichi Sakakura et.al show a significant decrease in the proportion of the intermediate subset in patients with oropharyngeal squamous cell cancer, and this immature status may associate with poor prognosis. However, because most studies on peripheral monocyte differentiation and their functions have been performed under normal physiological conditions, the mechanism controlling monocyte subsets differentiation and its function in disease states especially in cancer remains largely unknown.

1.5.6. Direct tumoricidal functions of monocytes

Monocytes display a cellular mechanism to directly kill malignant cells by cytokine-mediated induction of cell death and phagocytosis (Hagerling et al., 2019). In a study, it is reported that

circulating monocytes exhibit tumoricidal functions when exposed to IFN-γ or IFN-α by producing protein TRAIL (TNF-related apoptosis-inducing ligand), which can induce cell death TRAIL sensitive cancer cells. Further, the antibody mediated/dependent cellular cytotoxic effect of both $CD14^+$ and $CD16^+$ monocytes subsets have the capacity of cellular cytotoxicity, wherein $CD16^+$ monocytes subsets require direct contact with tumor cells and TNF- α signaling for induction of tumor cell cytolysis. Consequently, malignant cells in tumor maybe able to corrupt monocytes to adopt a phenotype that support tumorigenesis, the phenotypical switch overpower any programmed tumoricidal activities (Tecchio et al., 2004).

1.6. Emergency Myelopoiesis (originally termed Demand-Adapted Myelopoiesis)

In cancers, infections, or during other forms of immunological stress, there is an increased demand for leukocytes or in general the hematopoietic output to assist in combating the infection, to replace cells killed by invading microbes or consumed during the immune response, and to increase immune surveillance (Sica et al..). The adaptive immune system meets this demand by clonal expansion of T and B cells. In contrast, although there are some reports of proliferation of mature macrophages, the increased supply of most innate immune cells, which have a limited lifespan and must be regularly replenished, is achieved by "emergency myelopoiesis"(Sica et al.). However, the molecular mechanisms for this cancer-driven emergency myelopoiesis remain largely unknown there are few reported pathways which include Colony-stimulating factors (CSFs) as major orchestrators of hematopoietic development. Among these, granulocyte CSF (G-CSF) and granulocyte-macrophage CSF (GM-CSF) drive ''emergency myelopoiesis'' by securing supply of neutrophils and macrophages from bone marrow (BM) and hematopoietic stem cell niches (HSCs) (Metcalf, 2008; Ueha et al., 2011). Further, the macrophage CSF (M-CSF) promotes macrophage differentiation from medullar precursors and differentiation of tissue macrophages involved in tissue homeostasis (Hume and MacDonald, 2012) and tumor progression (Qian and Pollard, 2010). LauraStrauss et.,al reported that the continuous expansion of myeloid cells during cancer driven emergency myelopoiesis in tumor-bearing mice express PD-1 and PD-L1 .It is increasingly recognized that tumors can induce an immunosuppressive state characterized by the accumulation of immature myeloid cells (produced during emergency myelopoiesis) systemically and in the TME (Boscolo-Rizzo et al., 2018).

1.7. Tumor micro-environment (TME)

Malignant cells are just a small part of the complex ecosystem that makes up a tumor and facilitates its growth. The vasculature, lymphatics, stromal compartment, and extracellular matrix (ECM) composition are nonimmune cells components of the tumor microenvironment that pose unique challenges for delivering therapies and overcoming developed resistance. Monocytes and monocyte-derived cells can shape many of these microenvironmental features, often in a manner that promotes tumor growth and failure of therapy (Murciano-Goroff et al., 2020).

Malignancies alter the immune system's discriminating abilities, which are heavily influenced by host-pathogen interactions, and they benefit greatly from low antigenicity, PRR signaling with poor adjuvanticity, and a tumor microenvironment (TME) that resembles persistently inflamed and non-healing tissue (Tang et al., 2021). A TME with these characteristics is full of signals that encourage feedback inhibition processes and are detrimental to immune effector function. Like host-pathogen interactions, some aspects of this immune suppression might be "locked-in" and challenging to reverse. Tumors can limit anti-tumor immune responses in a variety of ways, including by altering adjuvanticity and antigenicity or by taking advantage of feedback inhibition (Petitprez et al., 2020). The significance of immunoediting and neo-antigens in cancer progression and immunotherapy response has been thoroughly established by seminal work in mice models and new genomic evidence from cancer patients (Liu et al., 2022).

Prolonged/ Chronic inflammation is a hallmark of cancer. Whether this inflammation initiates tumorigenesis or supports tumor growth is context dependent, but ultimately the global immune landscape beyond the tumor becomes significantly altered during tumor progression (Sica et al.,).

The tumor immunology field has focused heavily on local immune responses in the tumor microenvironment (TME), yet immunity is coordinated across tissues. For example, many myeloid cells are frequently replenished from hematopoietic precursors in the bone marrow, and critical T cell priming events typically occur in lymphoid tissues (Tiwari et al., 2022). The localized antitumor immune response cannot exist without continuous communication with the periphery. Furthermore, virtually every subset of immune cell has been implicated in cancer biology. Therefore, a thorough understanding of immune responses to cancer must

encompass all immune cell lineages across the peripheral immune system in addition to within the TME (Tang et al., 2016). **(FIGURE 6).**

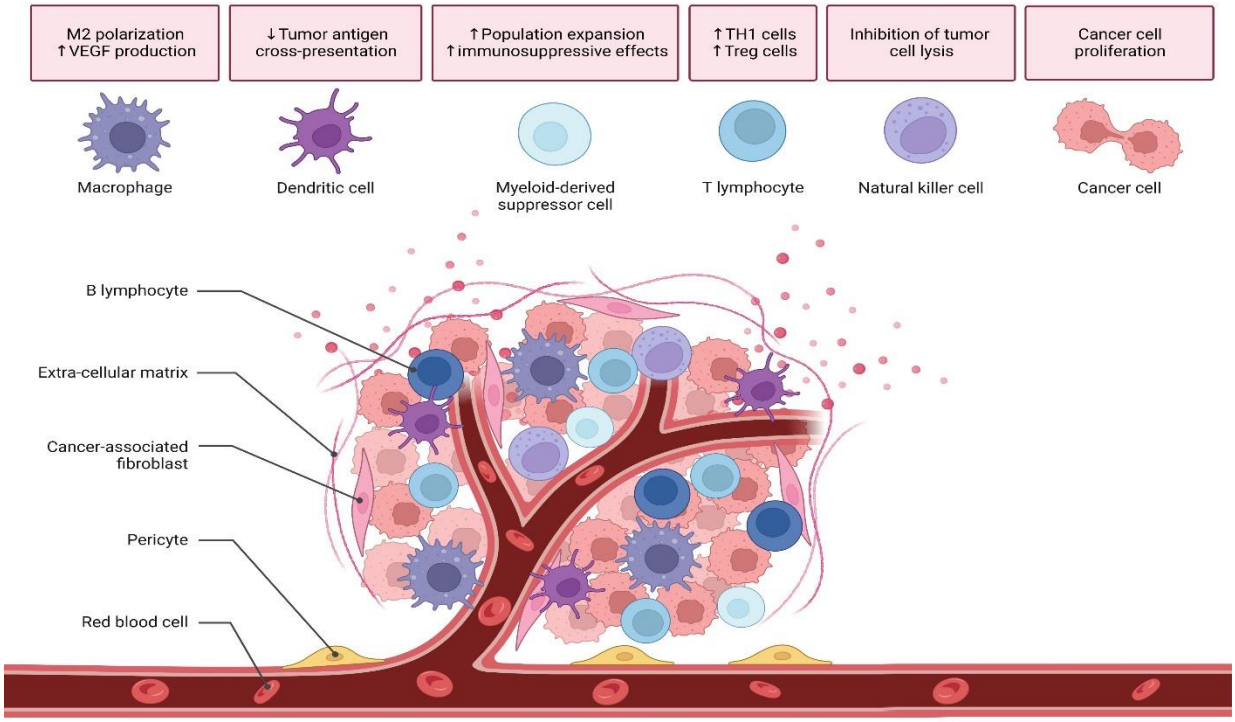

Figure 6 Tumor Microenvironment. The TME is composed of cancer cells and heterogenous nonmalignant cells integrated in a complex extracellular matrix (ECM). The main cellular components of the TME are T lymphocytes, tumor-associated macrophages (TAMs), myeloid-derived suppressor cells (MDSCs), natural killer (NK) cells, tumor-associated neutrophils (TANs), and cancer-associated fibroblasts (CAFs). Immune cells play a key role in tumor cell growth and dissemination.

1.8. Inflammation and cancer

Inflammatory processes in the immune system , irrespective of its occurrence weather in the context of chronic inflammatory diseases or in the appearance of a tumor-elicited smoldering inflammation, this has a tremendous effect on the dynamic composition of the TME, to the extent that it shapes the plasticity of tumor cells and also stromal cells , thus leaving the situation with two major choices: anti-tumorigenic function of immunity which is the result of immune-surveillance and immunological sculpting of tumor heterogeneity , at the same time pro-tumorigenic function of immunity favors cancer by blocking anti-tumor immunity (Zhao et al., 2021). This leads to shaping of a TME which tilts towards a more tumor-permissive state and exerts direct tumor -promoting signals and functions onto tumor stroma and malignant cells. Cancer-associated inflammation can be induced at different time points

of tumor development (Greten and Grivennikov, 2019). It can precede carcinogenesis in form of autoimmunity or infection, can be induced by malignant cells or can be triggered by anti-cancer therapy. Various cell intrinsic, host dependent or environmental factors can cause tumor-associated inflammation in different tumor types (Todoric et al., 2016).

1.9. Effector myeloid cells in the tumor microenvironment and their function

Myeloid cells constitute the predominant cellular population in TME, Myeloid cells are the predominant population which establishes an immunosuppressive milieu and leads to tumor immune evasion, the diverse myeloid cell population particularly TAMs (Tumor Associated Macrophages) (Porta et al., 2018) , TANs (Tumor Associated Neutrophils), DCs (Dendritic cells), and MDSCs, contribute to tumor progression, enhanced angiogenesis, metastasis, and immunotherapy resistance (Krishnamoorthy et al., 2021). Myeloid cells have all the critical attributes of playing a regulatory role in tumor biology. Therefore, deciphering the role of the individual myeloid cell population in TME is essential for understanding immunotherapy resistance and failure and developing combinatorial therapeutic strategies in cancer (Aghamajidi et al., 2022).

1.10. Cancer-induced phenotypical alterations in circulating monocytes.

The most frequently reported cancer-induced phenotypical change in human peripheral blood monocytes is the acquisition of immunosuppressive activity. The distant tumor not only skews the differentiation path of myeloid progenitors in hematopoietic tissue, but it also influences the phenotype of circulating monocytes. This typically occurs concurrently with the downregulation of the MHC class II surface protein HLA-DR, an important mediator of antigen presentation that is highly expressed on monocytes in healthy individuals (Canè et al., 2019).

The concept that a pathological state of immune activation is a common feature associated with the emergence of MDSCs, pathological activation arises from persistent stimulation of the myeloid cell compartment owing to the prolonged presence of myeloid growth factors and inflammatory signals in the settings of cancer, chronic infections or inflammation, and autoimmune diseases (Gabrilovich and Nagaraj, 2009). Examples of such activating signals include cytokines and various growth factors like granulocyte–macrophage colony-stimulating factor (GM-CSF), macrophage colony-stimulating factor (M-CSF; also known as

CSF1), IL-6, IL-1β, adenosine signaling or endoplasmic reticulum (ER) stress signaling (Veglia et al., 2021).

1.11. Myeloid derived suppressor cells (MDSCs)

1.11.1. Definition and Biological Dimension of MDSCs:

The definition of myeloid-derived suppressor cells (MDSC) that best captures both their origin and function is that they are immature myeloid cells with the capacity to dampen adaptative immune responses. Aside from cancer patients and experimental animals, MDSC accumulations have also been observed in other pathological circumstances such chronic/acute infections, autoimmune illnesses, and various forms of immunological stress (Gimeno and Barquinero, 2011). In each of these circumstances, MDSC may fulfill their physiological function by modifying both innate and adaptive immune responses that are typical. There are several different ways that MDSC functions, but they all include either cell-to-cell interaction or the release of soluble substances (Veglia et al., 2021).

The biological entity known as myeloid-derived suppressor cells (MDSCs) is one of the most spoken about in immunology. Although the context and classification of this type of cells have changed, MDSCs most frequently refer to cells that emerge during chronic inflammation, particularly late-stage malignancies, and are characterized by their immunosuppressive T cell activities. Although the MDSC idea has been useful in explaining myeloid phenomena linked to illness outcomes, it still lacks precise definitions and a paradigm that applies to all disorders (Scalea et al., 2018). Monocytic and granulocytic myeloid-derived suppressor cells (M-MDSCs and PMN-MDSCs, respectively) are the major myeloid populations associated with cancer development along with TAM (Millrud et al., 2016).

Although this MDSC idea has assisted in describing observed myeloid behaviors linked to disease outcome, efforts to distinguish MDSCs as discrete states, regulate them experimentally, and investigate their direct contribution to pathology have been impeded. MDSCs' primary characteristic, their immunosuppressive nature, does not set them apart from ordinary myeloid cells' immunoregulatory actions during inflammation (Dysthe and Parihar, 2020).

1.11.2. Phenotypes of MDSCs

Since the discovery of MDSC, multiple molecular markers have been proposed to define the MDSC population, and HLA-DR$^-$ Lin $^{low/-}$ CD33$^+$ CD11b$^+$ label is commonly used for MDSC recognition, even though MDSCs are frequently referred to as a distinct population, their phenotypic definition is constantly changing. Human M-MDSCs have typically been described as CD11b+CD14+CD33+HLA-DRlow/neg, while G-MDSCs have typically been described as CD11b+CD15+HLA-DRlowCD66b+. Lin$^-$ (including CD3, CD14, CD15, CD19, CD56) HLA-DR$^-$ CD33$^+$ cells is a mixed group of MDSC that tends to be more immature. And immature-MDSC (i-MDSC) or early-stage (e-MDSC) has been proposed to define these subsets. PMN-MDSC is phenotypically and morphologically similar to neutrophils (PMN), and the most abundant population of MDSC in most types of cancers. It is always a puzzle to distinctly differentiate the PMN-MDSC form PMN in cancer tissues. Strikingly, a recent study reported that lectin-type oxidized LDL receptor 1 (LOX-1) may serve as a specific marker of human PMN-MDSC and could be used to specifically identify PMN-MDSC (Bronte et al., 2016) **(FIGURE 7) .**

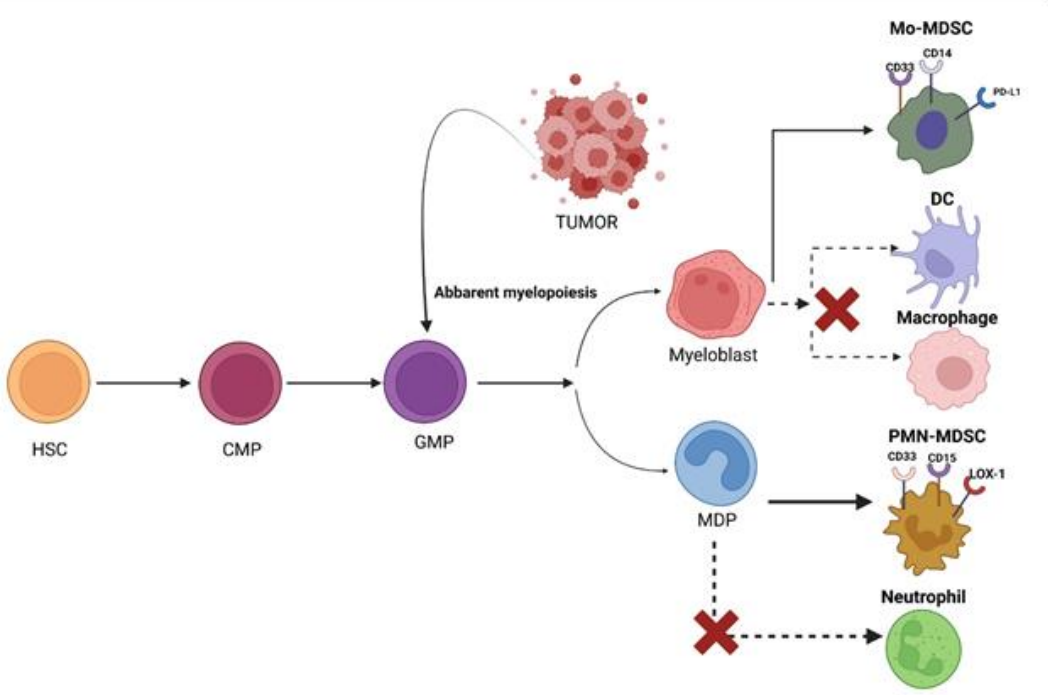

Figure 7 Myelopoiesis is altered under chronic inflammation. Under physiological conditions, hematopoietic progenitor cells (HPC) differentiate via common myeloid progenitor cells (CMP) into granulocyte/macrophage progenitor cells (GMP). These immature myeloid cells (IMC) further differentiate into monocytic/dendritic progenitor cells (MDP) or myeloblasts (MB) from which these cells further develop into dendritic cells (DCs)/macrophages or neutrophils, respectively. Under cancerous conditions, the tumor alters myelopoiesis in general and impairs further differentiation of progenitor cells, leading to the accumulation of monocytic myeloid-derived suppressor cells (M-MDSCs) and polymorphonuclear MDSCs (PMN-MDSCs)

1.11.3. Mechanisms of activity in cancer

Immunosuppressive pathways are affected generally by MDSC's, which promotes cancer growth and progression, MDSC's shows its presence in abundance in bone marrow and peripheral circulation of patients in several cancer types including terminal cancers and are corelated with disease stage and outcome. T-cell proliferation is strongly inhibited by MDSC's and patients with elevated MDSC's tend to have worse prognoses, IFN-γ production were markedly reduced in these patients, and this suppression was partially reversed by L-arginine or anti-TGFβ treatment. In gastrointestinal malignancies, upregulated plasma IL-6 was found to be linked with $CD33^{+}HLA\text{-}DR^{-}CD15^{+}$ MDSCs, while upregulated plasma IL-10 was linked with $CD33^{+}HLA\text{-}DR^{-}CD15^{-}$ MDSCs, which are associated with worse prognosis; additionally, the percentages of $CD15^{+}$ and $CD15^{-}$ cells were negatively linked with IFN-α-induced STAT1 phosphorylation in $CD4^{+}$ T cells. MDSC-derived S100A8/A9 interacts with RAGE and carboxylated glycans on colon cancer cells to facilitate activation of the MAPK/NF-κB axis, which promotes tumor growth and metastasis (Wu et al., 2022). MDSCs promoted hepatocellular carcinoma development and sensitization by inhibiting TLR ligand-induced IL-12 production in dendritic cells *via* generating IL-10 and suppressing T cell stimulatory activity in dendritic cells. Compared with controls, MDSCs are significantly elevated in pancreatic, esophageal, and gastric cancers; MDSC ratios, accompanied by arginase I and IL-13, are also correlated with an increased risk of death (Gao et al., 2022). In summary, MDSCs represent one of the many possible pathways used by tumors to create an immunosuppressive environment**. (FIGURE 8)**.

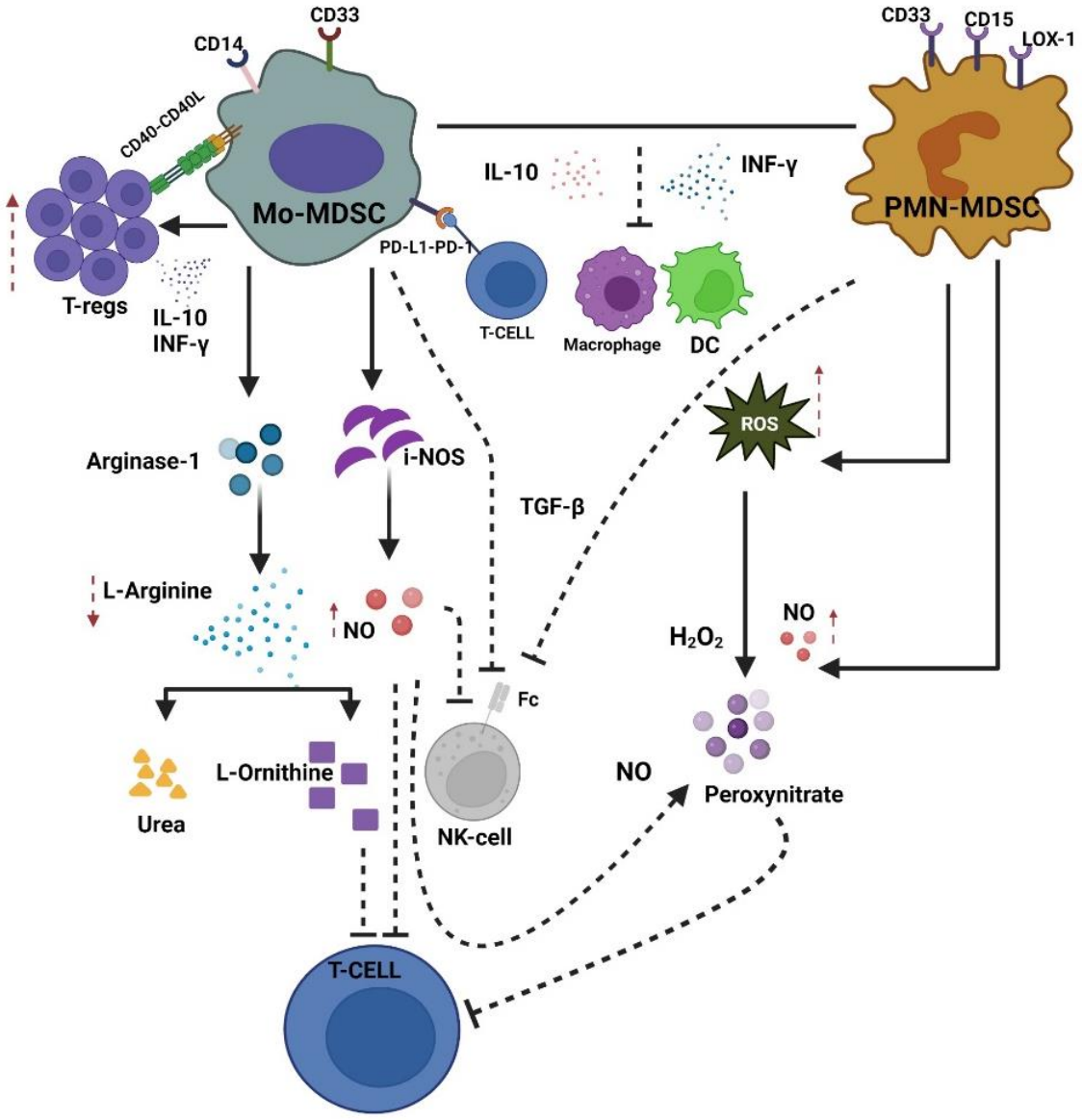

Figure 8 Immunosuppressive functions of MDSCs in the tumor microenvironment. DCs: dendritic cells; TAM: tumor-associated macrophage; ER: endoplasmic reticulum; Arg-1: arginase 1; iNOS: inducible nitric oxide synthase; In the tumor microenvironment, MDSCs are exposed to hypoxic conditions. This leads to an increase in HIF-1α-mediated elevation of Arg1 and iNOS and upregulation of inhibitory PD-L1 on the MDSC surface, all of which can suppress T cell immune activity. It also produces IL-10 and TGF-β, etc., which attract Treg cells to the tumor site and enhance their immunosuppressive functions, while suppressing the functions of NK cells, and DCs. Adenosine from MDSCs is a further major NK suppressive factor.

1.11.4. Immune Stimulation and Antitumor Activity of MDSCs

According to recent research, MDSCs can potentially operate as immunostimulants rather than just immunosuppressive, some studies have shown that the presence of MDSCs is not always associated with inhibited T cell function. When MDSCs are exposed to the appropriate cytokine milieu, they can develop immunostimulatory properties (Gao et al., 2022). MDSCs could develop into cells that present antigens, as demonstrated by Bronte et al. Additionally, their research showed that suppressive MDSC's cells are transformed into stimulatory cells (with CD86 overexpression) in the presence of IFN-, TNF-, or IL-12, which increases the cytotoxic T lymphocyte response in vitro (Hofer et al., 2021).

1.11.5. MDSC as a predictive and prognostic biomarker of ICI therapy in cancer patients

Overcoming the suppressive effects of MDSCs is a major hurdle in cancer immunotherapy. Diverse clinical criteria have been proposed as predictive indications for ICI therapy due to the limited response rate of ICI therapy. Numerous clinical studies have demonstrated high level of MDSC to be positively correlated with poor prognosis in patients with cancer (Diaz-Montero et al. 2014). Recently, MDSC have been suggested as a predictive biomarker for ICI therapy in certain types of cancer patients.

Numerous studies have revealed that MDSCs increase PD-L1 expression to induce T-cell anergy through interacting with PD-1 on T cells. Tumor-infiltrating MDSCs always come with higher PD-L1 expression compared with their counterparts in the periphery, indicating their acclimatization in the hypoxic microenvironment. Interestingly, Cassetta et al. reported that in cancer patients, profound PD-L1 expression was restricted to M-MDSCs and e-MDSCs, whereas LOX-1 expression was confined to PMN-MDSCs. Besides, MDSCs also express cytotoxic T lymphocyte-associated antigen 4 (CTLA-4), although the specific regulating mechanism is unclear. Blocking CTLA-4 has been reported to dampen the accumulation of granulocytic MDSCs and reduce their arginase 1 (ARG1) production in the peripheral blood of patients with metastatic melanoma.

Additionally, in preclinical models of melanoma, MDSCs have been shown to reduce the efficacy of anti-PD-1 and anti-CTLA4 therapies (Weber et al., 2018). MDSCs may be used as a prognostic marker for the efficacy of immunotherapy with ICIs. Meyer et al. show that MDSC frequencies in the peripheral blood of metastatic melanoma patients correlate with their response to ipilimumab, an anti-CTLA-4 antibody. Analysis of peripheral blood

mononuclear cells (PBMCs) via flow cytometry, before and during treatment with ipilimumab, indicated that patients with low frequencies of circulating M-MDSCs showed an improved clinical response to this therapy. Current research is focused on identifying a reliable and clinically relevant method to use MDSC frequency as a biomarker for the clinical response to ipilimumab in melanoma patients. In patients with advanced non-small-cell lung cancer (NSCLC), those who had progressive disease had higher percentages of PMN-MDSCs at baseline than those who showed a clinical response when treated with nivolumab, an anti-PD-1 antibody (Li et al., 2021). These clinical observations suggest that MDSCs contribute to primary resistance to immunotherapy regardless of cancer type or ICI administered (Krishnamoorthy et al., 2021).

The specific mechanisms of MDSC-mediated immunotherapy resistance in the previous studies were not explicitly stated; however, some studies have elucidated resistance mechanisms in their models. Gebhardt et al. demonstrated that in addition to elevated frequencies of MDSCs in the peripheral blood, MDSC activity was associated with poor clinical response in melanoma patients treated with ipilimumab. In this retrospective immune-monitoring study, a significant increase of M-MDSCs in the peripheral blood of non-responders was observed, while M-MDSC frequencies declined in responding patients compared to baseline values. This trend was observed after the first ipilimumab treatment in this cohort. In assessing the production of NO by MDSCs and concentration of S100A8/A9 proteins in serum, non-responders displayed elevated levels of both molecules after the first infusion of ipilimumab compared with responders. As NO and S100A8/A9 are employed by MDSCs and actively suppress anti-tumor immunity, this may indicate a mechanism by which MDSCs confer resistance to ICIs (Blattner et al., 2018).

As TGF-β signaling can amplify the immunosuppressive processes within the TME and beyond, these pathways also display a putative role in ICI resistance (Benjamin and Lyou, 2021). In a study in which a subset of patients with urothelial cancer unresponsive to the ICI, anti-PD-L1, RNA sequencing revealed that TGF-β is associated with poor response. Specifically, these patients expressed a TGF-β-induced cancer-associated fibroblast gene signature that was associated with an immune-excluded tumor phenotype (Song et al., 2019). Using colon adenocarcinoma (MC38) and mammary (EMT6) mouse models, this study revealed that therapeutic blockade of TGF-β with antibodies promoted CD8+ T-cell inflammation and anti-tumor immunity, sensitizing tumors to PD-L1 therapy (Lan et al., 2018). Evidence from another study using the MC38 mouse model revealed that anti-PD-1-

resistant tumors exhibited reduced infiltration of effector T-cells and NK cells when treated with anti-PD-1 (Bernardo et al..). Mice displaying resistance were found to have active TGF-β and Notch signaling. Inhibiting both pathways during treatment with anti-PD-1 decelerated tumor growth in resistant tumors (Denis et al., 2022).

Specific evidence of MDSC-mediated immunotherapy resistance through TGF-β production has been demonstrated using a 4T1 mammary mouse model. TGF-β neutralization was shown to promote anti-tumor activity of T-cells co-cultured with MDSCs (Dyck et al., 2022). Moreover, the depletion of MDSCs diminished anti-tumor effects mediated by TGF-β neutralization. These data indicate that TGF-β plays a vital role in the immunosuppressive activity of MDSCs and may contribute to the poor response associated with ICIs. Evidence using preclinical models suggests that combining specific TGF-β inhibitors with ICIs can facilitate effector T-cell infiltration and reduce the immunosuppressive myeloid compartment. In turn, this stimulates anti-tumor immunity and mitigates ICI resistance (Jayaraman et al., 2018).

1.11.6. Crosstalk between MDSCS and other immune cells

Apart from T cells, MDSCs also deliver immune inhibition on other tumoricidal immune cells such as NK cells, DCs, and B cells (Sanaei et al., 2020). It was reported that membrane-bound TGF-β1 on MDSCs contributed to suppressing the innate immune function of NK cells in mouse tumor models (Zalfa and Paust, 2021). Moreover, M-MDSCs from liver cancer patients were found to cause autologous NK cells anergy in vitro, mainly via the interaction of NKp30 receptor on NK cells with NKp30 ligand on MDSCs (Hoechst et al., 2009). Additionally, PMN-MDSCs were reported to block antigen cross-presentation of DCs by transferring oxidized lipids from PMN-MDSCs to DCs in tumor-bearing mice (Ugolini et al.).

MDSCs also can impair the function of B cells to suppress humoral immune responses, this was demonstrated on lung and breast cancer animal models (Wang et al., 2018) (Xu et al., 2017) . MDSCs can incite other immune inhibitory cells such as Tregs and TAMs to facilitate immunosuppression. Macrophage is another accomplice of MDSCs (Fujimura et al., 2012). The cell–cell interactions between MDSCs and macrophages can elicit a type 2 tumor-promoting immune response, which is mediated by elevated IL-10 production in MDSCs and downregulated IL-12 production in macrophages. Overall, MDSCs together with other

immune suppressive cells build an inhibitory network, crippling the cytotoxic effects on tumor cells (Kwak et al., 2020). **(FIGURE 9)**

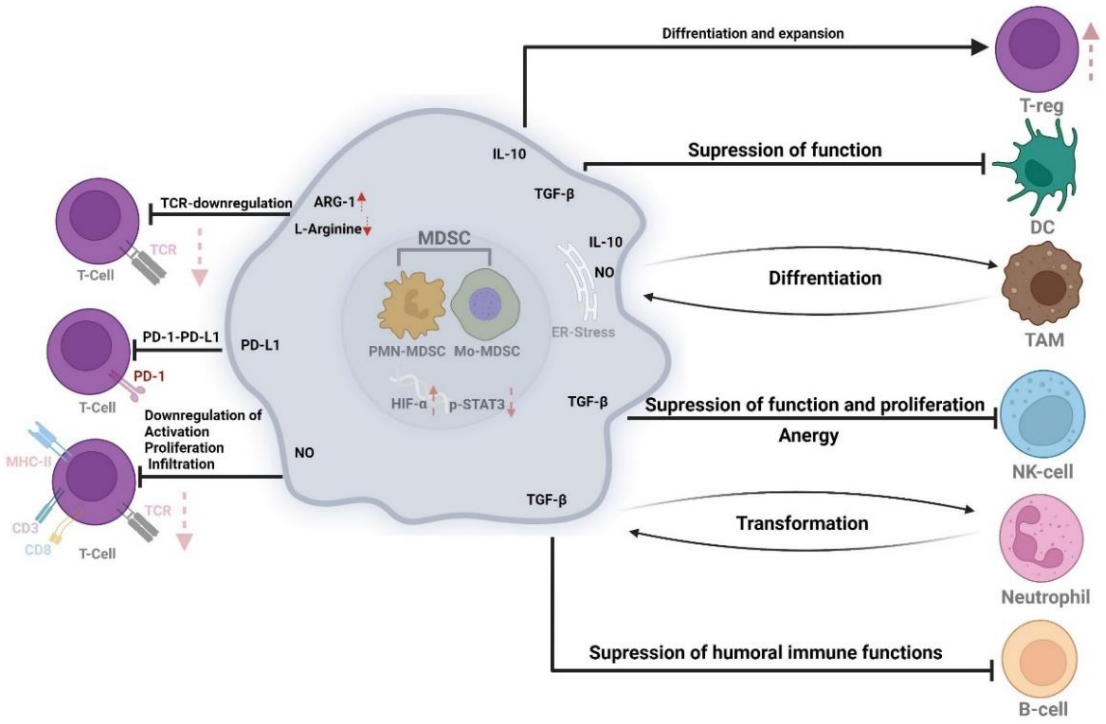

Figure 9 Crosstalk between MDSCs and other immune cells.

1.11.7. NON-IMMUNOLOGICAL FUNCTIONS OF MDSCS

Other than the effects on immune responses, MDSCs also contribute to tumor progression via multiple non-immunological mechanisms such as supporting angiogenesis, promoting stemness of tumor cells, facilitating epithelial–mesenchymal transition (EMT) and pre-metastatic niche formation (Murdoch et al., 2008).

1.12. HEME-OXIGENASE -1 (HO-1)

Endogenous iron protoporphyrin Heme is broken down by the enzyme heme oxygenase (HO), which catalyzes the reaction's rate-limiting step and generates ferrous ions, carbon monoxide (CO), and biliverdin (BV), whose reduction is carried out by biliverdin reductase and results in the synthesis of bilirubin (BR) (Tenhunen et al., 1968). In numerous pathological contexts, HO-1 displays important cytoprotective, anti-inflammatory, antioxidant, and antiapoptotic properties (Keyse and Tyrrell, 1989) (Petrache et al., 2000). Catalytic heme degradation requires an electron donor, that is Nicotinamide adenine

dinucleotide phosphate (NADPH) provided by P450 cytochrome reductase and oxygen (Applegate et al., 1991).

HMOX-1 and HMOX2 are two different genes which encodes for HO-1 and HO-2 respectively. Unlike HO-2 which is constitutive isoform expressed mainly in brain and testes, HO-1 is induced by variety of factors(Infante et al., 2010). This is a complex and dynamic cellular metabolism which is highly contextual and cell type specific. Among the most obvious advantage of HO-1 activity removal of free heme remains crucial because it is known to have pro-oxidant property, and it also regulates several transcriptional factors (Abraham, 1991) (Kietzmann et al., 2003). Moreover, heme can act as a damage -associated pattern (DAMP) and activate innate immune response (Murdoch et al., 2008) .

Apart from this, as known hematopoietic system transport all the necessary nutrients to the whole organism and provides immunological protection. Blood cells in circulation have high turnover, which calls for a dynamic control of this system, also a broad conditional regeneration potential is a must have. This complex system is regulated by HO-1 and sometimes its by-products from degradation (Jeney et al., 2002). **(FIGURE 10)**

1.12.1. Heme-degradation its by-products and their role

CO - Among all the heme degradation products, CO seems to be the most important in regulating the immune system. CO reduces the production of pro-inflammatory cytokines, IL-1, IL-6, TNF- α, and expression of adhesion molecules. This also simultaneously increase the production of anti-inflammatory IL-10. In terms of signal transmission from certain TLRs (Toll like receptors) CO plays a role, and this is a very important factor as this mechanism is responsible for the initiation of immune response (Otterbein et al., 2000).

Biliverdin- This is instantly converted to bilirubin-by-bilirubin reductase (BVR) and exhibits potent antixioxidant and anti-inflammatory factors. This is also an efficient scavenger of reactive oxygen species (ROS) and inhibits adhesion molecules signaling (Tenhunen et al., 1968) (Jansen and Daiber, 2012) (Mazzone et al., 2009).

Ferrous Ions- These can be considered harmful, however, the release of pro-oxidant Fe^{2+} ions induce the expression of ferritin, which apart from sequestering iron, also can have an anti-apoptotic effect. (Balla et al., 1992) (Walter-Nuno et al., 2018).

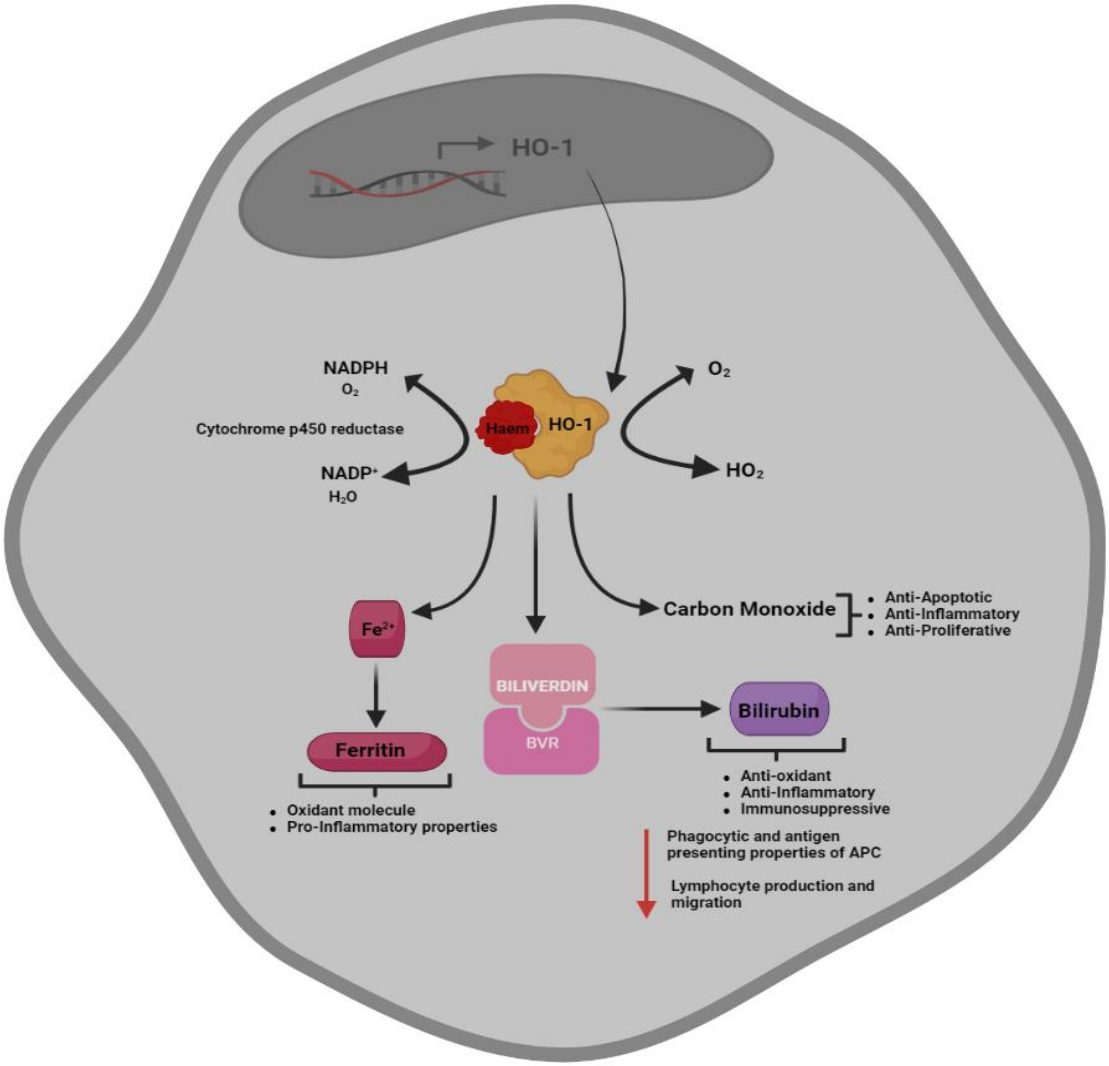

Figure 10 The oxidative degradation of heme by HO-1. In the first step of heme degradation, the ER membrane bound HO-1 interacts with the electron donor NADPH-cytochrome P450 reductase, and an oxygen molecule. The complex degrades heme to biliverdin, carbon monoxide (CO), and a ferrous iron (Fe2+). NADPH-biliverdin reductase competitively binds to HO-1 to reduce biliverdin to bilirubin, by using NADPH as an electron donor.

1.12.2. Role of HO-1 in regulation of innate immunity

A lot of evidence concerning the role of HO-1 in the normal and disease conditions were reported after the generation of genetically modified mice that lack the expression of HO-1 (HO-$1^{-/-}$). HO-$1^{-/-}$ mice are affected by a chronic proinflammatory state and dysregulated iron homeostasis (Kapturczak et al., 2004). In the context of alloreactivity, it is demonstrated that HO-1 contributes to the immunosuppressive properties of myeloid cells (Kapturczak et al., 2004). The current knowledge about the role of HO-1 in the regulation of Innate immunity is limited and points to a more complex scenario from affecting the production and regulation of above-mentioned inflammatory mediators to innate immunity in the context of

monocyte/macrophage lineage function (Cuitino et al., 2019). Studies have demonstrated that lack of HO-1 over activate pro-inflammatory phenotype of macrophages, the CO produced by HO-1 stimulates the production of IL-10 by macrophages, and this IL-10 in turn upregulates the HO-1 expression (Kietzmann et al., 2003). This indicates the presence of a positive feedback mechanism and emphasizes the importance of HO-1 in anti-inflammatory function of IL-10 (Kapturczak et al., 2004).

1.12.3. HO-1 in monocyte/macrophage lineage.

The role of HO-1 in monocyte/macrophage lineage is not limited to the regulation of the function of mature macrophages. Recent study evidenced that HO-1 is involved in the maturation of the myeloid cells from hematopoietic stem and progenitor cells. The specific deletion of HO-1 in myeloid lineage ($LysM^{Cre/+}Hmox1^{fl/fl}$) reduced the differentiation of myeloid progenitors toward macrophages (Wegiel et al., 2014). It was shown that CO, produced by HO-1, stimulates the differentiation of myeloid progenitors to macrophages, increases CD14 on their surface and enhances sensitivity to M-CSF (macrophage colony-stimulating factor) stimulation (Wegiel et al., 2014). The importance of HO-1 already in early differentiation steps of myeloid development was further confirmed by its role in myeloid-derived suppressor cells (MDSC). HO-1 was crucial for the immunosuppressive function of MDSC population in the IL-10-dependent manner (Condamine and Gabrilovich, 2011) .

As discussed and defined in earlier sections immunological stresses skews the myelopoietic output through emergency myelopoiesis, and this leads to generation of different myeloid populations endowed with pro-tumorigenic activities and to add to this in a clinical as well as biological point of view these population of immature cells and differentially programmed/adapted normal myeloid cells also hinders the activity of ICI's and limit their effect in the treatment of cancer (Stewart and Smyth, 2011). One example among this is TAM which represents final commitment of pro-tumoral reprogramming of myeloid lineage (Consonni et al., 2021) . The pro-tumoral functions of these cells are boosted by heterogenous (cancer specific, therapy induced, TME signals directed etc.) myeloid subsets and co-operatively fulfilled (Sica et al.).

As reported by A. Sica et., al transcription factors such as cEBPβ and RORγ (*Rorc*) regulate emergency myelopoiesis and contribute to the heterogeneous expansion of suppressive myeloid populations, nuclear factor-κB1 (NF-κB1, also known as p50) stimulates neutrophil production by induction of c/EBPα and promotes resolution of inflammation by diversion of

monocytes/macrophages toward a resolving anti-inflammatory M2-like phenotype. However, even though the resolution phase of acute inflammatory response is crucial for tissue homeostasis and is supported by an adaptation of hematopoietic output to inflammatory insults, no information is yet available on the mechanisms linking altered myelopoiesis to macrophage shift toward an alternative M2-polarized state, as observed in persistent infections and cancer (Gordon and Plüddemann, 2019).

1.13. The complement system as a regulator of tumor-promoting activities mediated by myeloid-derived suppressor cells. (CD5aR1/ CD88).

Existing and accumulating new evidence suggest that the complement system plays a major role in regulation of TME. Cancer cells along with the optimization of complement mediated functions remodel the TME and facilitate the tumor progression, metastasis, and evasion of immune system (Thurman et al., 2020) . Complement system a crucial player of innate immune response represents the first line of defense against harmful entities. The system compromises a set of more than 50 soluble membrane bound proteins, which are organized in independent but interactive networks (Zhang et al., 2019). To prevent damage to host tissues, complement is tightly controlled by fluid-phase and cell surface regulators. Defective or deregulated complement activation is associated with cancer. The enzymatic cleavage associated with complement activation leads to the production and release of a range of bioactive fragments, including C3a, C5a, C3b and C4b. Binding of the anaphylatoxins C3a and C5a to their respective cognate seven transmembrane domain receptors, C3a receptor (C3aR), C5a receptor 1 (C5aR1; CD88) or C5a receptor 2 (C5aR2; C5L2), plays a critical role in inflammation and immunomodulation (Thurman et al., 2020) (Wang et al., 2019).

C5a have been shown to inhibit antitumor response mediate CD4 T cells CD8 T cells or NK cells **(FIGURE 11)**. With these premises it is crucial to evaluate the intracellular activity of C5a, since C5a/ C5aR signaling promotes tumorigenesis through variety of mechanisms, including β-catenin stabilization (Melero et al., 2014) . One study reported that melanoma was reduced in C5aR1 deficient mice, but this is largely unexplored are and additional studies are required to understand the underlying complex mechanisms (“C5a receptors C5aR1 and C5aR2 mediate opposing pathologies in a mouse model of melanoma,” n.d.).

In a syngeneic model of metastatic breast cancer C5aR1 promoted angiogenesis and suppressed effector CD8 and DC4 T-cell response in the lungs (Vadrevu et al., 2014). The most astonishing aspect of this the mechanism of this suppression which involved the

recruitment of immature Myeloid cells, this connects the dot between tumor induced emergency myelopoiesis and skewed pro-tumorigenic immune landscape (Wang et al., 2019). Genetic abrogation of C5aR1 impaired M2-polarized TAMs, leading to a decrease of liver and lung metastases from colon cancer cells. Similarly, C5aR1 signaling activated a CXCL16-mediated osteoclastogenic program to sustain the osseous metastatic colonization of lung tumors. To sum up C5a/C5aR1 axis is involved in the distribution of MDSCs in the TME (Senent et al., 2022). Based on several evidence, a clinical trial was launched to evaluate the efficacy of the combined blockade of C5aR1 and PD-L1 in patients with solid tumors (Ajona et al., 2017).

Finally Complement-related biomarkers, such as circulating C5a or intratumorally C5a/C5aR1 levels, or C5aR1 levels on myeloid cells, may aid to identify those patients more likely to benefit from the ICI's and combination treatment.

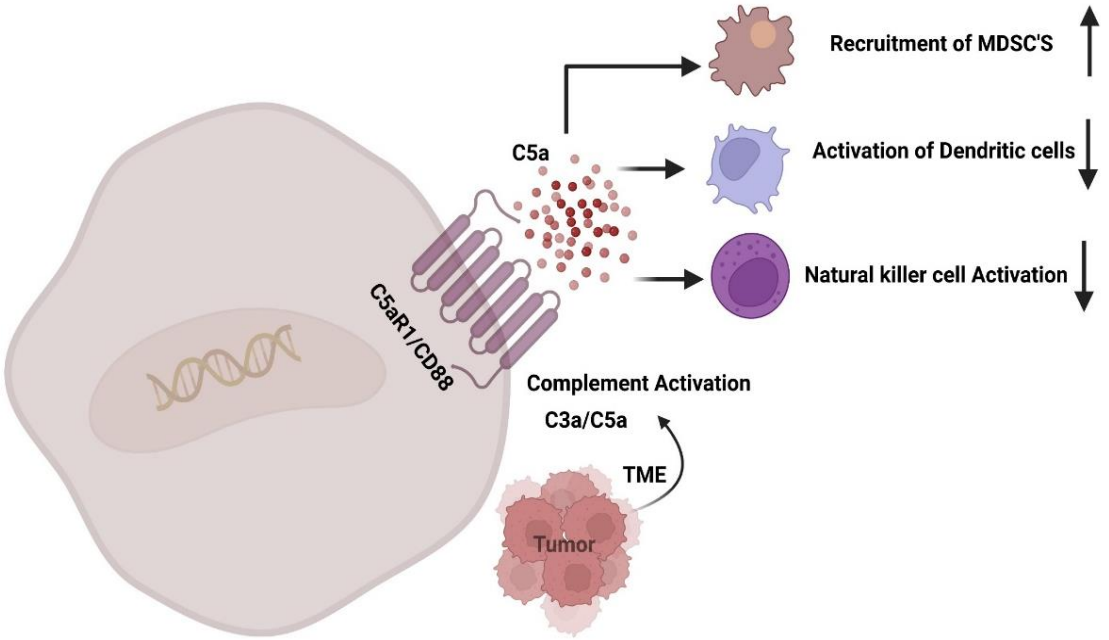

Figure 11 Complement system C5a/C5aR1 control the tumor microenvironment. Tumor cells actively promote complement activation by several mechanisms. Cancer cells also produced complement proteins, such as C5, which fuels local activation. Cancer cells can also release proteases, such as cathepsin L, which directly activate complement proteins. Complement activation within tumors likely causes apoptosis and necrosis of some target cells, but it also produces C3a and C5a which recruit inhibitory myeloid cells into the tumor microenvironment. These myeloid cells suppress the anti-tumor function of CD4 and CD8 T cells.

1.14. Cancer And Metabolism

As addressed in preclinical models challenged with hematopoietic stresses and metabolic influence has been shown to alter host metabolism, for example in the obese patients (Sica et al.). Indeed, obesity-induced chronic inflammation is a key component in the pathogenesis of both insulin resistance and metabolic syndrome and is characterized by continuous production of proinflammatory cytokines that can lead to significant alteration in HSCs function and output, ultimately leading to a skewed hematopoiesis, which might favor the pro-tumorigenic functions or alter the therapeutic outcomes to worse (Giles et al., 2016). Failure to efficiently resolve inflammatory insults can have serious consequences for tissue maintenance and function. Indeed, in the context of chronic inflammation due to metabolic diseases such as obesity and type 2 diabetes, the inflammatory stress fails to resolve, leading to a persistent inflammatory state. Parallelly diabetes negatively impacts the mobilization capacity of HSCs by altering chemokine expression in the BM niche. Obesity, presence of high levels of Insulin are only the few examples which favors the adverse outcome in the patient treated for several cancer types. There are emerging recent evidence that patients with higher Body Mass Index (BMI) have an improved outcome if treated with immunotherapy for advanced tumors (Bolton et al., 2019). This evidence indeed gives an indication that immune system, its targeting by cancer immunotherapy and patient metabolic status are all inter-connected (Sica et al.).

1.15. Existing and potential investigational liquid biomarkers in cancer and immunotherapy

It has become increasingly evident that the host immune response is critical in determining the magnitude of benefit from immunotherapy. Thus, multiple studies have examined routine blood-based parameters with response to immunotherapy (Arora et al., 2019). These blood-based parameters include absolute neutrophil counts (ANC), absolute or relative lymphocyte counts, total leucocyte counts, neutrophil-to-lymphocyte ratio (NLR), absolute or relative eosinophil counts, relative basophils, absolute monocyte counts (AMC), serum lactate dehydrogenase (LDH), and C-reactive protein (Arora et al., 2019) (Sankar et al., 2022).

Elevated leukocyte dehydrogenase (LDH) levels at baseline can indicate high tumor burden and have been shown to correlate with low response rate to immunotherapy such as

pembrolizumab (Wu et al., 2021). The overall response rate (ORR) to pembrolizumab in melanoma was noted to be 26% for patients with high LDH levels as compared to 40% in a general study patient population (Forkasiewicz et al., 2020). Similarly, response rates were 40% when LDH was in the normal range, 34% when LDH was up to 2 times the upper normal limit, and 8% when LDH is elevated over 2 times the upper normal limit in a first-line setting (Miao et al., 2013).

2. Materials and Methods

2.1. Study design and patients

This project is a mono-center, observational study that involves patients coming from the Hospital 'Maggiore della Carità', Novara, Italy.

Peripheral whole blood samples were collected from patients, who were eligible for ICIs therapy. 126 patients have been recruited so far. Informed consent was signed before the recruitment and the following inclusion/exclusion criteria was followed.

Inclusion criteria:

• Patients aged ≥ 18 years.

• Patients with a diagnosis of an advanced stage solid tumor (lung, melanoma, head and neck, renal).

• Patients who are candidates for immunotherapy with anti PD1 or anti PD-L1 or anti CTLA4 in any line of therapy for advanced disease, either alone or in combination with chemotherapy; other chemo-immunotherapy regimens could be included when available in clinical practice.

• Patients able to sign informed consent.

Exclusion criteria:

• Patients in psychological, family, social and geographical conditions that they could contraindicate compliance and adherence to proposed therapies.

• Pregnant patients

. • Patients that already received ICIs

. • Patients with blood tests non compatible with the treatment.

141 patients were screened through the collection of whole blood at baseline.

2.2. Blood Sample collection and processing

Whole blood samples were collected from patients diagnosed with advanced-stage cancers. 20 mL of peripheral blood were collected for each patient in 10 mL K2 or K3 potassium salt of EDTA (Ethylene Diamine Tetra Acetic acid) Vacutainer and were processed within 4

hours after collection. Each blood sample was diluted in a 50 mL falcon tube with 20 mL physiological solution, and then 15 mL of cell separation media (Ficoll-Paque Lympholyte, Cedarlane, Canada) was added. The tube was then centrifuged for 20 min at 800 xg without any application of brake. Peripheral blood mononuclear cells (PBMCs) were collected from the interphase between diluted plasma and cell separation media and washed twice by centrifugation at 400gx in physiological solution in the appropriate volume, and the pellet of PBMC was collected. **(Figure 12).**

2.3. Cells Staining and Flow cytometry.

2.3.1. Myeloid Derived Suppressor cells: MDSC'S

Fresh PBMCs were incubated with antibodies **(Table 1)** in pre-defined concentration and volumes for 15 minutes at room temperature and dark conditions. After a standard wash step by centrifugation, cells were resuspended in 200ul of staining buffer (2%FBS, 98% PBS 1X) and immediately acquired by Flow Cytometer (BD FACSymphony™ A5 Cell Analyzer, Milan, Italy) and the data were collected for analysis.

MDSC subpopulation phenotypes among lymphomonocyte gate ($CD45^{+)}$ were defined as follows:

M-MDSC: HLA-DR−/low CD33+ CD15− CD14+

PMN-MDSC: HLA-DR−/low CD33int CD15+ CD14−.

e-MDSC: HLA-DR−/low CD33int CD15− CD14−

Table 1

Antibody	Fluorophore	Volume/100uL	Source
CD45	BUV395	0.5 uL	(BD Bioscence, Milan, Italy
HLA-DR	BV605	1 uL	(BD Bioscence, Milan, Italy)
CD15	BV510	1 uL	(Thermo Fischer scientific, Waltham, USA)
CD14	BUV737	0.5 uL	(BD pharmingenTM, Milan, Italy
CD16	PE-CY	0.3 uL	(BD pharmingenTM, Milan, Italy
CD33	APC	5 uL	Life Technologies Corp,cartsbad, New York, USA)
Lox-1	PE	1 uL	Thermo-fisher Invitrogen , Monza, Italy.

Table 1 Antibodies, respective fluorophore, quantity used for identification of MDSCs.

2.3.2. Phenotyping Peripheral Blood monocyte subsets and measuring expression levels of intracellular Heme-oxygenase-1 and surface C5aR1/CD88:

Previously cryopreserved PBMC's were thawed in pre-warmed complete RPMI-1640 medium. Standard washing procedures were done, and cells were counted for vaibality in Burker chamber by diluting 1:10 with Turk solution.

Staining and Flow cytometry:

Cells were incubated with ZombieAqua solution for 20 minutes for live/dead cell discrimination. Then it was added with the listed antibodies for flow cytometry analysis: **(Table 2)**

Cells were incubated for pre-defined time period and in optimal conditions. standard wash steps were followed at the end of incubation. Cells were then incubated for 20 minutes on ice with BD Cytofix/Cytoperm solution (BD Bioscence, Milan, Italy), to permeabilize the membrane for the staining with intracellular heme-oxygenase-1. Finally, the HO-1 antibody (Prodotti Gianni Corp, Milano, Italy) was added to the solution with cells and incubated on ice for 30 minutes. After the incubation, the cells ware washed in BD Permeabilization buffer 1X, resuspended in 200uL of staining buffer and acquired Flow Cytometer (BD FACSymphony™ A5 Cell Analyzer, Milan, Italy).

Peripheral Blood monocyte subsets (Lineage negative) were phenotyped and gated as follows.

Classical monocytes (CD14++ CD16−),

Non-classical monocyte (CD14-CD16+) and

Intermediate monocytes (CD14+CD16+).

Geometric Mean Fluorescence Intensity (gMFI) was used to measure the expression of HO-1 and CD88, in all the three monocyte subsets.

Table 2

Antibody	Fluorophore	Volume/100uL	Source
CD45	BUV395	0.5 uL	(BD Bioscence, Milan, Italy)
CD16	PE-CY	0.3 uL	(BD pharmingenTM, Milan, Italy)
CD14	PE-CF594	1.25uL	(BD Bioscence, Milan, Italy)
CD3	PERCP.CY	1uL	(BD pharmingenTM, Milan, Italy)
CD56	PERCP.CY	1uL	(Biolegend, San Diego, USA)
CD19	PERCP.CY	1uL	(Thermo Fischer scientific, Waltham, USA)
CD88	PE	2.5uL	(Life Technologies Corp,cartsbad,New York, USA)
HO-1	FITC	1uL	(Prodotti Gianni Corp, Milano, Italy)

Table 2 Antibodies, respective fluorophore, quantity used for identification of monocyte subsets, expression of HO-1 and CD88.

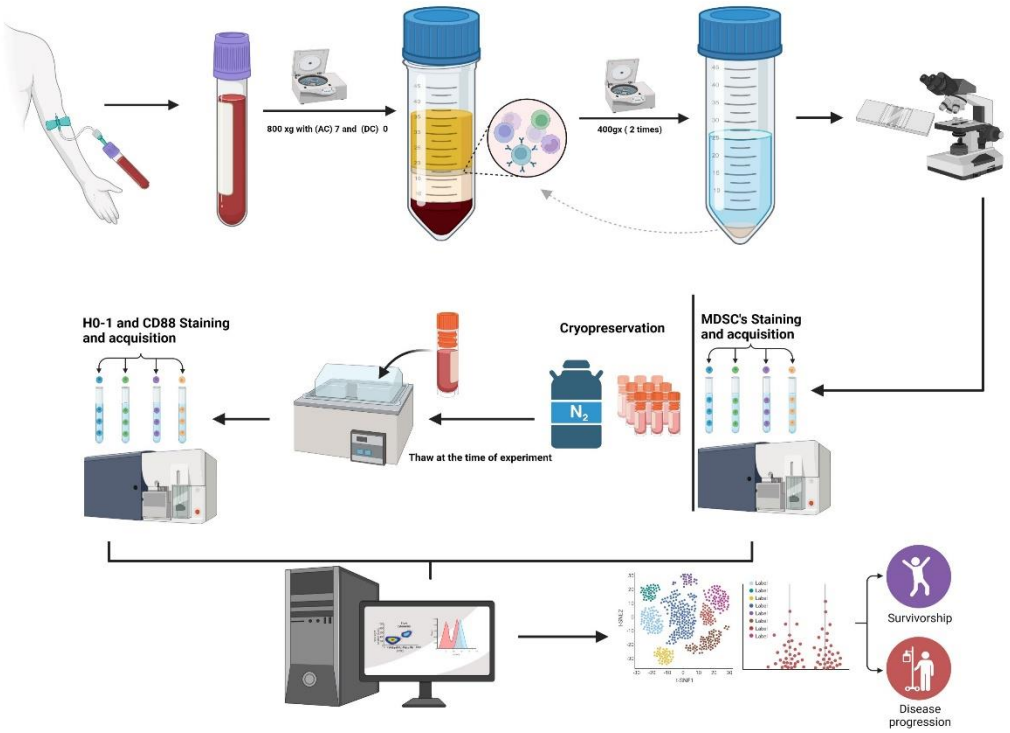

Figure 12: A schematic representation of workflow included in the study.

2.4. Blood Count Biomarker evaluation and quantification

Peripheral complete blood count was performed at baseline, and the absolute number of lymphocytes, platelets, monocytes and neutrophils determined to quantify absolute values of LMR, PLR, NLR, dNLR, NWR, SII as follows:

• LMR (lymphocyte monocyte ratio) was calculated by dividing the absolute lymphocyte value by the absolute monocyte value.

• NLR (Neutrophil Lymphocyte ratio) was calculated by dividing the absolute neutrophil value by the absolute lymphocyte value.

• PLR (Platelet lymphocyte ratio) was calculated by dividing the absolute platelet vale by the absolute lymphocyte value.

• dNLR (derived neutrophil lymphocyte ration) was calculated by dividing absolute neutrophil value by total white blood cells minus neutrophils.

• NWR (neutrophils to white blood cells ratio) was calculated by dividing absolute neutrophil value by total white blood cells value.

• SII (Systemic inflammation index) was calculated as (N×P)/L (N, P and L represent neutrophil counts, platelet counts and lymphocyte counts, respectively).

The other clinical parameters like cholesterol (LDL, HDL), Tri-acyl glycerol (TAG) , carboxy hemoglobin (COHb), glucose levels , body mass index , smoking status , ECOG scores were derived from the patient clinical profile at baseline of ICI therapy .

2.5. Statistics and Survival Data Analysis

Data were presented as mean, standard deviation (SD) and Standard Error of Mean (SEM). For statistical purposes, baseline characteristics were defined as categorical variables and reported as values and percentages. Statistical analysis was performed using Either one-way ANOVA or a Kruskal–Wallis test was used to compare multiple groups. A two-tailed, unpaired Student's *t*-test was used to compare unmatched groups with Gaussian distribution. A Mann–Whitney *U*-test was used in cases of non-Gaussian distribution. Flow cytometry Data was analyzed using BD FACSDiva v9.0 and FlowJo™ v10.8. Association of biomarkers with survival was tested by Kaplan-Meier model in the univariate approach using

Graph Pad prism V.7. Hazard ratio relative to a variation per unit of the scale was calculated, together with 95% confidence interval and associated P value.

2.6. Images

Bio render online platform was used to create images for introduction and materials and methods.

3. Results

3.1. Baseline characteristics and clinical predictors of advanced cancer patients treated with immune checkpoint inhibitors.

The present study enrolled a total of 126 patients undergoing immune checkpoint therapy for advanced solid tumors over the period between 03/2020-05/2022. Among which (n=89;71%), (n=13;10%), (n=14;11%), (n=10; 8%) were diagnosed with advanced lung cancer, melanoma, head and neck cancer, and renal cell carcinoma respectively. **(Table 3 to Table 6)** Clinical outcomes analyzed were OS and PFS. OS was defined as the time from randomization or initiation of treatment until death from any cause. PFS was defined as the time from randomization or initiation of treatment to first progression or death from any cause. The median overall survival rate (OS) and progression-free survival rate for the patient undergoing immune checkpoint inhibitor therapy were postulated using Kaplan Meier survival analysis. The median OS and PFS for lung cancer patients after the initiation of therapy were 22.2 months and 7.9 months respectively. In melanoma median OS and PFS rates were 5.3 months and 3.9 months respectively. In Head and neck cancer OS and PFS rates were 6.7 months and 3.3 months respectively, and in Renal cell carcinoma, median OS was not reached at the end of the study (16.3 months) more than 50% of patients were either alive or censored and hence OS remains undefined whereas PFS rate among patients was 6.7 months. Different clinical characteristics of patients are shown separately based on cancer type from **Table 3 to Table 6**. The median age for advanced lung cancer patients, melanoma patients, advanced head and neck cancer patients, and advanced renal cell carcinoma were 69.4 (37.6-88.7) years ,73.1(35-87) years, 63.6 (53.4-87) years,70.2 (49.8-78.8) years respectively. Among which 71.6%(n=63) were male and 28.4%(n=25) were female for lung cancer, 69.2%(n=9) were male and 30.7%(n=4) were female for melanoma, 85.7% (n=12) were male and 14.2% (n=2) were female for head and neck cancer, and 50%(n=5) were male and 50% (n=5) were female for renal cell carcinoma

3.2. Univariate Cox proportional hazard analysis of clinical characteristics

3.2.1. Smoking status:

Among lung cancer patients 10.2% (n=9), 70.4% (n=63), and 19.3% (n=17) were non, former, and active smokers respectively, in patients with melanoma 30.7% (n=4), 30.7% (n=4), 7.6% (n=1), were non, former and active smokers respectively, In head and neck

cancer patients 21.4% (n=3), 50% (n=7), 28.5% (n=4) were non, former and active smokers respectively, in renal cell carcinoma 50% (n=10), 30% (n=3), 20% (n=2) were non, former and active smokers respectively. Survival curves were derived using Kaplan Meier survival analysis for OS and PFS even though there was a difference in both OS and PFS between the three groups there was no statistical significance established.

3.2.2. ECOG Performance status:

We have compared the PFS, and OS of patients stratified by ECOG status. In lung cancer, melanoma, and head and neck cancer we observed a comparatively short PFS in those with higher ECOG status and this finding reflected on the OS except for head and neck cancer, the statistics are shown in (Table 3 to Table 6) and survival curves are shown in (Figure 13).

3.2.3. Therapy:

As shown in Tables 3 to 6, among the lung cancer patients, anti-PD-1/PD-L1 immunotherapy was given to 60.6 %/37.0%, whereas anti-CTLA-4 was used in 2.2% of patients, while 64.0% of patients were previously chemotherapy-treated group and 36% had no previous chemotherapy status. In melanoma patients, anti-PD-1/PD-L1 immunotherapy was given to 84.6%/15.3%, while no patients had a history of chemotherapy, for head and neck cancer patients, 100% patients were treated with anti-PD-1 immunotherapy, while 42.8% of patients were previously chemotherapy-treated group and 57.1% had no previous chemotherapy. In renal cell carcinoma patients, anti-PD-1 immunotherapy was given to 100%, while no patients were among the previously chemotherapy-treated group. There was no statistical significance found between the patients with previous chemotherapy status, both in terms of OS and PFS.

3.2.4. Body Mass Index:

With regards to BMI values, in this study, we stratified the BMI value into high BMI group and low BMI group by cutoff value (summarized in Table 3 to Table 6), which was obtained by median value independently for each cancer type. We analyzed Cox Proportional hazard ratios (HRs) with 95% confidence intervals for OS and PFS. In the analysis comparing survival differences between patients with high BMI and those with low BMI, no statistically significant difference in both OS and PFS patients treated with ICIs therapy was found, in any of the advanced cancer types.

LUNG CANCER	n , %	OS (Median) (Months)	PFS (Median) (Months)	HR		95% CI		p-VALUE	
SURVIVAL RATE (Median)		22.2	7.9	**OS**	**PFS**	**OS**	**PFS**	**OS**	**PFS**
SEX, (n) %				2.3	0.91	1.20-4.6	0.52-1.6	**0.0276**	0.7599
Male	64 (71.6%)	13.9	7.8						
Female	25 (28.4%)	25.2	15.05						
Age (Years)				0.63	0.69	0.32-1.22	0.42-1.14	0.1601	0.6998
Median	69.4	16.2 (>69.4),25.2 (<69.4)	10.1 (<69.4), 7.6 (>69.4)						
Range	37.6-88.7								
Smoking history (n)									
Never	9 (10.2%)	6.8	5.0						
Former	63 (70.4%)	NR	7.9						
Active	17 (19.3%)	13.09	11.3						
ECOG performance status, (n)								**0.0001**	**0.0163**
0	52 (58.4%)	25.2	10.8						
1	33 (37.0%)	7.9	4.8						
2	4 (4.4%)	2.3	1.6						
BMI				0.84	1.23	0.44-1.63	0.72-2.18	0.6145	0.4238
> 23.58	46 (51.6%)	13.9	10.7						
< 23.58	43 (48.3%)	22.2	7.9						
ICI given , (n)									
Anti-PD-1	54 (60.6%)								
Anti-PD-L1	33 (37.0%)								
Anti-CTLA-4	2 (2.2%)								
Previous Chemotherapy				0.79	0.89	0.407-1.55	0.54-1.47	0.4920	0.6533
Yes	57 (64.0%)	16.2	7.1						
No	32 (35.9%)	22.2	9.0						

Table 3: Baseline clinical characteristics of patients with advanced lung cancer treated with ICI's. n: number, %: percentage, BMI: Body mass index, ICI: immune checkpoint Inhibitor, OS: overall survival, PFS: Progression free survival, HR: Hazard ratio, 95% CI: 95% confidence interval, Y: years, PD-1: Programmed Cell Death Protein 1, PD-L1: Programmed Cell Death ligand 1, CTLA-4: Cytotoxic T-lymphocyte-associated protein 4. Significant p-Values are represented in bold.

MELANOMA	n , %	OS (Median) (Months)	PFS (Median) (Months)	HR		95% CI		p-VALUE	
SURVIVAL		5.3	3.9	**OS**	**PFS**	**OS**	**PFS**	**OS**	**PFS**
SEX, (n)				0.67	0.98	0.14-3.11	0.23-4.1	0.5709	0.9831
Male	9 (69.2%)	5.3	3.9						
Female	4 (30.7%)	6.3	3.1						
Age (Years)				1.69	2.6	0.42-6.78	0.62-10.79	0.4576	0.1617
Median	73.1	5.3 (<73.1), 6.1 (>73.1)	1.7 (<73.1),4.5 (>73.1)						
Range	35-87								
Smoking history (n)				0.72		0.18-2.9		0.65569	0.0833
Never	4 (30.7%)	5.0	3.9						
Fromer	4 (30.7%)	6.5	4.5						
Active	1 (7.6%)	5.3	1.3						
ECOG performance status, (n)								**0.0019**	**0.0019**
0	11 (84.6%)	6.1	3.9						
1	2 (15.3%)	1.6	1.1						
2	-	-	-						
BMI				1.39	0.78	0.30-6.3	0.19-3.1	0.6190	0.7409
> 25.97	5 (38.4%)	5.3	3.8						
< 25.97	7 (53.8%)	6.1	3.9						
ICI given , N									
Anti-PD-1	11 (84.6%)								
Anti-PD-L1	2 (15.3%)								
Anti-CTLA-4									
Previous Chemotherapy, (n)									
Yes	0								
No	13 (100%)								

Table 4: Baseline clinical characteristics of patients with melanoma treated with ICI's. n: number, %: percentage, BMI: Body mass index, ICI: immune checkpoint Inhibitor, OS: overall survival, PFS: Progression free survival, HR: Hazard ratio, 95% CI: 95% confidence interval, Y: years, PD-1: Programmed Cell Death Protein 1, PD-L1: Programmed Cell Death ligand 1, CTLA-4: Cytotoxic T-lymphocyte-associated protein 4. Significant p-Values are represented in bold.

Head and Neck Cancer	n , %	OS (Median) (Months)	PFS (Median) (Months)	HR		95% CI		p-VALUE	
SURVIVAL		6.7	3.3	**OS**	**PFS**	**OS**	**PFS**	**OS**	**PFS**
SEX, (n)				0.6	0.82	0.09-3.8	0.16-4.13	0.5313	0.7894
Male	12 (85.7%)	6.7	3.3						
Female	2 (14.2%)	6.7	3.6						
Age (Years)				1.46	0.29	0.35-6.02	0.67-1.28	0.5655	0.0555
Median	63.6	6.8 (> 63.6Y) ,6.6 (<63.6 Y)	4.8 (> 63.6Y) , 2.8 (<63.6 Y)						
Range	53.4-81.9								
Smoking history (n)								0.6602	0.5075
Never	3 (21.4%)	6.6	2.8						
Fromer	7 (50%)	7.1	3.4						
Active	4 (28.5%)	6.7	3.6						
ECOG performance status, (n)								0.5652	**0.0117**
0	8 (57.1%)	6.7	4.4						
1	3 (21.4%)	6.2	2.3						
2	3 (21.4%)	4.1	1.9						
BMI				2.125	1.71	0.52-8.5	0.56-5.19	0.2676	0.2797
> 22.53	7 (50%)	7.1	3.1						
< 22.53	7 (50%)	6.7	3.4						
ICI given , (n)									
Anti-PD-1	14 (100%)								
Anti-PD-L1	0								
Anti-CTLA-4	0								
Previous Chemotherapy				1.28	1.6	0.31-5.8	0.54-4.78	0.7228	0.3564
Yes	6 (42.8%)	6.7	3.3						
No	8 (57.1%)	6.6	3.8						

Table 5: Baseline clinical characteristics of patients with advanced head and neck cancer treated with ICI's. n: number, %: percentage, BMI: Body mass index, ICI: immune checkpoint Inhibitor, OS: overall survival, PFS: Progression free survival, HR: Hazard ratio, 95% CI: 95% confidence interval, Y: years, PD-1: Programmed Cell Death Protein 1, PD-L1: Programmed Cell Death ligand 1, CTLA-4: Cytotoxic T-lymphocyte-associated protein 4. Significant p-Values are represented in bold.

RENAL CELL CARCINOMA	n , %	OS (Months)	PFS (Months)	HR		95% CI		p-VALUE	
SURVIVAL RATE (MEDIAN)		NR	6.8	OS	PFS	OS	PFS	OS	PFS
SEX, (n)				0.5	1.93	0.05-4.8	0.42-8.73	0.563	0.2786
Male	5 (50%)	NR	1.5						
Female	5 (50%)	11.9	6.7						
Age (Years)				0.35	0.20	0.03-3.5	0.04-0.97	0.3657	**0.0250**
Median	70.2	NR (>70.2), NR (<70.2)	2.5 (>70.2),9.2 (<70.2)						
Range	49.8-78.8								
Smoking history (n)					1.5		0.24-9.2	0.4205	0.6224
Never	5 (50%)	NR	6.6						
Fromer	3 (30%)	11.9	6.7						
Active	2 (20%)	6.3	5.3						
ECOG performance status, (n)								0.1070	0.9581
0	8 (80%)	NR	6.6						
1	2 (20%)	10.18	6.7						
2	-								
BMI				1.13	0.34	0.10-11.9	0.05-2.15	0.91	0.0907
> 23.34	5 (50%)	NR	6.6						
< 23.34	5 (50%)	13.1	6.8						
ICI given , (n)									
Anti-PD-1	10 (100%)								
Anti-PD-L1	-								
Anti-CTLA-4	-								
Previous Chemotherapy									
Yes	0								
No	10 (100%)								

Table 6: Baseline clinical characteristics of patients with advanced renal cell carcinoma treated with ICIs. n: number, %: percentage, BMI: Body mass index, ICI: immune checkpoint Inhibitor, OS: overall survival, PFS: Progression-free survival, HR: Hazard ratio, 95% CI: 95% confidence interval, Y: years, PD-1: Programmed Cell Death Protein 1, PD-L1: Programmed Cell Death ligand 1, CTLA-4: Cytotoxic T-lymphocyte-associated protein 4. Significant p-Values are represented in bold.

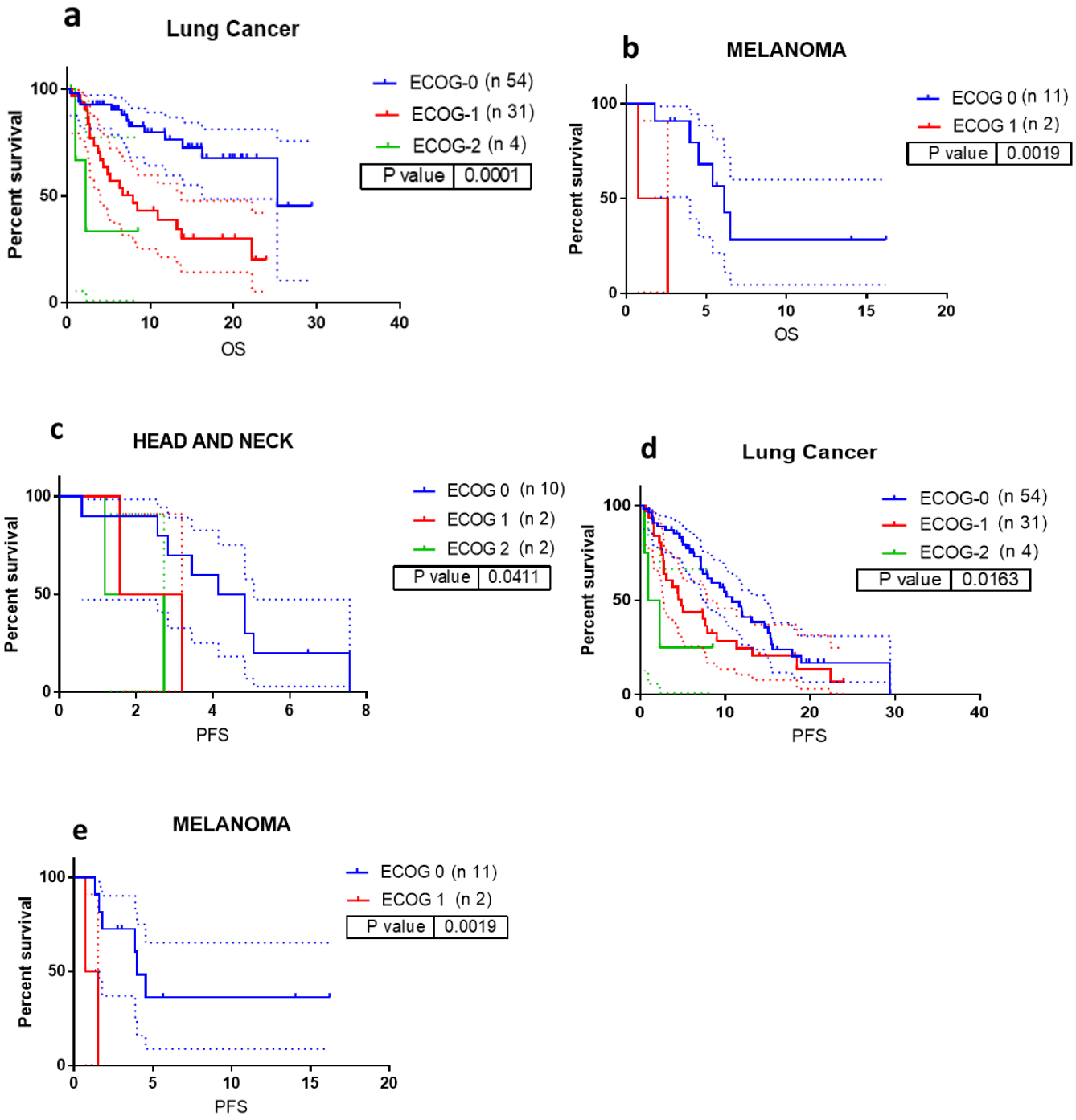

Figure 13: Kaplan-Meier Survival Curves with 95% CI for Overall Survival (OS; a, b,) and Progression-Free Survival (PFS; c,d, e) of advanced Lung Cancer, head and neck and melanoma Patients treated With ICI's. Time is represented in months at baseline. (a) (OS; advanced lung cancer patient) and (b) (OS; melanoma patients) (c,d,e) (PFS; advanced head and neck cancer , advanced lung cancer patient and melanoma patient respectively) , patients are stratified by ECOG score 0, 1 and 2 .Blue line represents ECOG;0 Red line represents ECOG;1 and Green line represents ECOG;2 . Dotted lines represent upper and lower limit of 95% CI (Confidence Interval) . Results are from univariable cox proportional Hazard model. (ECOG; Eastern Cooperative Oncology Group status).

3.2.5. Serum lipids and Glucose:

Cox Proportional hazard ratios (HRs) with 95% confidence intervals for the association between the serum biomarkers and ICI therapy outcome (OS and PFS) among the study population at the time of the end of the study are displayed at **(Table 7-10),** the patients were divided into low and high-value groups based upon cut-off value (median value) individualized for each cancer type for, Total cholesterol, low-density lipoprotein (LDL), high-density lipoprotein (HDL), triacylglyceride (TAG), and glucose levels, no statistically significant difference in both OS and PFS after receiving ICIs therapy was found, in any of the advanced cancer types for total cholesterol, LDL, HDL, TAG and Glucose levels **(Table 7-10)**.

3.2.6. Carboxyhaemoglobin (COHb):

The circulation levels of CO (measured as COHb) that is majorly derived from HO-1 catalyzed heme metabolism, were obtained for all the patients included in the study, the cut-off values were defined as median levels (in%) among individual advanced cancer type (Table 7-10), no statistically significant difference in both OS and PFS was observed for COHb levels (Table 7-10).

SURVIVAL RATE (MEDIAN)		OS	PFS	OS	PFS	OS	PFS	OS (Median) (Months)		PFS (Median) (Months)	
LIPOPROTEIN/COHb/GLUCOSE	CUT OFF VALUES	HR		95% CI		p-VALUE		High	Low	High	Low
Cholestrol Total	185 mg/dL	3	1.38	0.72-13.1	0.46-4.12	0.0731	0.5295	7.1	6.7	4.0	3.0
High Density Lipoprotein (HDL)	45 mg/dL	0.86	1.27	0.20- 3.74	0.42-3.78	0.8322	0.6385	6.7	6.7	3.4	2.8
Low Density Lipoprotein (LDL)	126 mg/dL	1.91	1.08	0.44-8.26	0.36-3.24	0.3032	0.8733	7.1	6.7	3.4	3.1
Triacyl glyceride (TAG)	121 mg/dL	3.08	1.18	0.72-13.1	0.39-3.55	0.0768	0.7498	7.1	6.6	3.1	3.4
Carboxyhemoglobin (COHb)	1.50%	1.1	1.74	0.27-4.42	0.57-5.29	0.8824	0.2821	6.7	6.6	4.1	2.8
Glycemia	106 (mg/dL)	3.53	2.12	0.80-15.6	0.68-6.63	0.0522	0.1429	6.8	6.6	4.1	2.7

Table 7: Represents baseline lipoproteins HDL, LDL, TAG and total cholesterol levels, COHb levels and glucose levels of advanced lung cancer patients treated with ICI'S. OS; overall survival PFS; progression free survival, ICI'S; Immune checkpoint inhibitors. Results are from univariable cox proportional Hazard model. Significant p-Values are represented in bold.

SURVIVAL RATE (MEDIAN)		OS	PFS	OS	PFS	OS	PFS	OS (Median) (Months)		PFS (Median) (Months)	
LIPOPROTEIN/COHb/GLUCOSE	**CUT OFF VALUES**	**HR**		**95% CI**		**p-VALUE**		**High**	**Low**	**High**	**Low**
Cholestrol Total	186 mg/dL	1.2	2.06	0.29-4.82	0.51-8.3	0.7926	0.3103	6.1	4.5	3.9	2.8
High Density Lipoprotein (HDL)	50 mg/dL	2.09	2.06	0.51-8.44	0.51-8.30	0.2909	0.3103	6.1	3.5	3.9	2.8
Low Density Lipoprotein (LDL)	116 mg/dL	1.46	1.07	0.36-5.85	0.25-4.43	0.5932	0.9237	6.1	4.5	1.7	3.9
Triacyl glyceride (TAG)	98 mg/dL	0.58	0.70	0.14-2.49	0.17-2.89	0.4435	0.6236	4.5	6.1	3.1	3.9
Carboxyhemoglobin (COHb)	1.70%	Undefined	Undefined	Undefined	Undefined	0.6005	0.4750	NR	5.3	NR	3.8
Glycemia	101 (mg/dL)	0.93	0.84	0.22-3.86	0.20-3.45	0.9248	0.8177	6.1	5.3	7.9	3.9

Table 8: Represents baseline lipoproteins HDL, LDL, TAG and total cholesterol levels, COHb levels and glucose levels of melanoma patients treated with ICI'S. OS; overall survival PFS; progression free survival, ICI'S; Immune checkpoint inhibitors. Results are from univariable cox proportional Hazard model. Significant p-Values are represented in bold.

SURVIVAL RATE (MEDIAN)		OS	PFS	OS	PFS	OS	PFS	OS (Median) (Months)		PFS (Median) (Months)	
LIPOPROTEIN/COHb/GLUCOSE	**CUT OFF VALUES**	**HR**		**95% CI**		**p-VALUE**		**High**	**Low**	**High**	**Low**
Cholestrol Total	176 mg/dL	1.28	1.06	0.66-2.47	0.64-1.73	0.4498	0.8126	16.2	22.2	8.3	7.9
High Density Lipoprotein (HDL)	48.5 mg/dL	1.21	1.02	0.62-2.32	0.62-1.67	0.5579	0.9110	25.2	22.2	7.6	9.0
Low Density Lipoprotein (LDL)	102 mg/dL	1.07	0.99	0.55-2.07	0.60-1.61	0.8272	0.9689	16.2	22.2	9.0	7.8
Triacyl glyceride (TAG)	116.5 mg/dL	0.49	0.77	0.23-1.08	0.47-1.27	0.0784	0.3093	16.2	22.2	7.3	9.8
Carboxyhemoglobin (COHb)	1.40%	1.36	1.10	0.70-2.65	0.66-1.82	0.3681	0.6997	25.25	22.2	10.1	7.6
Glycemia	100 (mg/dL)	1.08	0.85	0.49-2.38	0.52-1.40	0.838	0.5402	22.2	NR	7.1	10.8

Table 9: Represents baseline lipoproteins HDL, LDL, TAG and total cholesterol levels, COHb levels and glucose levels of advanced head and neck cancer patients treated with ICI'S. OS; overall survival PFS; progression free survival, ICI'S; Immune checkpoint inhibitors. Results are from univariable cox proportional Hazard model. Significant p-Values are represented in bold.

SURVIVAL RATE (MEDIAN)		OS	PFS	OS	PFS	OS	PFS	OS (Median) (Months)		PFS (Median) (Months)	
LIPOPROTEIN/COHb/GLUCOSE	CUT OFF VALUES	HR		95% CI		p-VALUE		High	Low	High	Low
Cholestrol Total	169 mg/dL	0.74	0.28	0.05-9.5	0.39-1.98	0.8075	0.0501	NR	NR	2.5	6.8
High Density Lipoprotein (HDL)	39 mg/dL	0.11	0.46	0.006-2.09	0.08-2.51	**0.0199**	0.4624	8.4	11.9	2.5	6.7
Low Density Lipoprotein (LDL)	90 mg/dL	0.30	0.42	0.01-8.5	0.05-3.48	0.2207	0.2295	NR	NR	2.5	6.7
Triacyl glyceride (TAG)	114 mg/dL	undefined	0.66	undefined	0.10-4.10	0.2779	0.5768	NR	11.9	6.6	6.7
Carboxyhemoglobin (COHb)	1.00%	1.49	0.72	0.14-14.18	0.15-3.42	0.7630	0.6517	NR	NR	6.6	6.7
Glycemia	103 (mg/dL)	1.8	2.23	0.31-10.57	0.57-8.72	0.4953	0.1694	NR	11.9	6.8	6.6

Table 10: Represents baseline lipoproteins HDL, LDL, TAG and total cholesterol levels, COHb levels, and glucose levels of advanced renal cell carcinoma patients treated with ICI'S. OS; overall survival PFS; progression-free survival, ICI'S; Immune checkpoint inhibitors. Results are from the univariable cox proportional Hazard model. Significant p-Values are represented in bold.

3.2.7. Baseline Peripheral blood count biomarkers are associated with therapy outcomes in advanced cancer patients treated with ICIs:

To identify peripheral blood biomarker candidates for advanced cancer patients treated with ICIs, we examined nine peripheral blood parameters, measured at treatment initiation or baseline **(Table 11-14)**. Univariable Cox proportional hazard analysis of these factors revealed that in lung cancer ANC of $5.64x10^3$/uL or higher was associated with poor OS (HR = 0.52, 95% CI: 0.26-1.02, p = 0.0488), NLR of 4.38 or higher was associated with poor OS (HR = 0.45, 95% CI: 0.23-.0.88, p = 0.0172). dNLR of 2.58 or higher was associated with poor OS (HR = 0.45, 95% CI: 0.23-.0.88, p = 0.0156) and PFS (HR = 0.57, 95% CI: 0.34-0.95, p = 0.0204). SII of 1227 or higher was associated with poor OS (HR = 0.38, 95% CI: 0.19-0.73, p = 0.0055) and PFS (HR = 0.61, 95% CI: 0.37-1.01, p = 0.0486). In contrast, a trend toward a better OS (HR = 2.91, 95% CI: 1.51-5.61, p = 0.0033) and PFS (HR = 1.18, 95% CI: 1.12-2.98, p = 0.0158) was apparent in patients with an LMR of 2.45. **(Table 11) (Figure 14).**In patients with melanoma an NWR of 0.68 or higher was associated with poor

PFS (HR = 0.24, 95% CI: 0.05-1.12, p = 0.0208), an NLR of 3.3 or higher was associated with poor PFS (HR = 0.24, 95% CI: 0.05-1.12, p = 0.0208, a dNLR of 2.58 or higher was associated with poor PFS (HR = 0.21, 95% CI: 0.05-0.89, p = 0.0248), a PLR of 178.2 or higher was associated with poor PFS (HR = 0.14, 95% CI: 0.06-1.11, p = 0.019). On the contrary, no parameter showed any statistically significant effect on OS. **(Table 12) (Figure 15)**. In patients with advanced Head and neck cancer ALC of $1.47x10^3$/uL or higher was associated with better PFS (HR = 2.7, 95% CI: 0.84-9.21, p = 0.0337), an NWR of 0.66 or higher was associated with better PFS (HR = 2.7, 95% CI: 0.88-8.44, p = 0.0391). No parameter showed any statistical significance for OS. **(Table 13) (Figure 16)**. In a patient with advanced Renal cell carcinoma, none of the nine-parameter analyzed has shown a statistically significant effect on both OS and PFS. **(Table 15).**

SURVIVAL RATE		OS (Median) (Months)		PFS (Median) (Months)		OS	PFS	OS	PFS	OS	PFS
BLOOD COUNT BIOMARKERS	CUT OFF VALUES	High	Low	High	Low	HR		95% CI		p-VALUE	
Absolute Neutophil Count (ANC)	5.64 X10³/µL	9.3	22.2	7.9	8.3	0.52	0.71	0.26-1.02	0.43-1.16	**0.0488**	0.1616
Absolute Monocyte Count (AMC)	0.58 X10³/µL	10.9	25.2	7.1	10.8	0.6	0.82	0.31-1.16	0.50-1.35	0.122	0.4425
Absolute Lymphocyte Count (ALC)	1.35 X103/µL	25.2	13.2	10.8	7.1	1.48	1.3	0.76-2.84	0.79-2.12	0.2442	0.2828
Neutophil:WBC (NWR)	0.72	9.3	25.2	7.6	9.8	0.64	0.9	0.33-1.25	0.54-1.48	0.183	0.6761
Neutrophil:Lymphocyte (NLR)	4.38	8.4	25.2	7.3	10.8	0.45	0.84	0.23-.0.88	0.51-1.38	**0.0172**	0.484
Derived Neutrophil:Lymphocyte (dNLR)	2.58	7.9	22.2	5.3	11.9	0.45	0.57	0.23-.0.88	0.34-0.95	**0.0156**	**0.0204**
Platelet:Lymphocyte (PLR)	219.6	NR	22.2	7.1	11.3	0.76	0.81	0.39-1.48	0.49-1.33	0.7674	0.3934
Lymphocyte:Monocyte (LMR)	2.45	25.2	8.4	11.9	5.3	2.91	1.18	1.51-5.61	1.12-2.98	**0.0033**	**0.0158**
Systemic Inflammation Index (SII)	1227	8.4	25.2	5.8	11.9	0.38	0.61	0.19-0.73	0.37-1.01	**0.0055**	**0.0486**

Table 11: Summarizes the blood count-based biomarkers in advanced lung cancer patients treated with ICIs. OS; overall survival PFS; progression-free survival ICI'S; Immune checkpoint inhibitors. Results are from the univariable cox proportional Hazard model. Significant p-Values are represented in bold.

SURVIVAL RATE		OS (Median) (Months)		PFS (Median) (Months)		OS	PFS	OS	PFS	OS	PFS
BLOOD COUNT BIOMARKERS	CUT OFF VALUES	High	Low	High	Low	HR		95% CI		p-VALUE	
Absolute Neutophil Count (ANC)	5.52 X10^3/µL	4.5	6.5	1.6	NR	0.32	0.31	0.07-1.38	0.07-1.36	0.0858	0.0862
Absolute Monocyte Count (AMC)	0.44 X10^3/µL	4.5	1.3	4.5	3.8	0.66	1.08	0.14-3.07	0.26-4.48	0.567	0.9077
Absolute Lymphocyte Count (ALC)	1.46 X10^3/µL	6.1	5.3	4.5	3.8	1.46	1.77	0.36-5.81	0.44-7.10	0.598	0.4152
Neutophil:WBC (NWR)	0.68	5.3	NR	1.5	NR	0.47	0.244	0.11-1.93	0.05-1.12	0.2998	**0.0208**
Neutrophil:Lymphocyte (NLR)	3.3	5.3	NR	1.6	NR	0.47	0.244	0.11-1.93	0.05-1.12	0.2998	**0.0208**
Derived Neutrophil:Lymphocyte (dNLR)	2.2	5.3	NR	1.7	NR	0.32	0.21	0.08-1.27	0.05-0.89	0.1388	**0.0248**
Platelet:Lymphocyte (PLR)	178.2	5.3	NR	1.6	NR	0.27	0.14	0.06-1.11	0.03-0.64	0.0895	**0.019**
Lymphocyte:Monocyte (LMR)	3	NR	4.5	NR	2.8	3.92	3.69	0.97-15.9	0.91-14.9	0.0615	0.0712
Systemic Inflammation Index (SII)	881	3.9	NR	1.5	NR	0.24	0.1	0.06-0.99	0.02-0.53	0.588	0.0003

Table 12: Summarizes the blood count-based biomarkers in melanoma patients treated with ICIs. OS; overall survival PFS; progression-free survival ICI'S; Immune checkpoint inhibitors. Results are from the univariable cox proportional Hazard model. Significant p-Values are represented in bold.

SURVIVAL RATE		OS (Median) (Months)		PFS (Median) (Months)		OS	PFS	OS	PFS	OS	PFS
BLOOD COUNT BIOMARKERS	CUT OFF VALUES	High	Low	High	Low	HR		95% CI		p-VALUE	
Absolute Neutophil Count (ANC)	5.72 X10^3/µL	6.7	6.8	3.4	3.1	1.14	0.92	0.28-4.60	0.31-2.75	0.8395	0.8832
Absolute Monocyte Count (AMC)	0.715 X10^3/µL	7.1	6.7	3.4	2.8	1.78	1.16	0.44-7.13	0.38-3.49	0.4065	0.771
Absolute Lymphocyte Count (ALC)	1.47X10^3/µL	6.7	6.8	4.8	2.7	1.27	2.7	0.31-5.17	0.84-9.21	0.7244	**0.0337**
Neutophil:WBC (NWR)	0.66	6.7	6.7	4.9	2.7	1.57	2.7	0.36-6.75	0.88-8.44	0.5647	**0.0391**
Neutrophil:Lymphocyte (NLR)	3.73	6.8	6.7	2.6	4.4	0.91	0.41	0.21-3.88	0.12-1.42	0.895	0.0783
Derived Neutrophil:Lymphocyte (dNLR)	2.34	6.6	6.7	2.6	4.4	1.29	0.41	0.28-5.87	0.12-1.42	0.7392	0.0783
Platelet:Lymphocyte (PLR)	197.87	6..7	6.8	3.3	3.4	0.71	1.02	0.18 -2.68	0.34-3.04	0.61	0.9671
Lymphocyte:Monocyte (LMR)	2.37	6.7	6.7	4.9	2.7	1.57	2.7	0.36-6.75	0.88-8.44	0.5647	0.0391
Systemic Inflammation Index (SII)	840.75	6.6	6.8	3.1	4.0	0.59	0.52	0.14-2.47	0.16-1.70	0,4348	0.2082

Table 13: Summarizes the blood count-based biomarkers in advanced head and neck cancer patients treated with ICIs. OS; overall survival PFS; progression-free survival ICI'S; Immune checkpoint inhibitors. Results are from the univariable cox proportional Hazard model. Significant p-Values are represented in bold.

SURVIVAL RATE		OS (Median) (Months)		PFS (Median) (Months)		OS	PFS	OS	PFS	OS	PFS
BLOOD COUNT BIOMARKERS	CUT OFF VALUES	High	Low	High	Low	HR		95% CI		p-VALUE	
Absolute Neutophil Count (ANC)	5.15 X103/µL	NR	12.2	6.8	6.6	0.71	1.71	0.07-7.14	0.34-8.54	0.7822	0.4233
Absolute Monocyte Count (AMC)	0.39 X103/µL	NR	11.9	8.0	6.6	2	3.28	0.20-19.23	0.64-16.81	0.5637	0.0675
Absolute Lymphocyte Count (ALC)	1.34 X103/µL	NR	11.9	6.6	6.7	2.5	0.44	0.25-24.38	0.08-2.2	0.4328	0.5014
Neutophil:WBC (NWR)	0.68	NR	14.1	6.8	6.6	0.5	1.71	0.05-4.80	0.34-8.54	0.5637	0.4233
Neutrophil:Lymphocyte (NLR)	3.28	NR	NR	2.5	6.7	0.35	0.72	0.03-3.54	0.16-3.18	0.3657	0.6678
Derived Neutrophil:Lymphocyte (dNLR)	2.22	8.4	NR	4.7	6.7	0.24	1.14	0.02-2.71	0.25-5.04	0.2072	0.8596
Platelet:Lymphocyte (PLR)	213.9	NR	NR	6.7	6.6	0.7	1.37	0.07-6.94	0.29-6.49	0.763	0.6517
Lymphocyte:Monocyte (LMR)	2.88	11.9	NR	9.2	6.7	0.62	0.58	0.62-6.09	0.13-2.59	0.6949	0.5826
Systemic Inflammation Index (SII)	1115.7	NR	NR	6.7	6.6	0.7	1.37	0.07-6.94	029-6.49	0.763	0.6517

Table 14: Summarizes the blood count-based biomarkers in advanced renal cell carcinoma patients treated with ICIs. OS; overall survival PFS; progression-free survival ICI'S; Immune checkpoint inhibitors. Results are from the univariable cox proportional Hazard model. Significant p-Values are represented in bold.

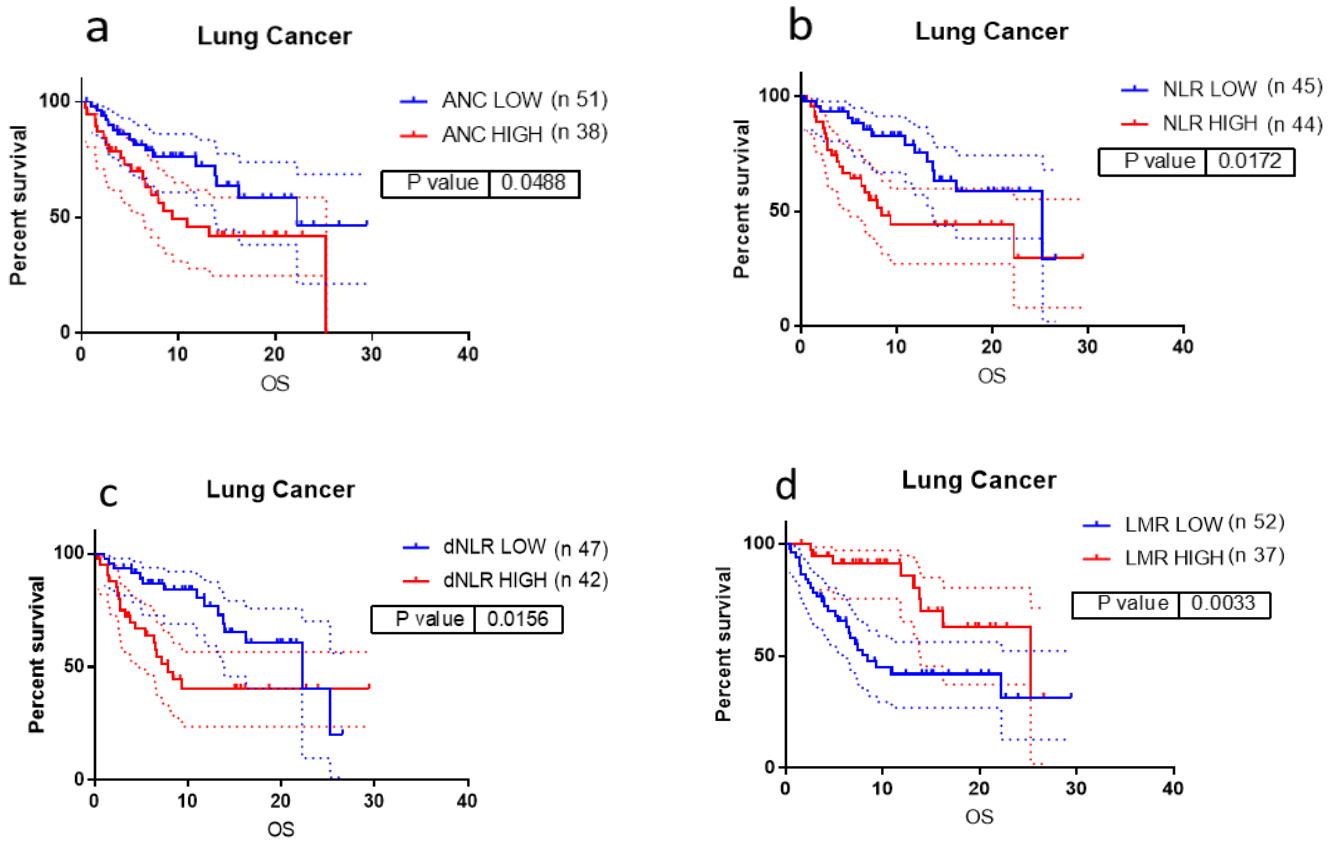

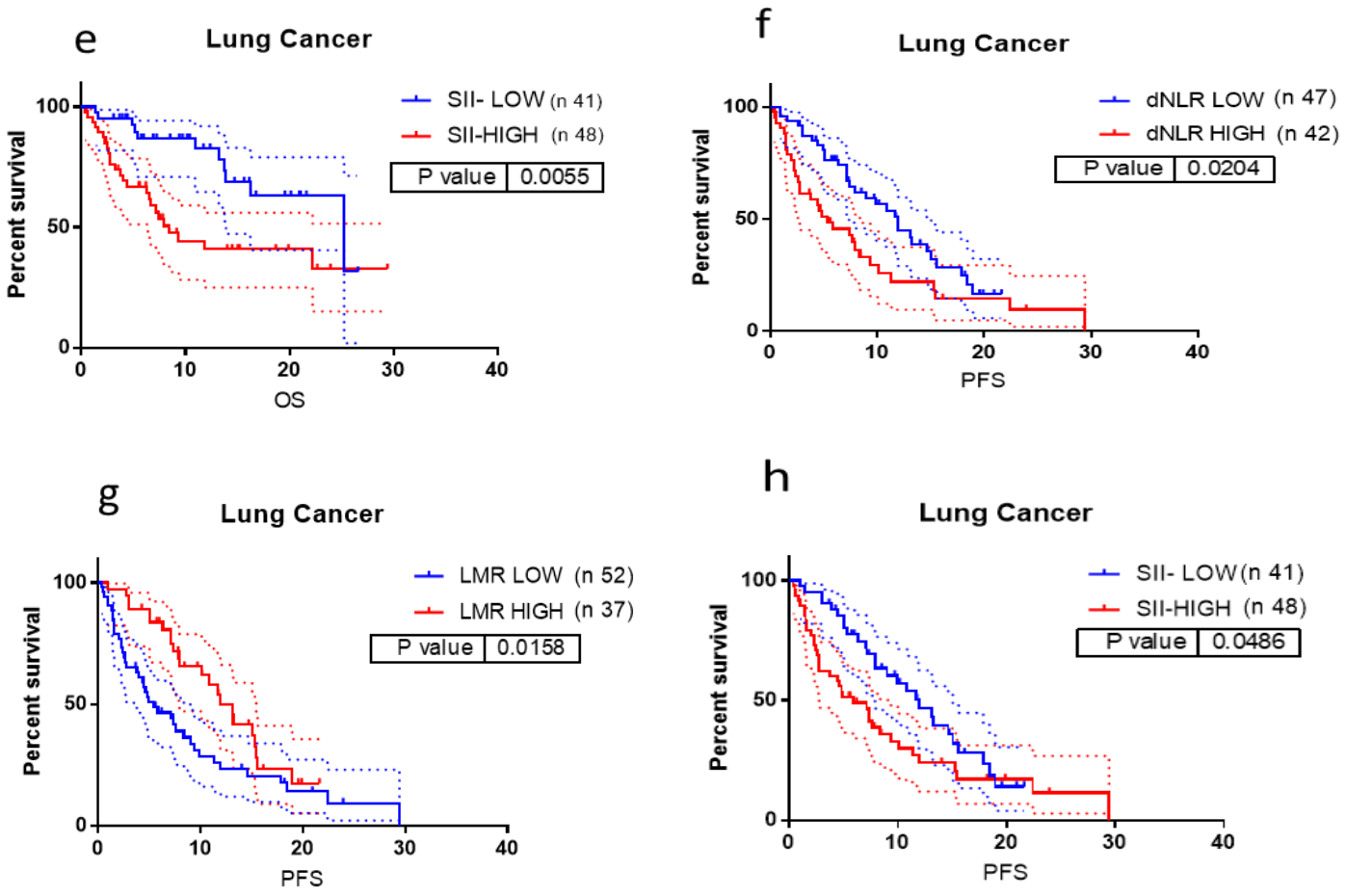

Figure 14: Kaplan-Meier Survival Curves with 95% CI for Overall survival (OS; a,b,c,d,e) Progression-Free Survival (PFS; f,g,h) of advanced lung cancer Patients treated With ICIs. Time is represented in months at baseline. (a) OS; ANC > 5.15 X103/µL (red line) v/s ANC < 5.15 X103/µL(blue line) , (b) OS; NLR > 4.38 (red line) v/s NLR < 4.38 (blue line), (c) OS; dNLR > 2.58 (red line) v/s dNLR < 2.58 (blue line) (d) OS; LMR > 2.88 (red line) v/s LMR < 2.88 (blue line) (e) OS; SII > 1115.7 (red line) v/s SII< 1115.7 (blue line) (f) PFS; dNLR > 2.58 (red line) v/s dNLR < 2.58 (blue line) (g) PFS; LMR > 2.88 (red line) v/s LMR < 2.88 (blue line) (h) PFS; SII > 1115.7 (red line) v/s SII< 1115.7 (blue line) . The dotted lines represent the upper and lower limit of 95% CI (Confidence Interval). Results are from the univariable cox proportional Hazard model. (NWR; Neutrophil to white blood cell ratio, NLR; Neutrophil to lymphocyte ratio, dNLR; Derived Neutrophil to lymphocyte ratio, LMR; Lymphocyte to monocyte ratio, SII, Systemic Inflammatory Index, OS; overall survival PFS; progression-free survival).

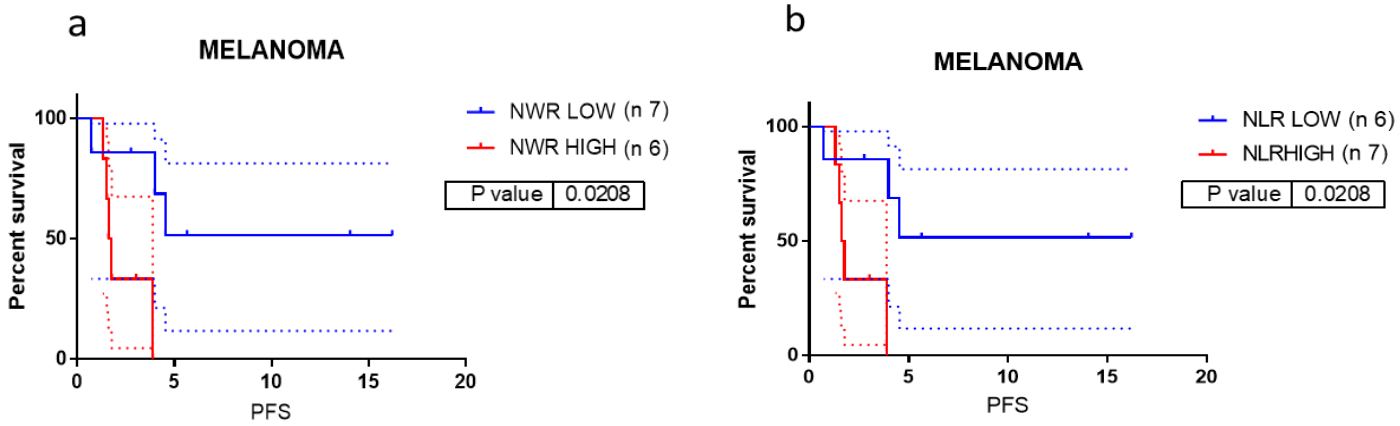

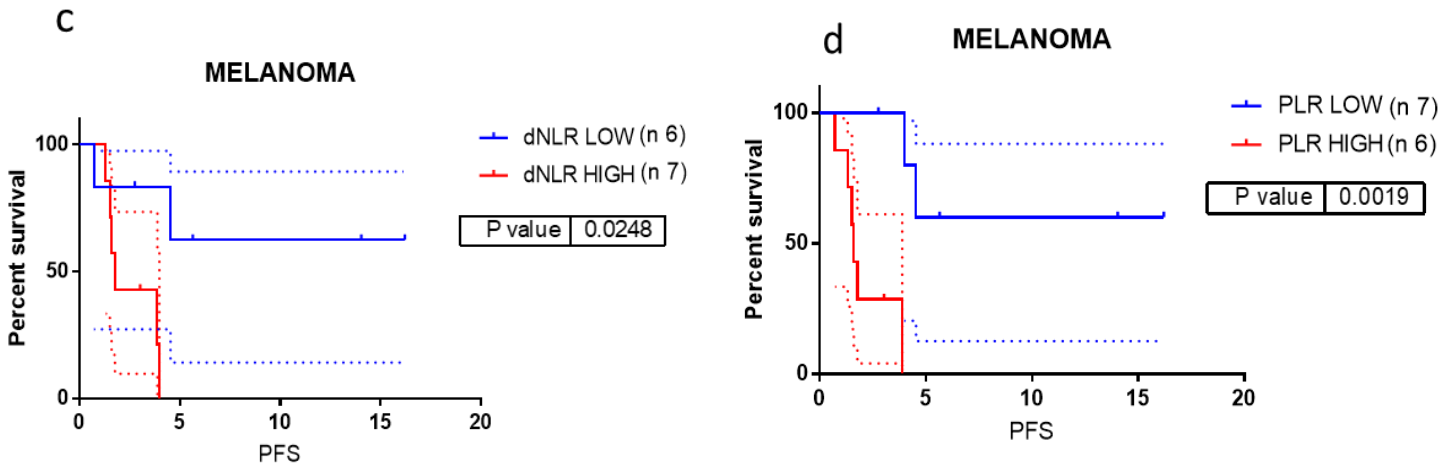

Figure 15: Kaplan-Meier Survival Curves with 95% CI for Progression-Free Survival (PFS; a,b,c,d) of melanoma Patients treated With ICIs. Time is represented in months at baseline. (a) PFS; NWR > 0.68 (red line) v/s NWR < 0.68 (blue line), (b) PFS; NLR > 3.3 (red line) v/s NLR < 3.3 (blue line), (c) PFS; dNLR > 2.2 (red line) v/s dNLR < 2.2 (blue line) (d) PFS; PLR > 178.2 (red line) v/s PLR < 178.2 (blue line) . The dotted lines represent upper and lower limits of 95% CI (Confidence Interval). Results are from the univariable cox proportional Hazard model. (NWR; Neutrophil to white blood cell ratio, NLR; Neutrophil to lymphocyte ratio, dNLR; Derived Neutrophil to lymphocyte ratio, PLR; Platelet to lymphocyte ratio, OS; overall survival PFS; progression-free survival)**.**

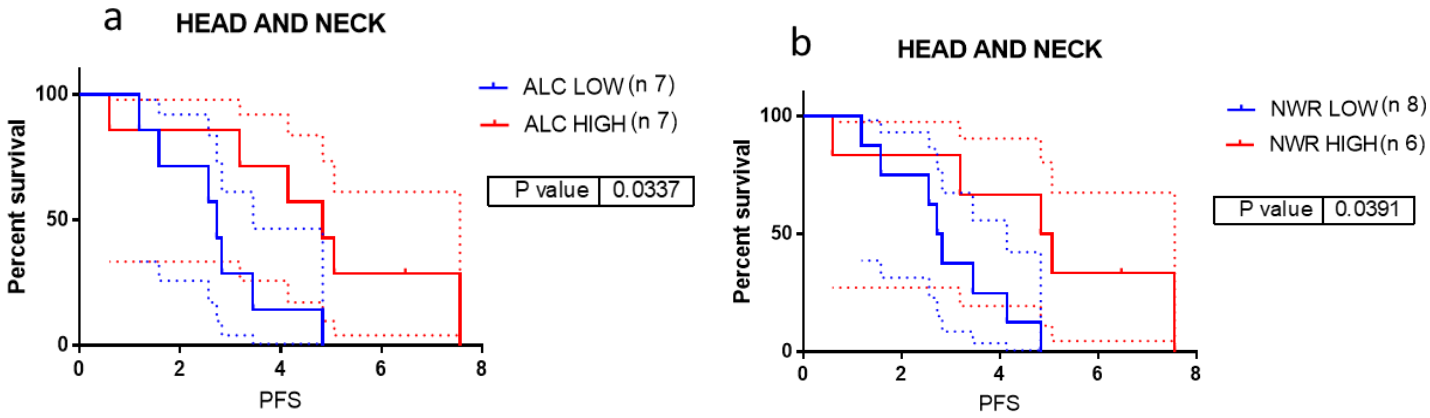

Figure 16: Kaplan-Meier Survival Curves with 95% CI for Progression-Free Survival (PFS; a,b) of advanced head and neck Patients treated With ICI's. Time is represented in months at baseline. (a) PFS; ALC > $1.47X10^3$/µL (red line) v/s ALC < $1.47X10^3$/µL (blue line) and (b) PFS; NWR > 0.66 (red line) v/s NWR < 0.66 (blue line). The dotted lines represent the upper and lower limit of 95% CI (Confidence Interval). Results are from the univariable cox proportional Hazard model. (ALC; absolute lymphocyte count NWR; Neutrophil to white blood cell ratio, PFS; progression-free survival).

3.3. Identification of MDSCs in Peripheral Blood of advanced cancer patients.

A panel of seven markers and nine parameters were used to phenotype the population of MDSCs using flow cytometry which was sub-categorized as Mo-MDSCs, e-MDSCs, PMN-MDSCs a novel marker LOX-1 was used to define LOX 1+ PMN-MDSCs, PBMC were stained for CD45, HLA-DR, CD15, CD16, CD14, CD33, and LOX-1. The initial gating was done for the physical parameters of PBMC SSC-A and FSC-A, further doublets were excluded using FSC-A and FSC-H. We then selected CD45+ cells using SSC-A on the X-axis on a dot plot to gate lymphomonocytes, HLA-DR-positive cells were excluded using a tight gate on the HLA-DR-negative population on an HLA-DR vs CD33 dot plot, which consistently placed the HLA-DR positive/negative threshold, leading to a slightly more stringent definition of MDSC's. Finally, total MDSCs were identified by expression of $CD33^{+}$ and $HLA\text{-}DR^{-}$, while polymorphonuclear (PMN-MDSC) and monocytic (Mo-MDSC) subpopulations were determined by CD15 and CD14 expression, respectively. Cells that did not express either CD14 or CD15 were considered and are referred to as early stage-MDSC (e-MDSC). **(Figure 16)**.

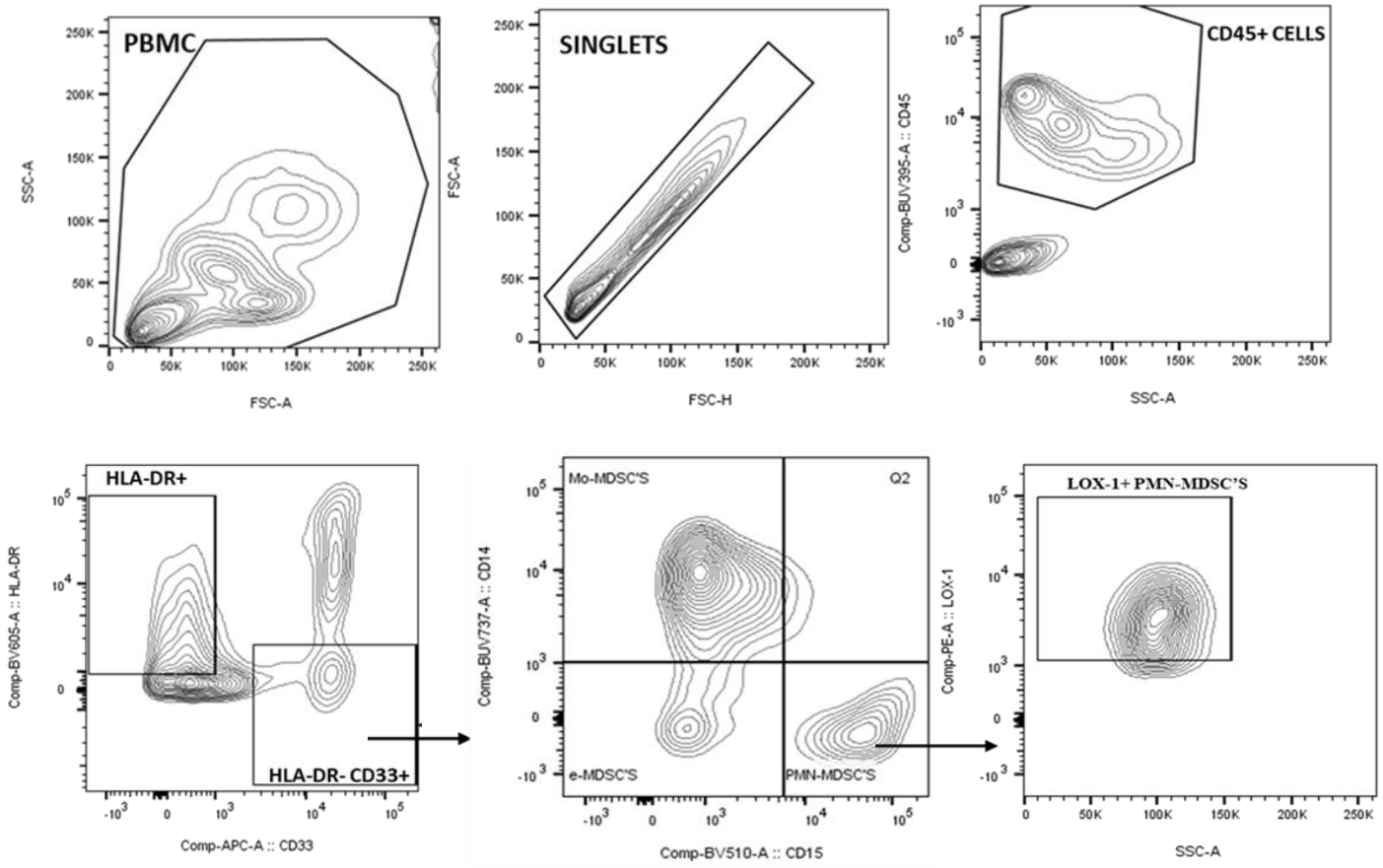

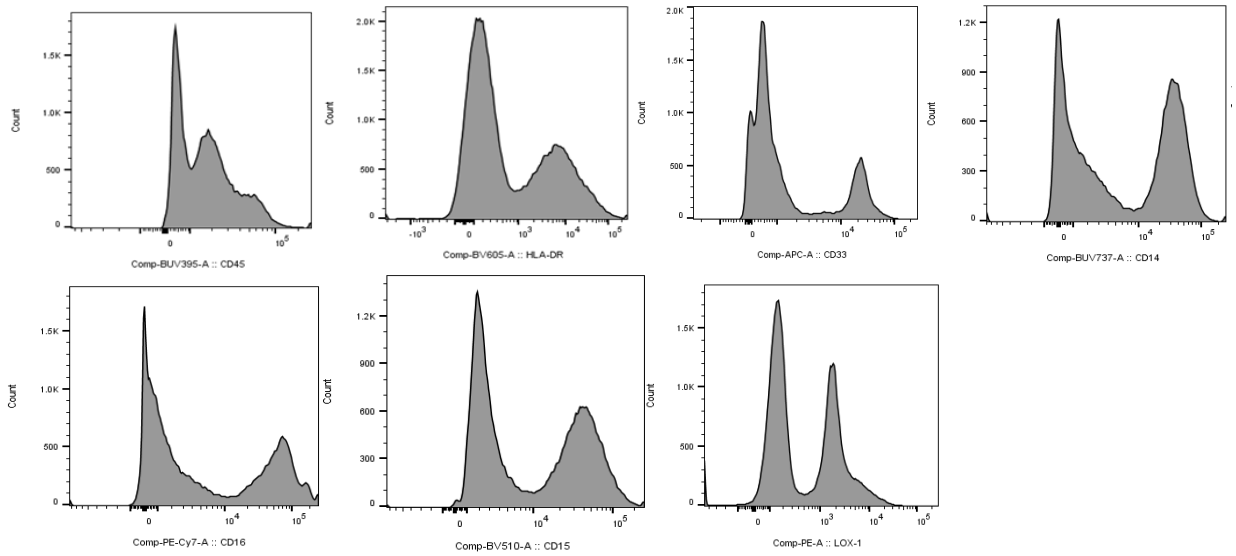

Figure 17: Gating strategy for identification of MDSCs in peripheral blood mononuclear cells of advanced cancer patients treated with ICI'S. Contour plots - (PBMC; Peripheral Blood Mononuclear Cells, HLA-DR; Human Leucocyte Antigen, MDSC; Myeloid-Derived Suppressor Cells, Mo-MDSC; Monocytic-Myeloid Derived Suppressor Cells, PMN-MDSC; Polymorphonuclear-Myeloid Derived Suppressor Cells, e-MDSC; Early Stage Myeloid-Derived Suppressor Cells SSC-A; Side Scatter Area, FSC-A; Forward Scatter Area, FSC-H; Forward Scatter- Height)

3.4. MDSCs: levels in Peripheral blood of advanced cancer patients:

We analyzed the proportion of Mo-MDSCs, e-MDSCs, and PMN-MDSCs in the PBMCs of advanced cancer patients using the mentioned gating strategy.

Flow cytometry data were analyzed using FlowJo v10.8.1 software. t-SNE was run using default FlowJo parameters (iterations = 1000, perplexity = 30). A range of 10000 to 60000 $CD45^+$ live cells was acquired. In each figure, all samples were derived from the same t-SNE run. Individual flow cytometry standard files from each t-SNE run were combined into a single flow cytometry standard file to assist in defining spatially distinct populations using the concatenation tool. t-SNE heat maps show the fluorescent intensity of each marker for each event. Scales on the heat maps are individually generated for each surface marker from low to high expression.

In advanced lung cancer patients and head and neck cancer patients presence of all three subsets of MDSCs was identified and analyzed for 56 and 11 patient samples respectively, Mo-MDSCs were the most prevalent among all the three subsets, followed by e-MDSCs PMN-MDSCs and LOX-1^+PMN-MDSCs were least abundant population among all the MDSCs. **(Figure 18), (Figure 20).** In 7 patient samples with melanoma, the trend was similar

except there was no statistically significant difference between the frequency of Mo-MDSCs and e-MDSCs population. **(Figure 19)**. Whereas in 9 samples of patients with renal carcinoma e-MDSCs were most prevalent followed by Mo-MDSCs and PMN-MDSCs **(Figure 21)**.

FIGURES 18-21

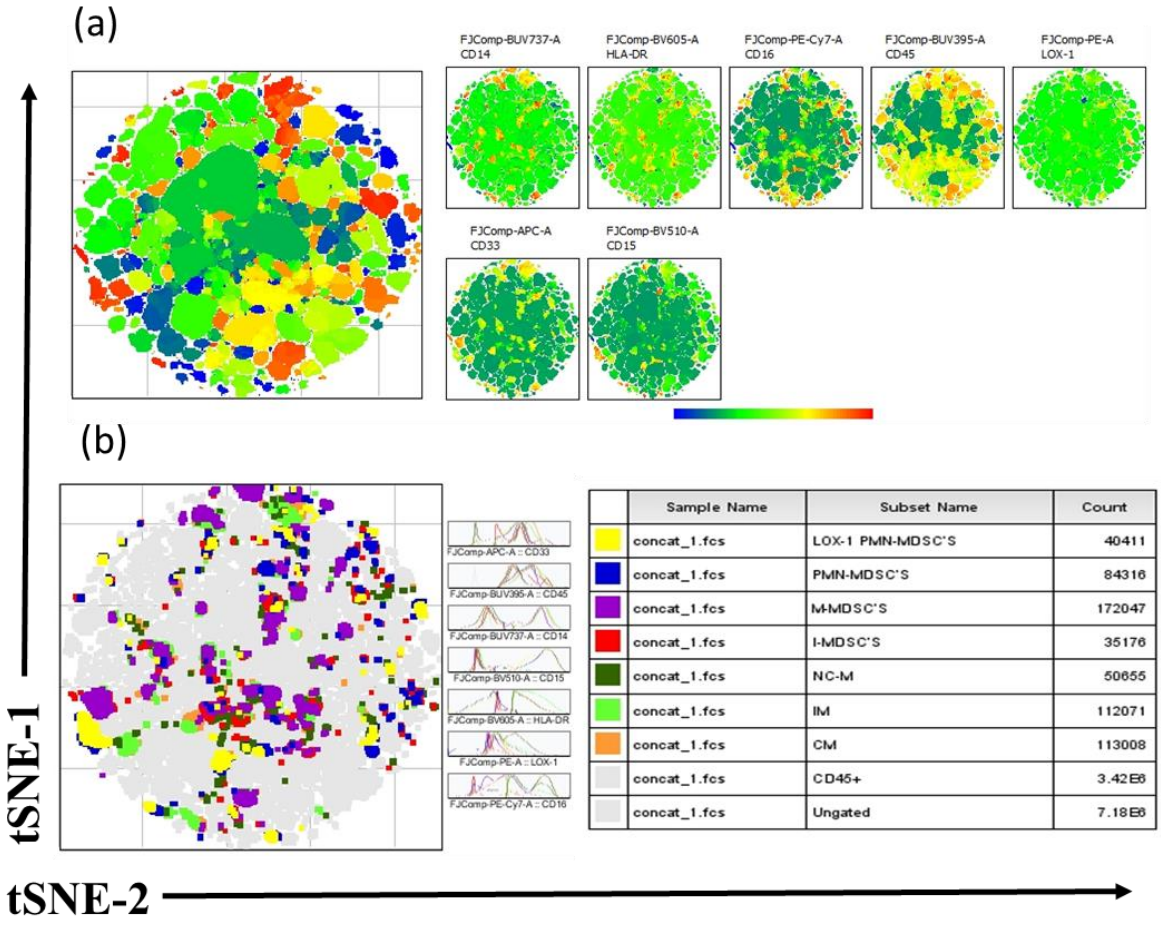

Figure 18 (a,b): Identification of MDSCs and their subsets in peripheral blood mononuclear cells of advanced lung cancer patients. (a) tSNE plot of concatenated 56 whole PBMC samples stained for seven markers (represented with heat map) for identification of MDSCs, (b) tSNE plot, Clusters of monocyte subsets and MDSCs; Purple large dots represents Mo-MDSCs, Red large dots represents e-MDSCs, Blue large dots represents PMN-MDSCs and yellow large dots represents LOX-1^{+} PMN-MDSCs .

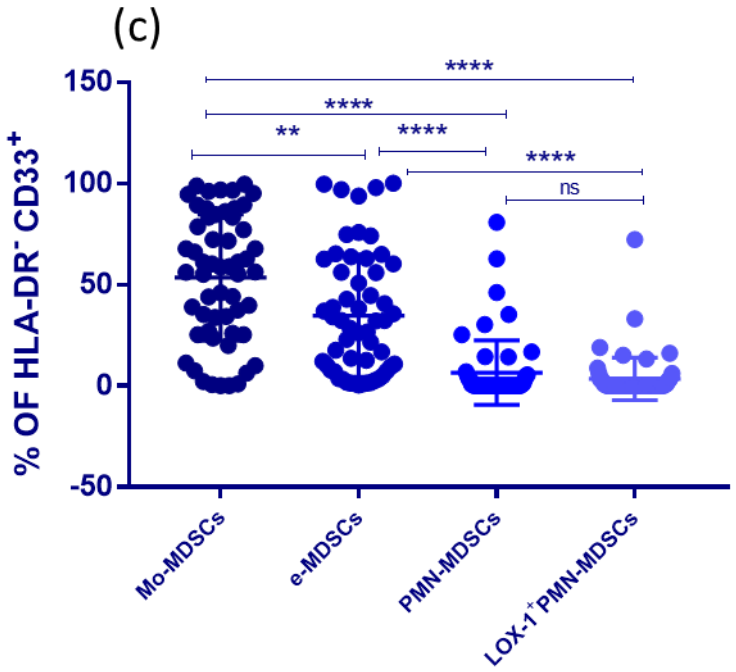

	Mo-MDSCs	e-MDSCs	PMN-MDSCs	LOX-1+PMN-MDSCs
Mean	53.44	34.63	6.452	3.36
Std. Deviation	31.22	30.26	15.9	10.5
Std. Error of Mean	4.172	4.043	2.124	1.323

Figure 18 (c): Scatter plot representing percentage of MDSCs subset among HLA-DR^{-} and CD33^{+} population with corresponding column statistics. P-values are represented as (ns:P > 0.05 , * : P ≤ 0.05, ** : P ≤ 0.01 *** : P ≤ 0.001 ; **** : P ≤ 0.0001) .

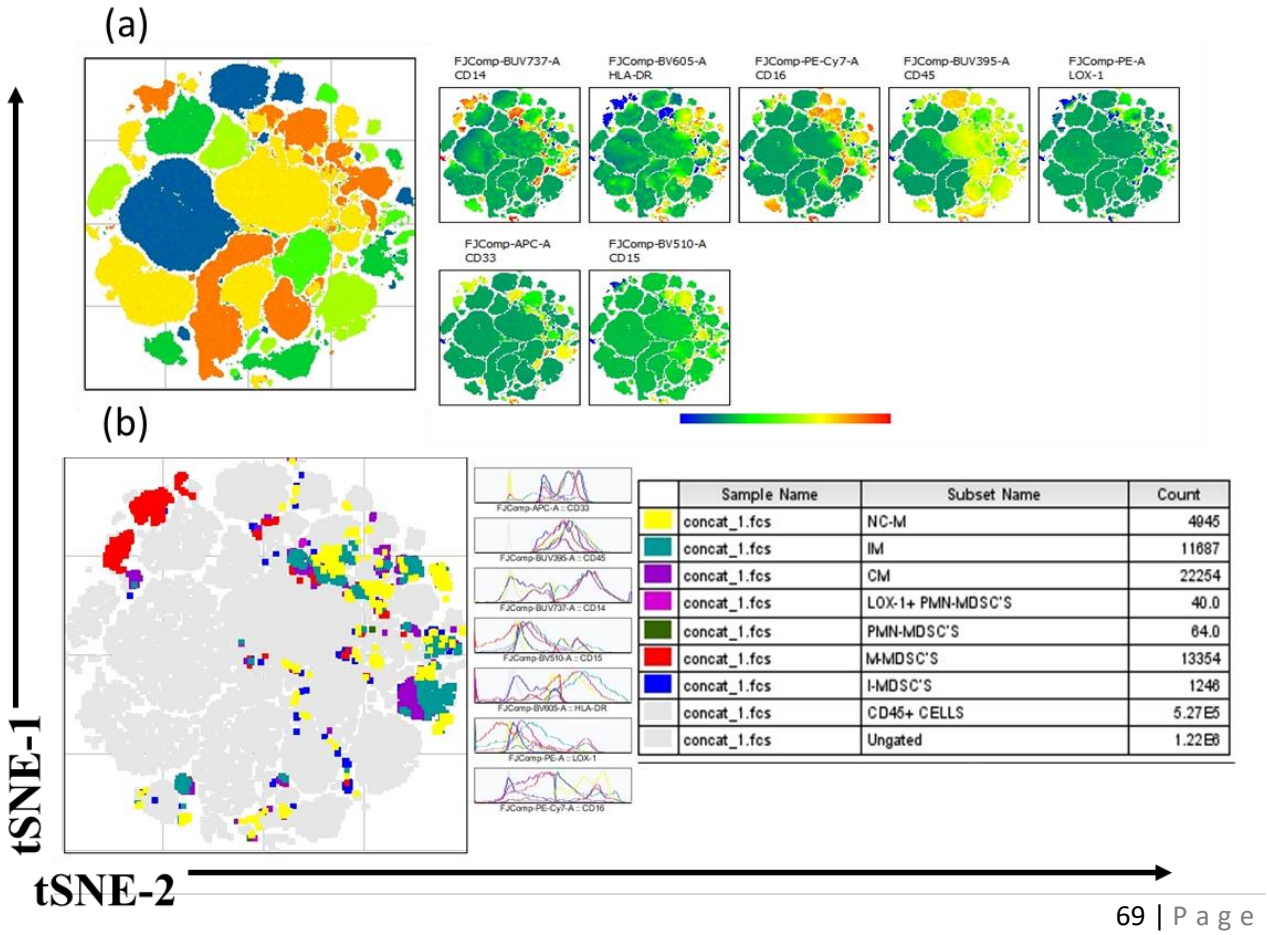

	Sample Name	Subset Name	Count
	concat_1.fcs	NC-M	4945
	concat_1.fcs	IM	11687
	concat_1.fcs	CM	22254
	concat_1.fcs	LOX-1+ PMN-MDSC'S	40.0
	concat_1.fcs	PMN-MDSC'S	64.0
	concat_1.fcs	M-MDSC'S	13354
	concat_1.fcs	I-MDSC'S	1246
	concat_1.fcs	CD45+ CELLS	5.27E5
	concat_1.fcs	Ungated	1.22E6

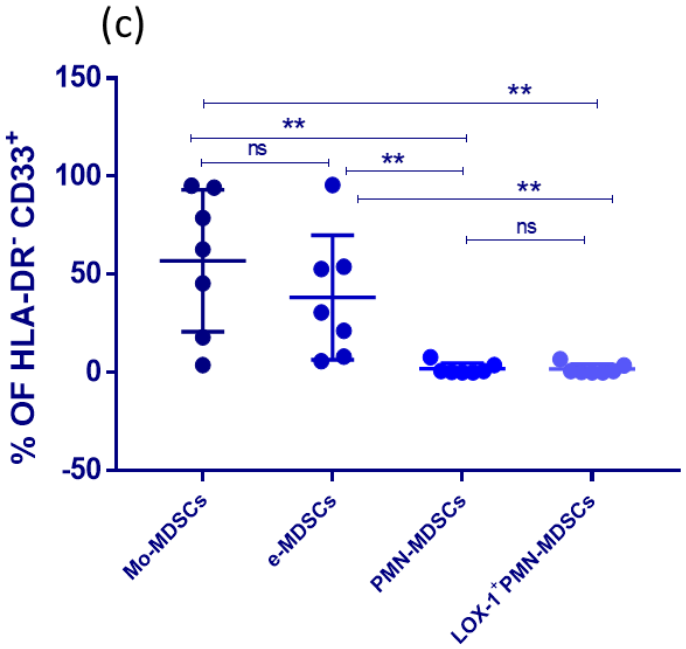

	Mo-MDSCs	e-MDSCs	PMN-MDSCs	LOX-1^{+}PMN-MDSCs
Mean	56.88	38.22	1.91	1.739
Std. Deviation	36.19	31.76	2.892	2.531
Std. Error of Mean	13.68	12	1.093	0.9566

Figure 19: Identification of MDSCs and their subsets in peripheral blood mononuclear cells of melanoma patients. (a) tSNE plot of concatenated 7 whole PBMC samples stained for seven markers (represented with heat map) for identification of MDSCs , (b) tSNE plot , Clusters of monocyte subsets and MDSCs ; RED large dots represents Mo-MDSC'S, Blue large dots represents e- MDSCs, Dark green large dots represents PMN- MDSCs and Pink large dots represents LOX-1^{+} PMN- MDSCs . (C) Scatter plot representing percentage of MDSCs subset among HLA-DR^{-} and CD33^{+} population With corresponding column statistics. P-values are represented as (ns:$P > 0.05$, * : $P \leq 0.05$, ** : $P \leq 0.01$ *** : $P \leq 0.001$; **** : $P \leq 0.0001$.

(a)

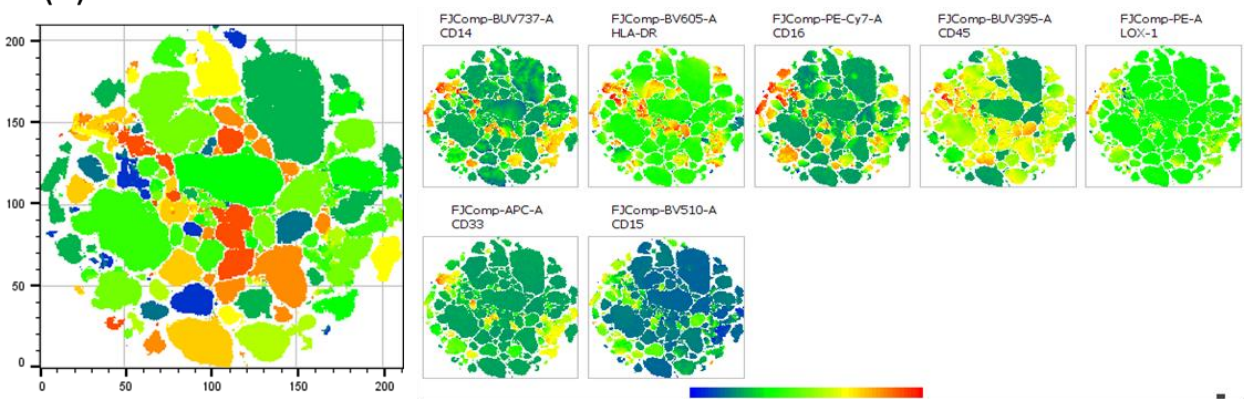

(b)

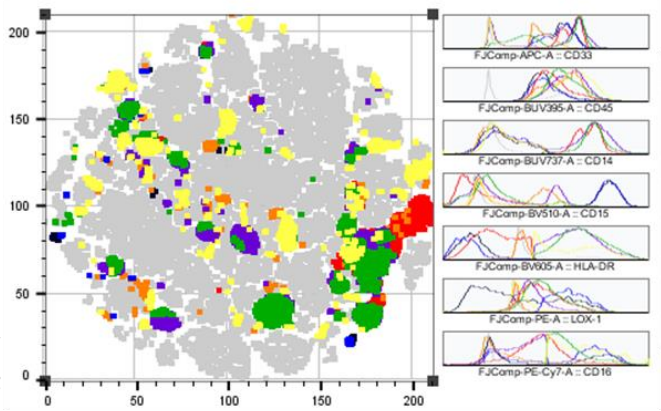

	Sample Name	Subset Name	Count
	concat_1.fcs	Non-classical-monocytes	19777
	concat_1.fcs	Intermediate-monocytes	56490
	concat_1.fcs	classical monocytes	58428
	concat_1.fcs	LOX-1-PMN-MDSC'S	610
	concat_1.fcs	I-MDSC'S	2448
	concat_1.fcs	Mo-MDSC'S	18583
	concat_1.fcs	PMN-MDSC'S	1986
	concat_1.fcs	Ungated	1.68E6

tSNE-1

tSNE-2

(c)

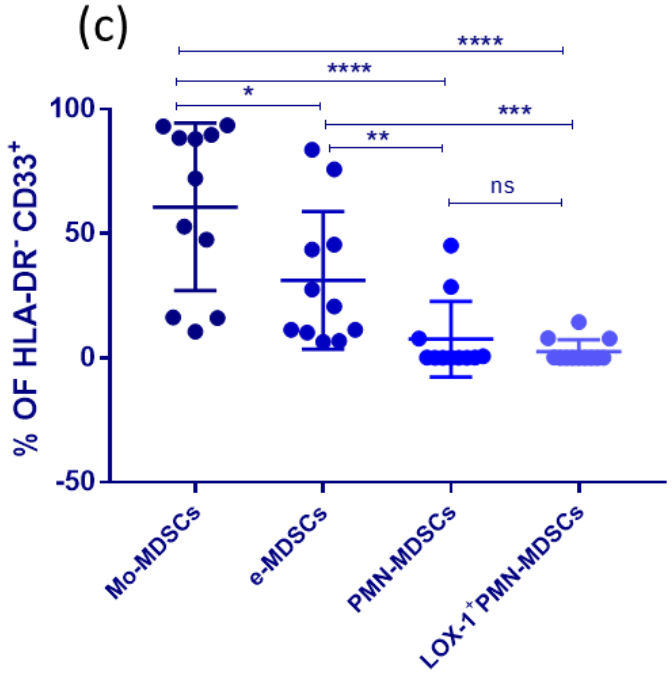

	Mo-MDSCs	e-MDSCs	PMN-MDSCs	LOX-1+PMN-MDSCs
Mean	60.75	31.18	7.501	2.536
Std. Deviation	33.68	27.69	15.18	4.825
Std. Error of Mean	10.15	8.349	4.576	1.393

Figure 20: Identification of MDSCs and their subsets in peripheral blood mononuclear cells of advanced head and neck cancer patients. (a) tSNE plot of concatenated 11 whole PBMC samples stained for seven markers (represented with heat map) for identification of MDSCs , (b) tSNE plot , Clusters of monocyte subsets and MDSCs ; RED large dots represents Mo- MDSCs, Orange large dots represents e- MDSCs, Black large dots represents PMN- MDSCs and Bluelarge dots represents LOX-1^{+} PMN- MDSCs . (C) Scatter plot representing percentage of MDSCs subset among HLA-DR^{-} and CD33^{+} population With corresponding column statistics. P-values are represented as (ns:P > 0.05 , * : P ≤ 0.05, ** : P ≤ 0.01 *** : P ≤ 0.001 ; **** : P ≤ 0.0001 .

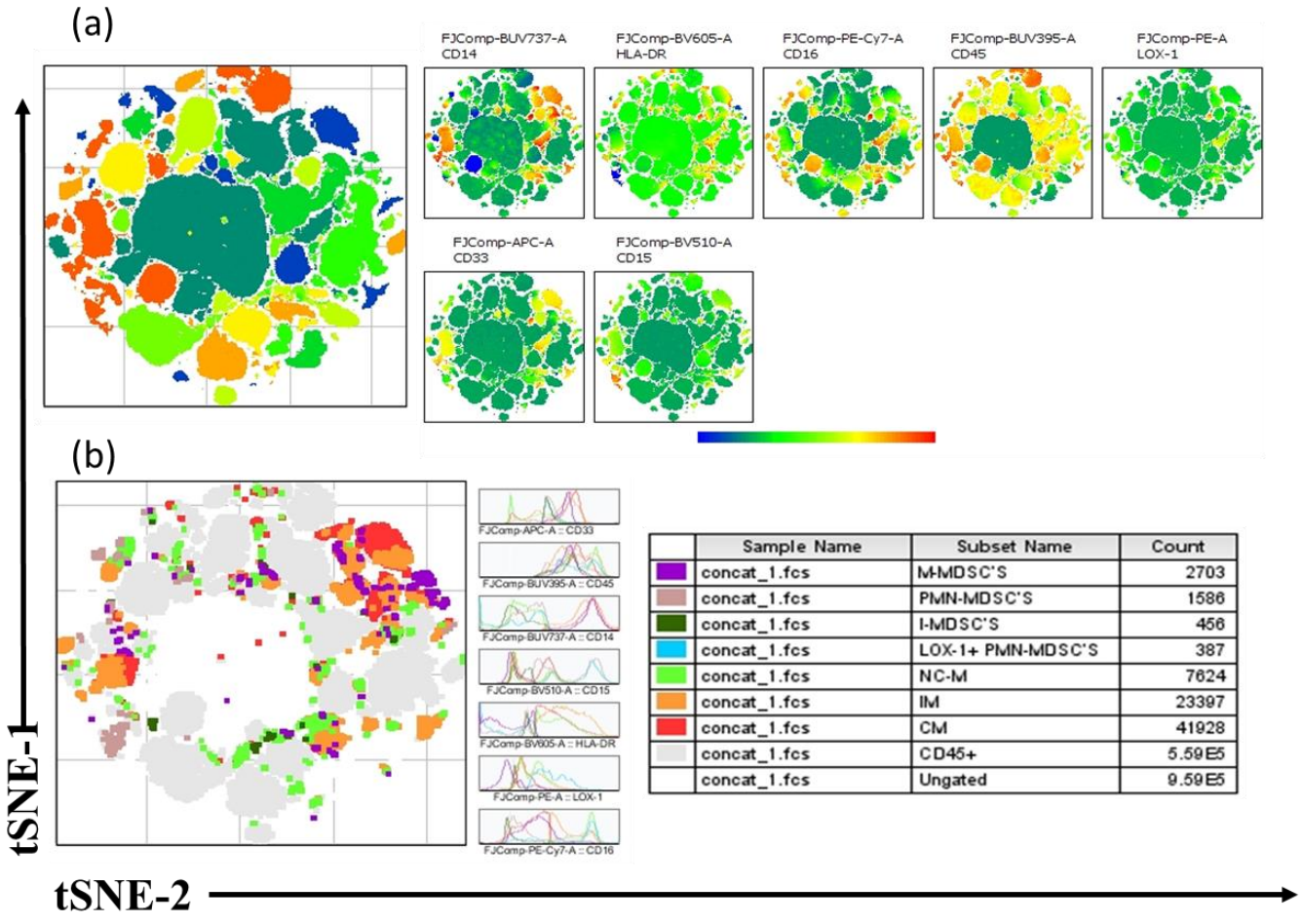

	Sample Name	Subset Name	Count
	concat_1.fcs	M-MDSC'S	2703
	concat_1.fcs	PMN-MDSC'S	1586
	concat_1.fcs	I-MDSC'S	456
	concat_1.fcs	LOX-1+ PMN-MDSC'S	387
	concat_1.fcs	NC-M	7624
	concat_1.fcs	IM	23397
	concat_1.fcs	CM	41928
	concat_1.fcs	CD45+	5.59E5
	concat_1.fcs	Ungated	9.59E5

Figure 21 (a,b) : Identification of MDSCs and their subsets in peripheral blood mononuclear cells of advanced renal cell carcinoma patients. (a) tSNE plot of concatenated 9 whole PBMC samples stained for seven markers (represented with heat map) for identification of MDSCs, (b) tSNE plot, Clusters of monocyte subsets and MDSCs ; Purple large dots represents Mo- MDSCs, Dark green large dots represents e- MDSCs, Lavender large dots represents PMN- MDSCs and Light Blue large dots represents LOX-1^{+} PMN-MDSCs.

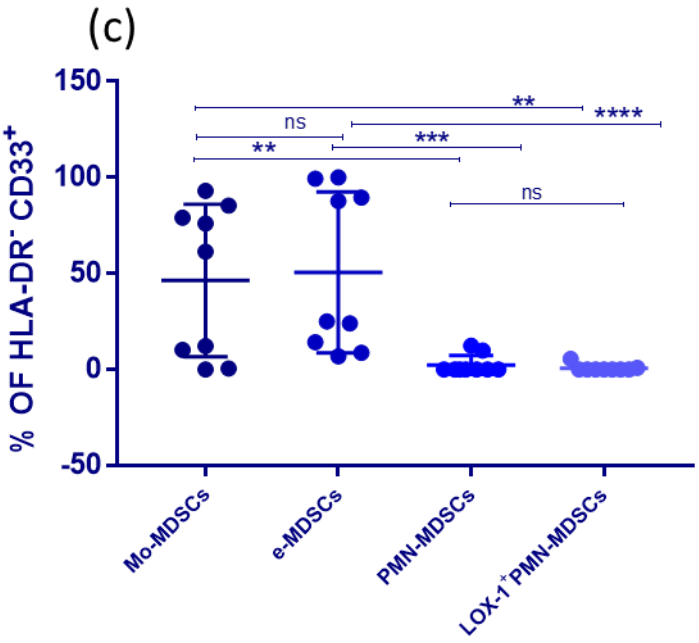

	Mo-MDSCs	e-MDSCs	PMN-MDSCs	LOX-1$^+$PMN-MDSCs
Mean	46.44	50.63	2.482	0.7091
Std. Deviation	39.67	41.92	4.964	1.829
Std. Error of Mean	13.22	13.97	1.655	0.6095

Figure 21 (C): Scatter plot representing percentage of MDSCs subset among HLA-DR$^-$ and CD33$^+$ population with corresponding column statistics. P-values are represented as (ns:P > 0.05, *: P ≤ 0.05, **: P ≤ 0.01 ***: P ≤ 0.001; ****: P ≤ 0.0001.

3.5. Levels MDSCs are associated with therapy outcomes in advanced cancer patients treated with ICIs.

The patients were divided into low and high-frequency groups for each MDSCs subtype, for all the cancer types in the study. Univariable Cox proportional hazard analysis was performed, and Kaplan Meier survival curves were generated, the cut-off value was decided on the median percentage values of each MDSCs subset among total MDSCs. In advanced lung cancer patients, the frequency of Mo-MDSCs higher than 56.2% within total MDSCs was associated with poor PFS (HR = 0.477, 95% CI: 0.24-0.93, p = 0.0214) **(Figure 22a)**. In head and neck cancer patients, the frequency of Mo-MDSCs higher than 72.2% within total MDSCs was associated with poor OS (HR = 0.25, 95% CI: 0.01-3.18, p = 0.0422) **(Figure 22b)**. The PMN-MDSCs and e-MDSCs did not show any statistically significant effect on the outcome of therapy in terms of both OS and PFS, also no statistical significance on therapy outcome was established for patients with melanoma and renal cell carcinoma.

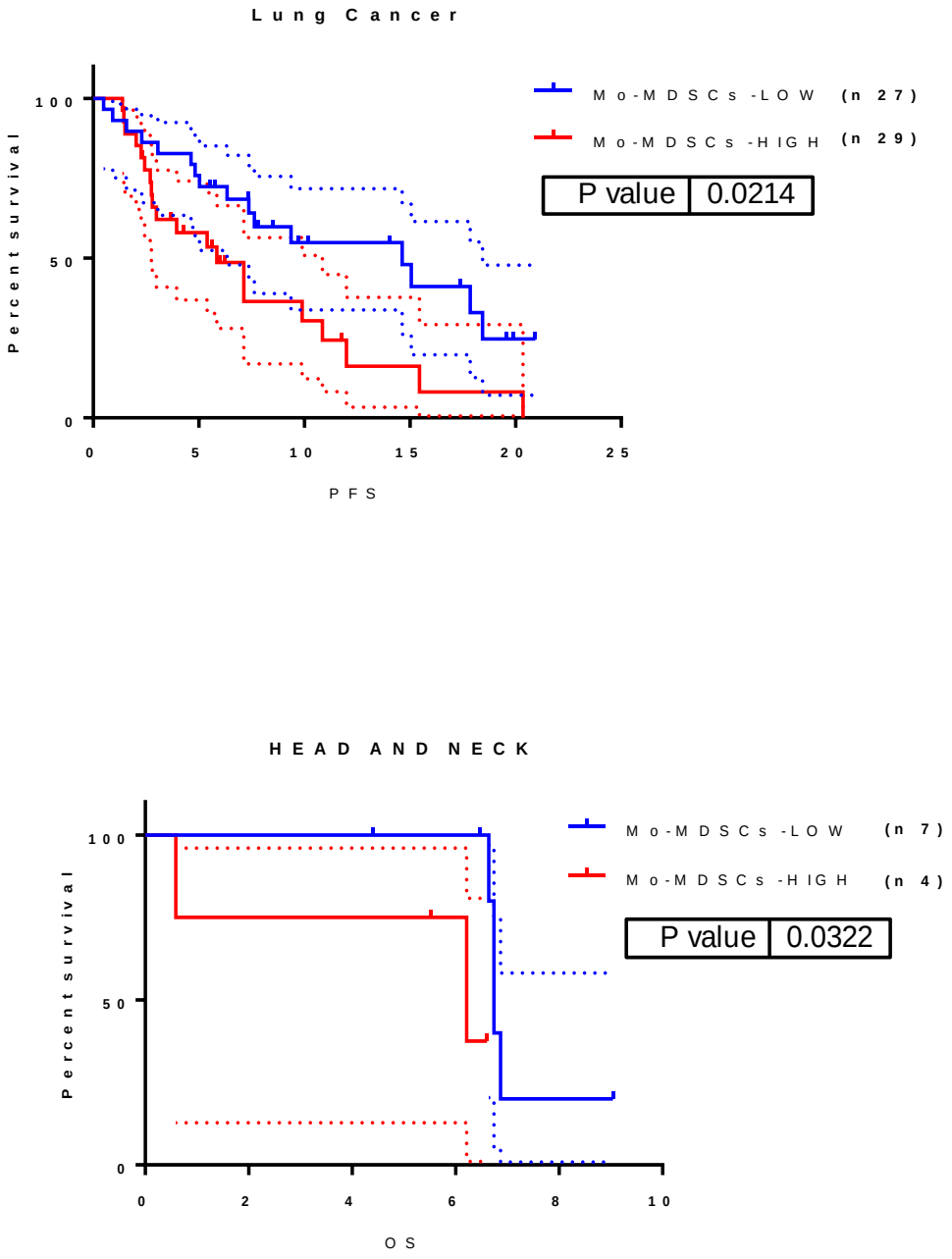

Figure 22: Kaplan-Meier Survival Curves with 95% CI for Overall survival (OS; a) Progression-Free Survival (PFS; b) of advanced head and neck cancer and lung cancer Patients respectively treated With ICI's. Time is represented in months at baseline. (a) PFS; Mo- MDSCs high (red line) v/s Mo- MDSCs Low (blue line), (b) OS; Mo- MDSCs high (red line) v/s Mo- MDSCs Low (blue line). Dotted lines represent upper and lower limit of 95% CI (Confidence Interval). Results are from univariable cox proportional Hazard model (OS; overall survival PFS; progression free survival).

3.6. Identification of monocyte subsets in human blood

To properly identify monocyte subpopulations in blood, we employed a negative exclusion gating strategy, firstly the physical parameters were plotted on a dot plot using SSC-A and FSC-A, and the doublets were excluded using FSC-A and FSC-H dot plots then the lympho-monocyte population of cells was gated as $CD45^+$ population among this population a negative selection was gated for monocytes which excluded $CD3^+$, $CD56^+$ and $CD19^+$ T-cells, NK-cells and B-cells respectively. The left-over population was concluded as true or lineage-negative monocytes. The resulting final population was discriminated on CD14 and CD16 surface expression to give three distinct monocyte subsets. **(Figure 22)**. As Classical monocytes (CD14+ CD16−), Non-classical monocyte (CD14-CD16+) and Intermediate monocytes (CD14+CD16+).

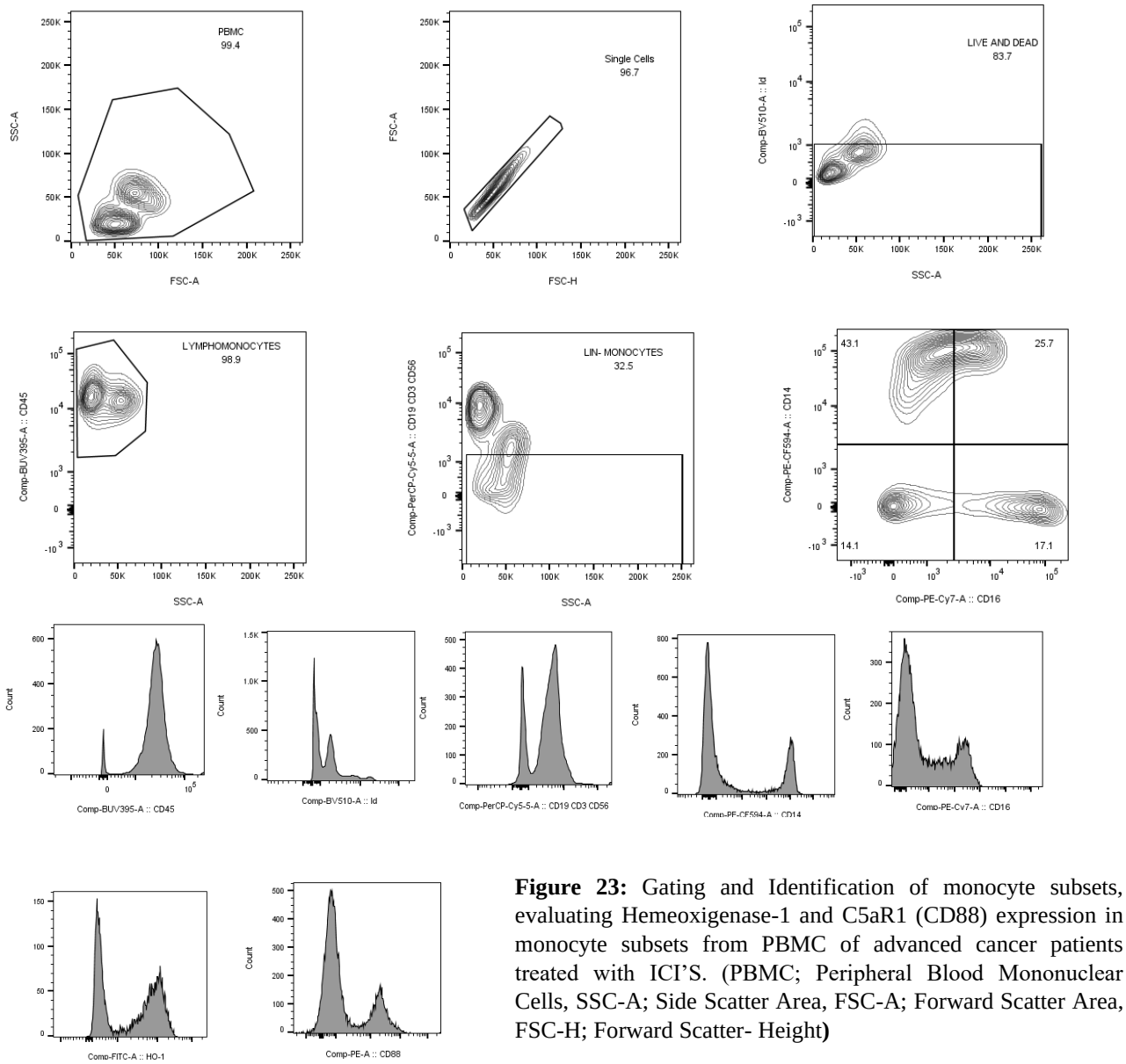

Figure 23: Gating and Identification of monocyte subsets, evaluating Hemeoxigenase-1 and C5aR1 (CD88) expression in monocyte subsets from PBMC of advanced cancer patients treated with ICI'S. (PBMC; Peripheral Blood Mononuclear Cells, SSC-A; Side Scatter Area, FSC-A; Forward Scatter Area, FSC-H; Forward Scatter- Height**)**

3.7. Frequency of monocyte subset in advanced cancer patients peripheral blood treated with ICIs:

In advanced lung cancer patients' peripheral blood, the frequency of classical monocytes was 37.4%, the intermediate monocytes were 26.4%, and the non-classical monocytes were 36%. In head and neck cancer patients' peripheral blood, the frequency of classical monocytes was 37.8%, the intermediate monocytes were 10.9%, and the non-classical monocytes were 52.2%. In melanoma patients' peripheral blood, the frequency of classical monocytes was 28.0%, the intermediate monocytes were 12.7%, and the non-classical monocytes were 59.2%. In renal cell carcinoma patients' peripheral blood, the frequency of classical monocytes was 23.9%, the intermediate monocytes were 12.2%, and the non-classical monocytes were 63.8%. These results suggest that except for advanced lung cancer patients the predominant circulating monocyte subset is non-classical monocytes, however since this data is on a small patient population it requires further validation. **(Figure 24-Figure 27)**.

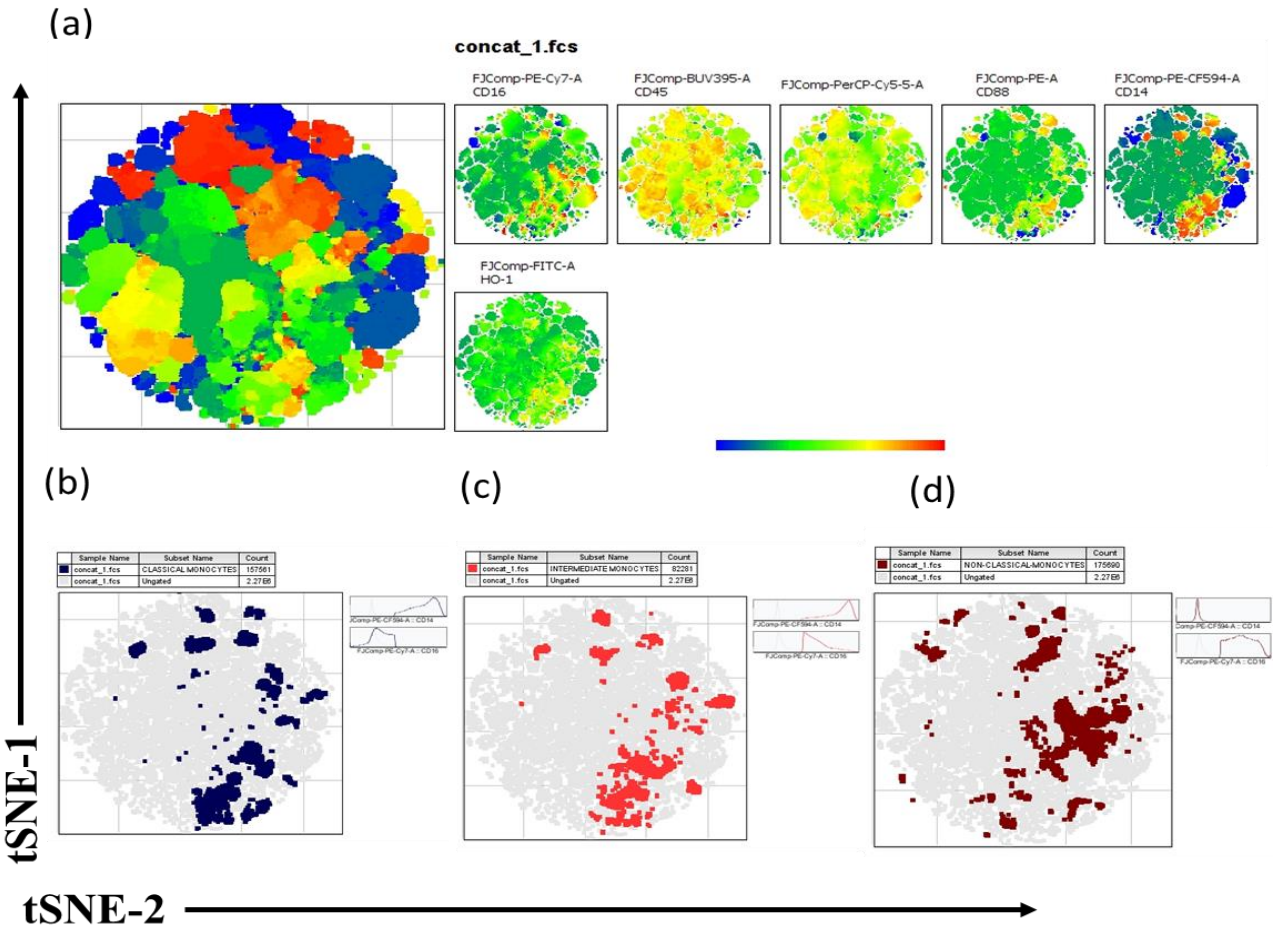

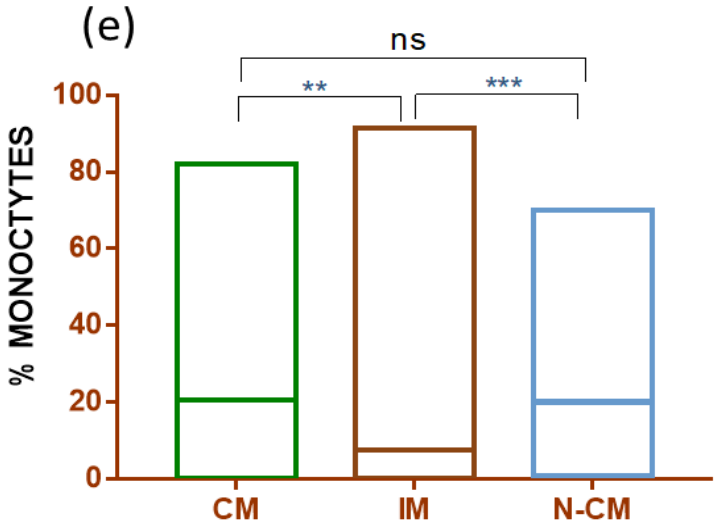

	CM	IM	N-CM
Mean	25.36	17.95	24.44
Std. Deviation	22.25	22.26	20.04
Std. Error of Mean	2.428	2.429	2.186

Figure 24: Identification of circulating monocyte subsets in peripheral blood mononuclear cells of advanced lung cancer patients. (a) tSNE plot of concatenated 84 whole PBMC samples stained for nine markers (represented with heat map) for identification of monocyte subset, (b) tSNE plot, Clusters of monocyte subsets ; Dark Blue large dots represents classical monocyte subset, (c) tSNE plot , Clusters of monocyte subsets ; Red large dots represents intermediate monocyte subset, (d) tSNE plot , Clusters of monocyte subsets ; Red large dots represents non-classical monocyte subset . (e) Box and Whisker plot representing percentage of Monocyte subset among total monocyte population With corresponding column statistics. P-values are represented as (ns:P > 0.05 , * : P ≤ 0.05, ** : P ≤ 0.01 *** : P ≤ 0.001 ; **** : P ≤ 0.0001) (CM; classical Monocytes, N-CM; Non- classical Monocytes IM; Intermediate Monocytes) .

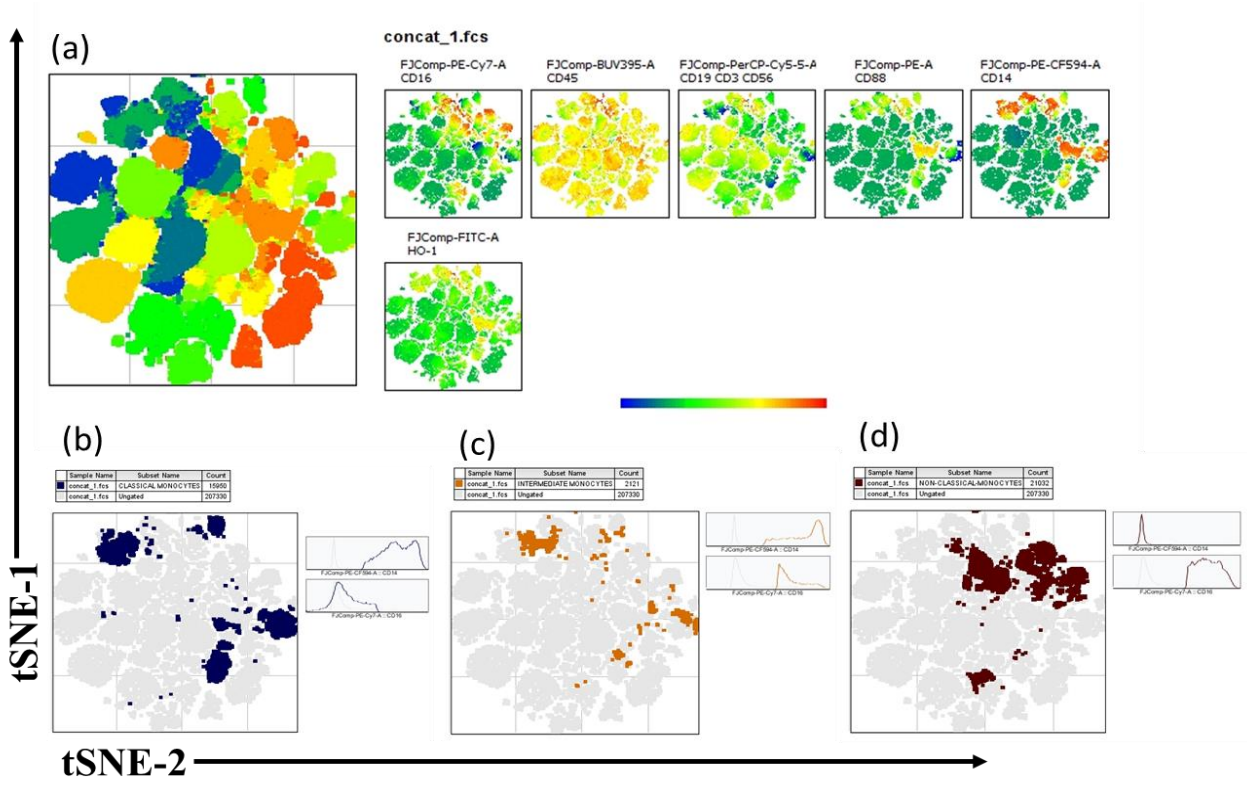

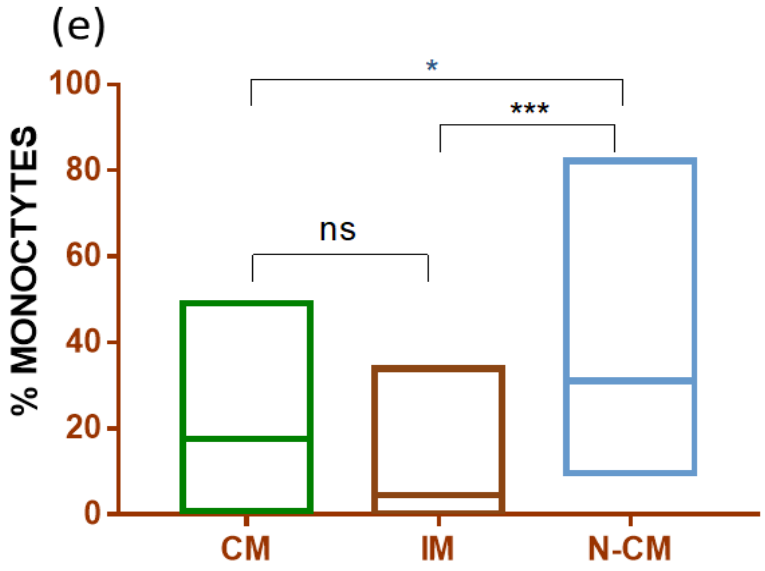

	CM	IM	N-CM
Mean	19.15	8.769	40.42
Std. Deviation	16.58	11.62	24.47
Std. Error of Mean	4.999	3.502	7.379

Figure 25: Identification of circulating monocyte subsets in peripheral blood mononuclear cells of melanoma patients. (a) tSNE plot of concatenated 11 whole PBMC samples stained for nine markers (represented with heat map) for identification of monocyte subset, (b) tSNE plot , Clusters of monocyte subsets ; Dark Blue large dots represents classical monocyte subset, (c) tSNE plot , Clusters of monocyte subsets ; Brown large dots represents intermediate monocyte subset, (d) tSNE plot , Clusters of monocyte subsets ; Dark brown large dots represents non-classical monocyte subset . (e) Box and Whisker plot representing percentage of Monocyte subset among total monocyte population with corresponding column statistics. P-values are represented as (ns:P > 0.05, *: P ≤ 0.05, **: P ≤ 0.01 ***: P ≤ 0.001; ****: P ≤ 0.0001) . (CM; classical Monocytes, N-CM; Non- classical Monocytes IM; Intermediate Monocytes).

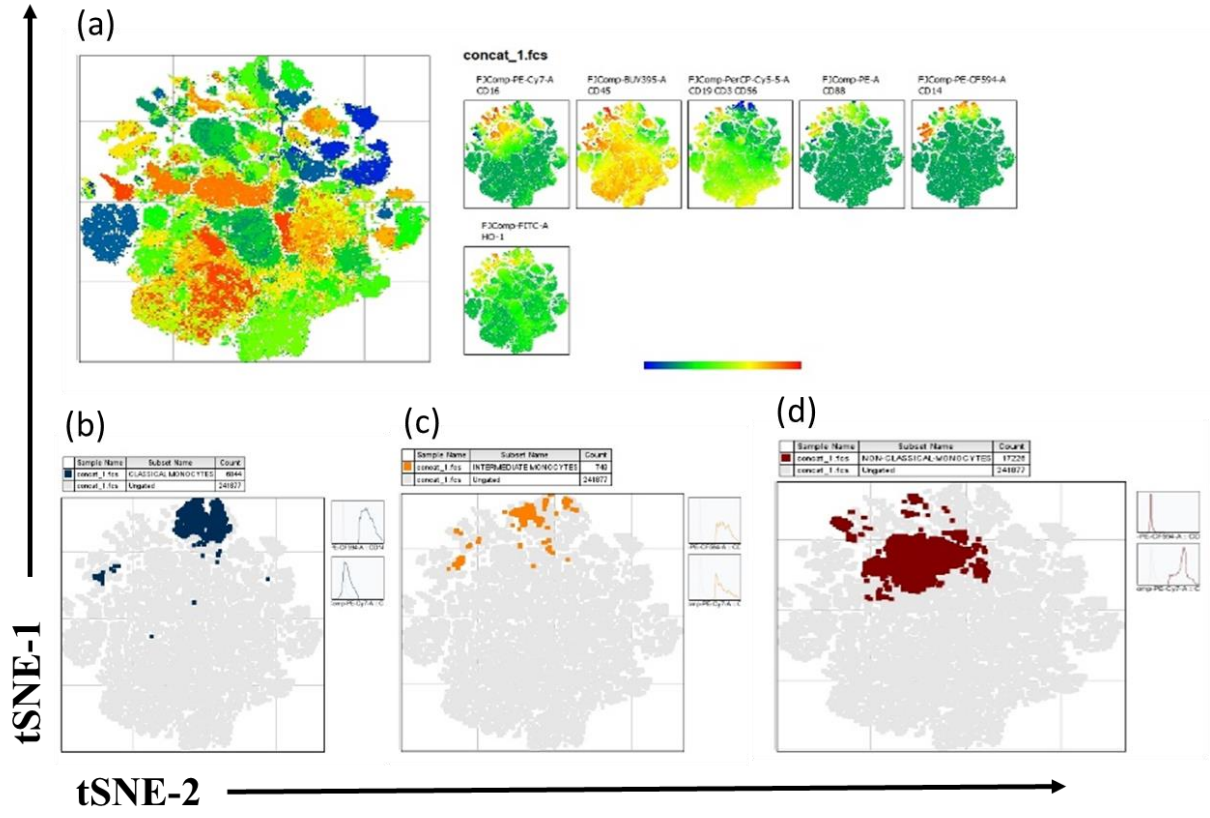

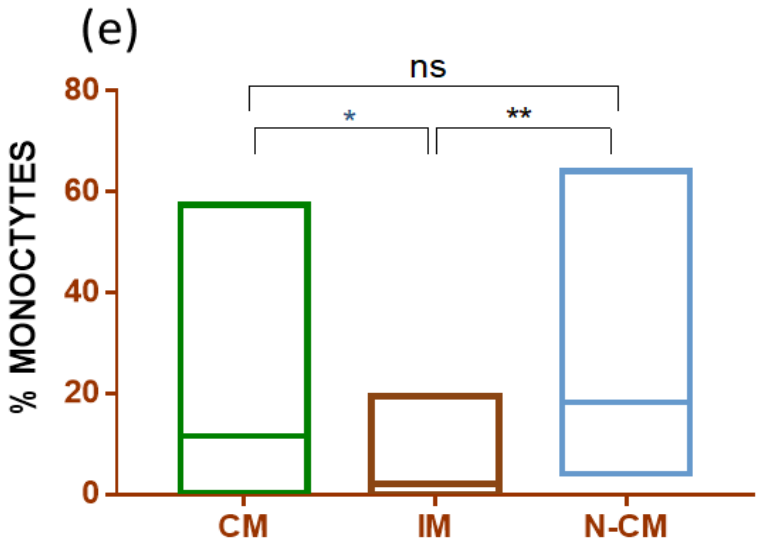

	CM	IM	N-CM
Mean	19.11	5.767	27.11
Std. Deviation	18.06	6.532	21.89
Std. Error of Mean	4.826	1.746	5.851

Figure 26: Identification of circulating monocyte subsets in peripheral blood mononuclear cells of advanced head and neck cancer patients. (a) tSNE plot of concatenated 14 whole PBMC samples stained for nine markers (represented with heat map) for identification of monocyte subset , (b) tSNE plot , Clusters of monocyte subsets ; Dark Emrald large dots represents classical monocyte subset, (c) tSNE plot , Clusters of monocyte subsets ; Orange large dots represents intermediate monocyte subset, (d) tSNE plot , Clusters of monocyte subsets ; Brown large dots represents non-classical monocyte subset . (e) Box and Whisker plot representing percentage of Monocyte subset among total monocyte population With corresponding column statistics. P-values are represented as (ns:P > 0.05 , * : P ≤ 0.05, ** : P ≤ 0.01 *** : P ≤ 0.001 ; **** : P ≤ 0.0001) . (CM; classical Monocytes, N-CM; Non- classical Monocytes IM; Intermediate Monocytes) .

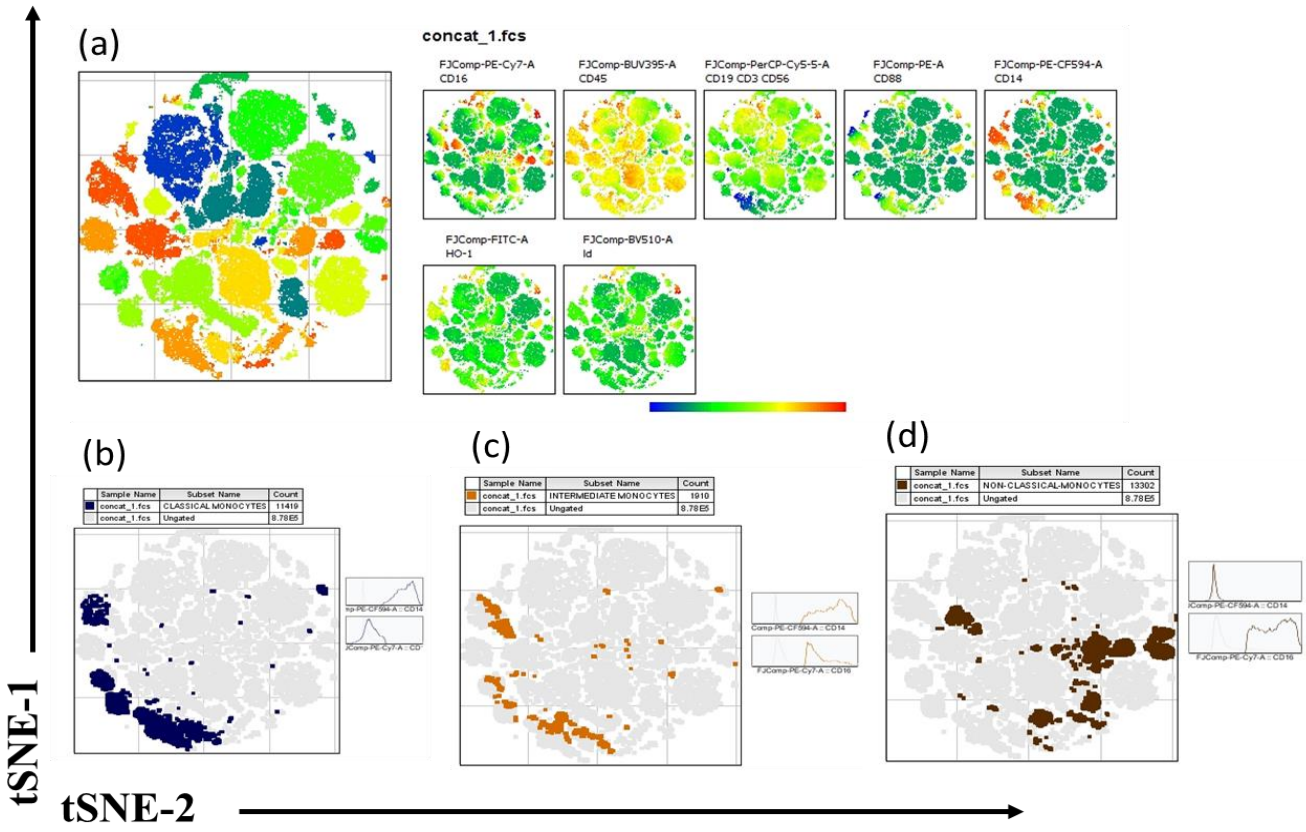

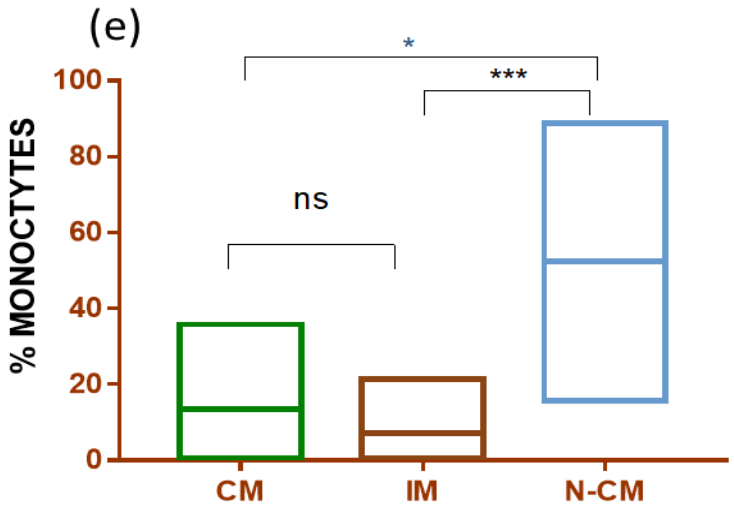

	CM	IM	N-CM
Mean	17.57	8.973	46.88
Std. Deviation	13.37	7.338	24.64
Std. Error of Mean	4.457	2.446	8.214

Figure 27: Identification of circulating monocyte subsets in peripheral blood mononuclear cells of advanced renal cell carcinoma. (a) tSNE plot of concatenated 10 whole PBMC samples stained for nine markers (represented with heat map) for identification of monocyte subset, (b) tSNE plot , Clusters of monocyte subsets ; Dark blue large dots represents classical monocyte subset, (c) tSNE plot , Clusters of monocyte subsets ; Orange large dots represents intermediate monocyte subset, (d) tSNE plot , Clusters of monocyte subsets ; Brown large dots represents non-classical monocyte subset . (e) Box and Whisker plot representing percentage of Monocyte subset among total monocyte population with corresponding column statistics. P-values are represented as (ns:P > 0.05, *: P ≤ 0.05, **: P ≤ 0.01 ***: P ≤ 0.001; ****: P ≤ 0.0001). (CM; classical Monocytes, N-CM; Non- classical Monocytes IM; Intermediate Monocytes) .

3.8. Circulating monocyte subsets are associated with therapy outcomes in advanced cancer patients treated with ICIs.

In advanced lung cancer presence of a higher level of classical monocytes had a higher risk of poor OS and PFS, a median percentage was set as the cutoff value, and patients who had above 51% of classical monocytes in peripheral blood had a higher risk of poor outcome, OS (HR = 0.55, 95% CI: 0.28-1.07, p = 0.077), PFS (HR = 0.71, 95% CI: 0.42-1.18, p = 0.1748). Although this result was not statistically significant the median OS was reduced to 9.7 months in the higher classical monocyte group compared to the low classical monocyte group for which the median OS was 22.2 months. similarly, the median PFS was 11.3 months in the low classical monocyte group v/s 7.1 months for patients who had a higher percentage of classical monocytes. **(Figure 28).**

A similar trend was also observed in the intermediate monocytes where the higher levels (cutoff value10.9%) of this subset were associated with higher risk both in terms of OS (HR = 0.65, 95% CI: 0.33-1.26, p = 0.2091) and PFS (HR = 0.70, 95% CI: 0.42-1.16, p = 0.1686). The median OS was 22.2 months v/s 10.9 months for the low v/s high intermediate

monocytes group and the median PFS was 9.8 months v/s 6.3 months for the low v/s high intermediate monocytes group **(Figure 28)**. There was no significant effect on OS and PFS was established for the presence of the non-classical monocytes' subset. In advanced head and neck cancer, melanoma, and renal cell carcinoma the results remained inconclusive.

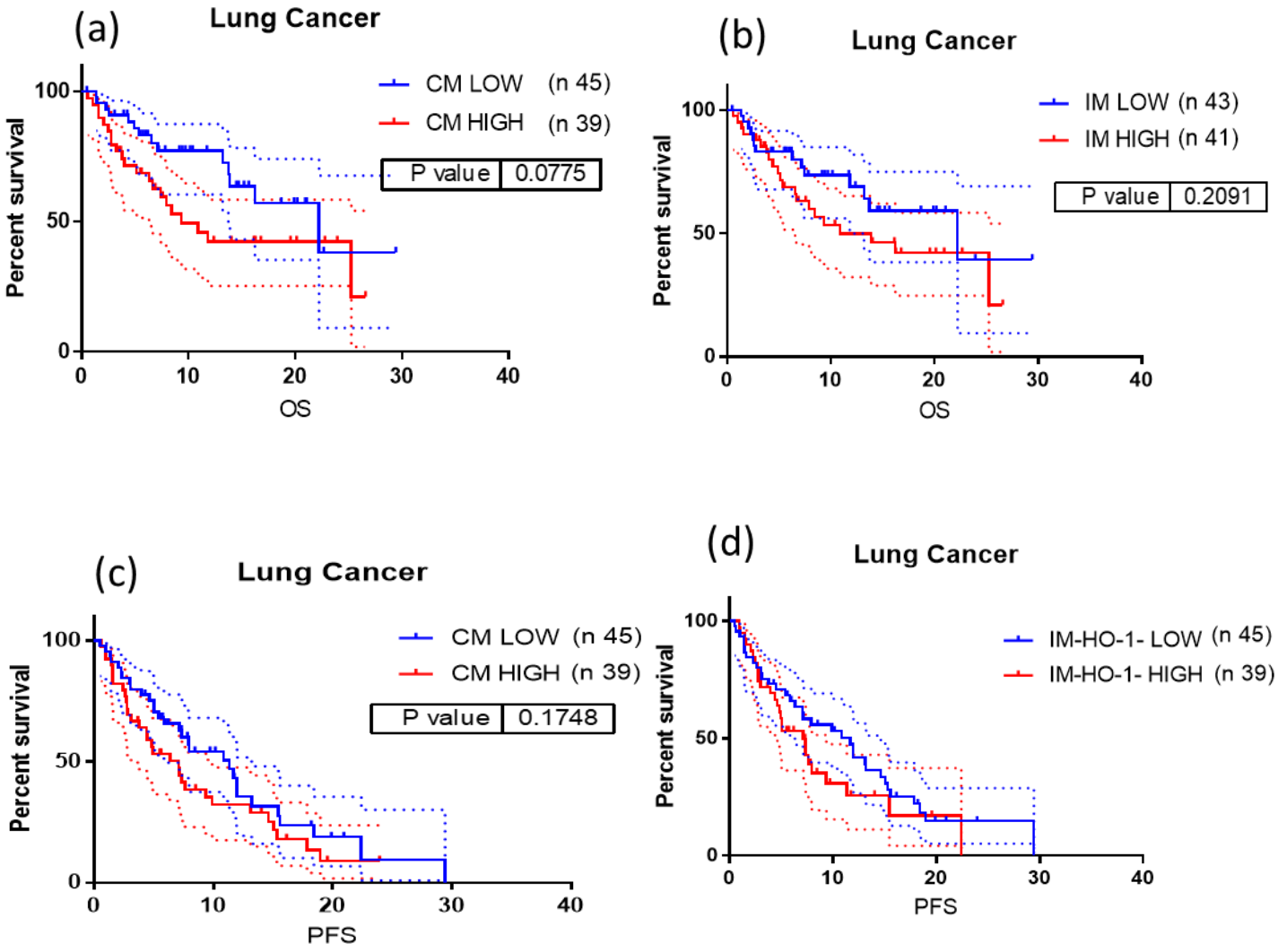

Figure 28: Kaplan-Meier Survival Curves with 95% CI for Overall survival (OS; a) Progression-Free Survival (PFS; b) of advanced lung cancer Patients respectively treated With ICI's. Time is represented in months at baseline. (a) OS; CM high (red line) v/s CM Low (blue line), (b) OS; IM high (red line) v/s IM Low (blue line) (c) PFS; CM high (red line) v/s CM Low (blue line), (d) PFS; IM high (red line) v/s IM Low (blue line). Dotted lines represent upper and lower limit of 95% CI (Confidence Interval). Results are from univariable cox proportional Hazard model (OS; overall survival PFS; progression free survival CM; classical Monocytes, IM; Intermediate Monocytes**).**

3.9. Heme-oxygenase-1 (HO-1) in peripheral blood Monocytes and therapy outcome in advanced cancer patients.

The expression of HO-1 in all the three identified monocyte subsets was measured as gMFI, HO-1 predominately showed higher expression among the classical monocyte subset followed by intermediate and non-classical monocytes in all cancer types, however, there was no significant difference was observed for melanoma between classical and non-classical monocyte subset.

Advanced lung cancer: In classical monocytes, HO-1 was expressed significantly higher compared to the other two subsets gMFI Mean±SD: classical monocytes 5317±5099; intermediate monocytes 3577±3814; non-classical monocytes 1347±1242. P<0.0001 (Kruskal-Wallis test) **(Figure 29)**

Melanoma: In classical monocytes, HO-1 was significantly expressed higher compared to other non-classical monocytes, there was no statistically significant difference in expression levels between classical and intermediate monocyte subset, gMFI Mean±SD: classical monocytes 5406±4412; intermediate monocytes 4479±5093; non-classical monocytes 988±442. P=0.0013 (Kruskal-Wallis test) **(Figure 30)**

Advanced head and neck cancer: In classical monocytes HO-1 was significantly expressed higher compared to other two subsets gMFI Mean±SD: classical monocytes 8004±6699; intermediate monocytes 3051±3135; non-classical monocytes 861±508 P<0.0001 (Kruskal-Wallis test) **(Figure 31)**

Renal Cell Carcinoma: In classical monocytes, HO-1 was significantly expressed higher compared to the other two subsets gMFI Mean±SD: classical monocytes 6124±5978; intermediate monocytes 2625±2880; non-classical monocytes 892±682. P=0.0005 (Kruskal-Wallis test) **(Figure 32).**

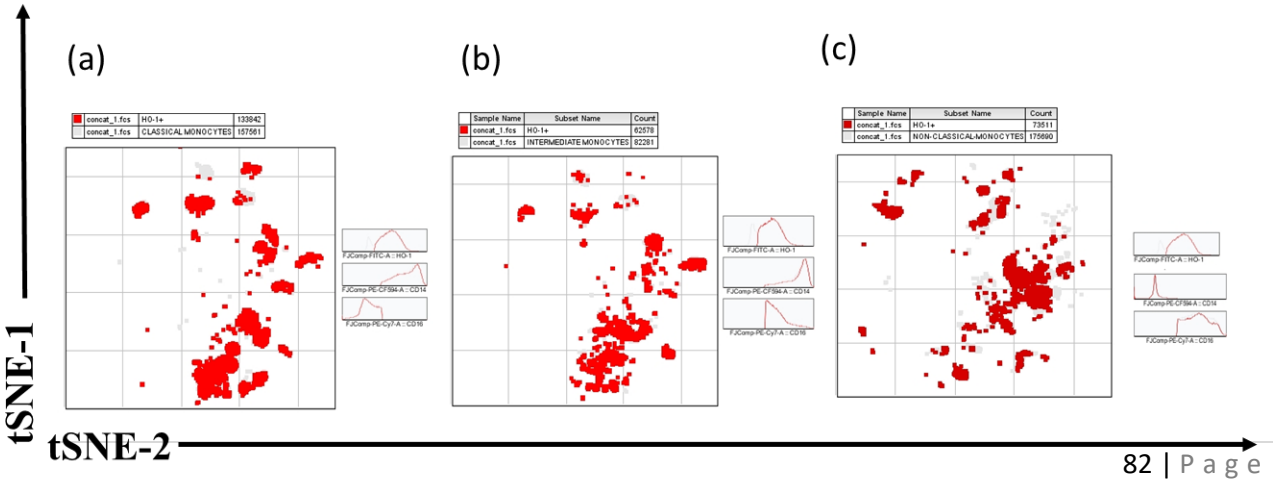

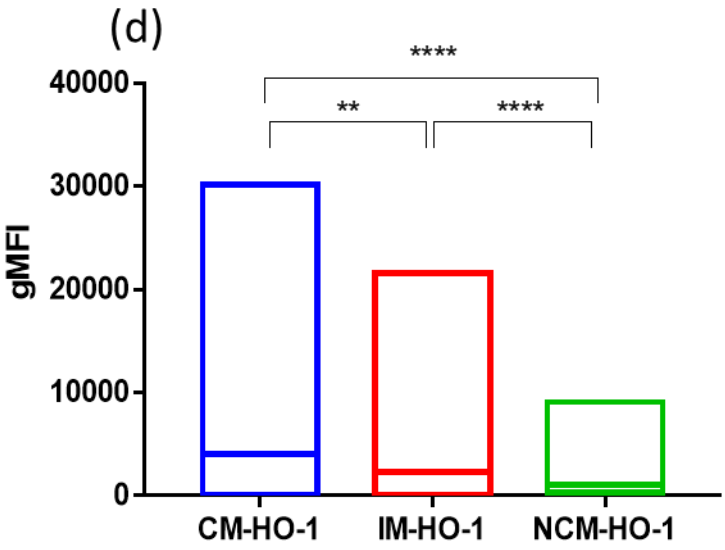

	CM-HO-1	IM-HO-1	NCM-HO-1
Mean	5317	3577	1347
Std. Deviation	5099	3814	1242
Std. Error of Mean	556.3	416.2	135.6

Figure 29: Expression of HO-1 in three monocyte subsets in peripheral blood mononuclear cells of advanced lung cancer patients. (a) tSNE plot of HO-1 expressing classical monocyte subset, (b) tSNE plot of HO-1 expressing intermediate monocyte subset; (c) tSNE plot of HO-1 expressing non-classical monocyte subset (d) Box and Whisker plot representing gMFI of HO-1 in classical, intermediate and non-classical monocyte subsets With corresponding column statistics. P-values are represented as (ns:P > 0.05, * : P ≤ 0.05, ** : P ≤ 0.01 *** : P ≤ 0.001 ; **** : P ≤ 0.0001) . (H0-1; hemeoxigenase-1, gMFI; geometric mean fluorescent intensity, CM; classical Monocytes, N-CM; Non- classical Monocytes IM; Intermediate Monocytes).

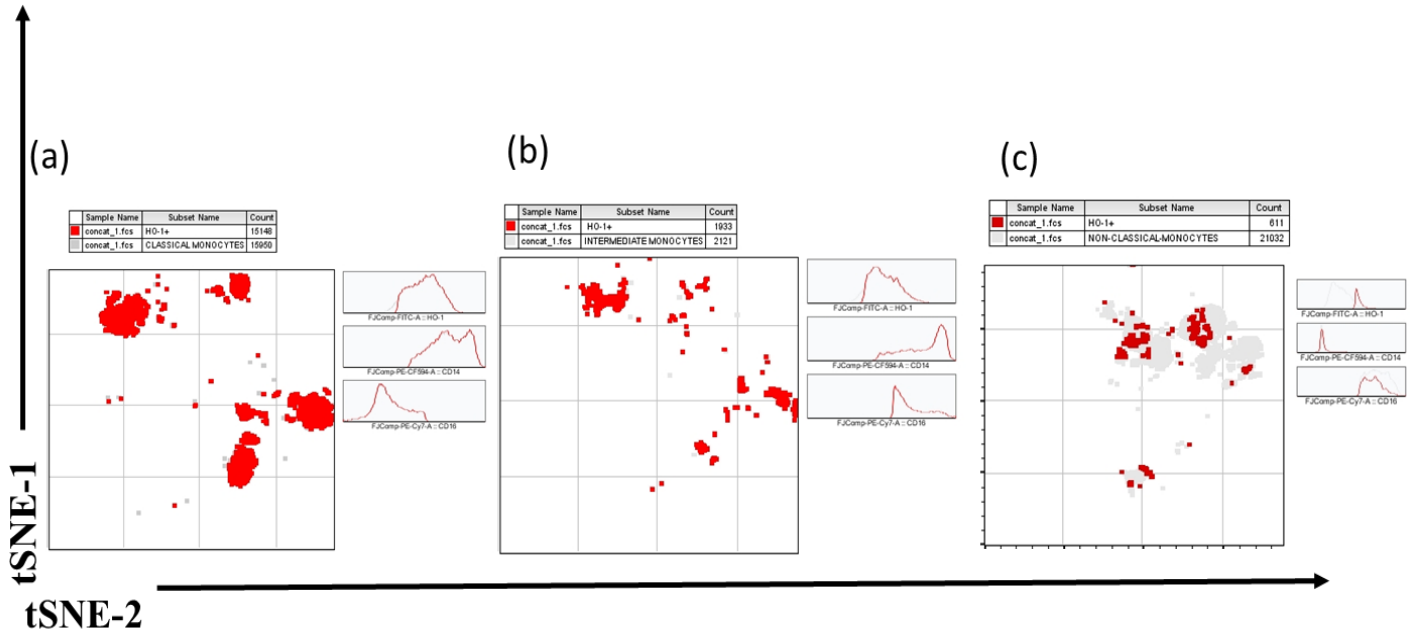

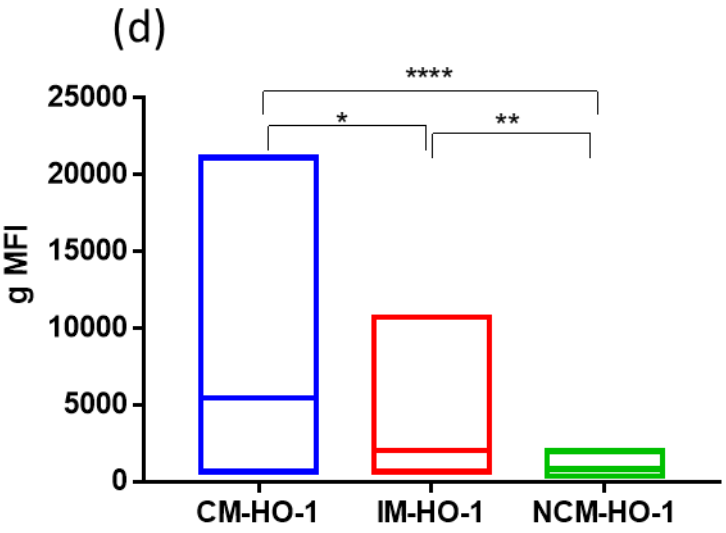

	CM-HO-1	IM-HO-1	NCM-HO-1
Mean	8004	3051	861.9
Std. Deviation	6699	3135	508.9
Std. Error of Mean	1790	837.8	136

Figure 30: Expression of HO-1 in three monocyte subsets in peripheral blood mononuclear cells of Melanoma patients. (a) tSNE plot of HO-1 expressing classical monocyte subset, (b) tSNE plot of HO-1 expressing intermediate monocyte subset; (c) tSNE plot of HO-1 expressing non-classical monocyte subset (d) Box and Whisker plot representing gMFI of HO-1 in classical, intermediate and non-classical monocyte subsets with corresponding column statistics. P-values are represented as (ns:P > 0.05, * : P ≤ 0.05, ** : P ≤ 0.01 *** : P ≤ 0.001 ; **** : P ≤ 0.0001) . (H0-1; hemeoxigenase-1, gMFI; geometric mean fluorescent intensity, CM; classical Monocytes, N-CM; Non- classical Monocytes IM; Intermediate Monocytes).

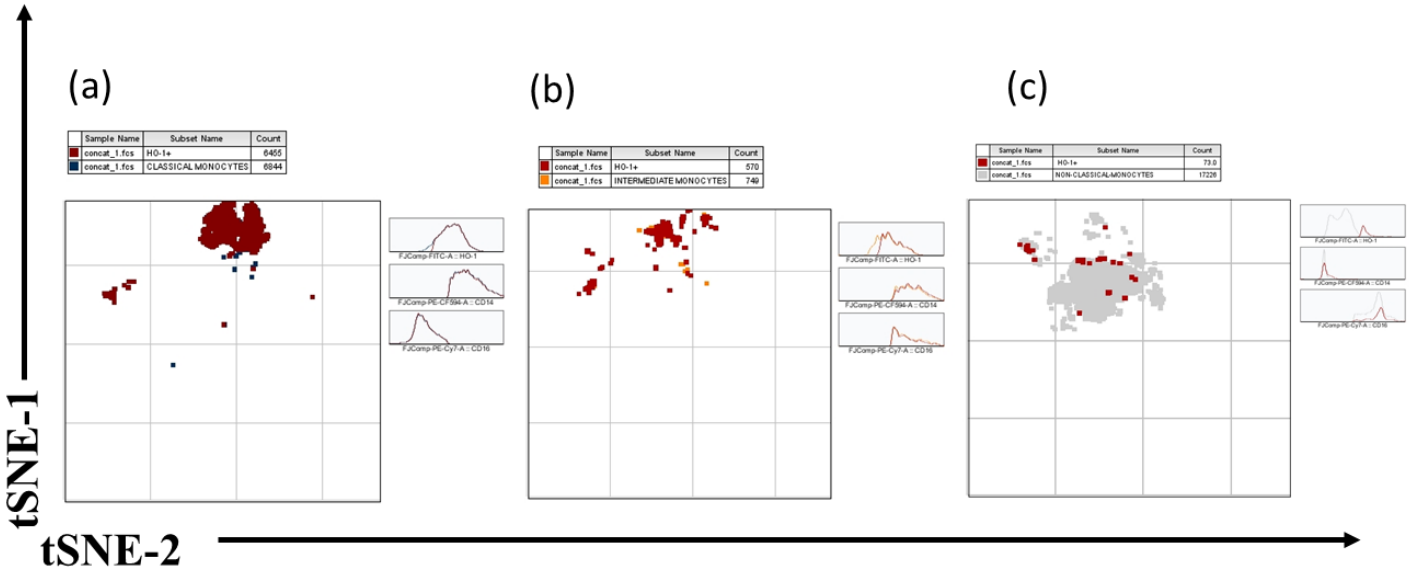

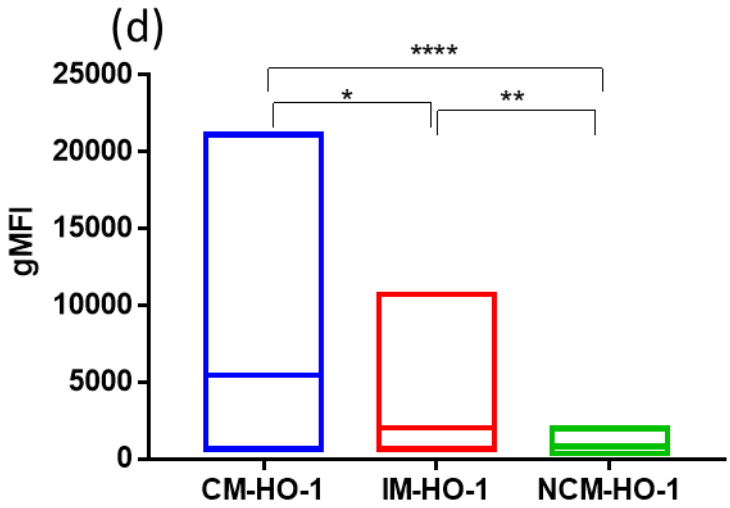

	CM-HO-1	IM-HO-1	NCM-HO-1
Mean	8004	3051	861.9
Std. Deviation	6699	3135	508.9
Std. Error of Mean	1790	837.8	136

Figure 31: Expression of HO-1 in three monocyte subsets in peripheral blood mononuclear cells of advanced head and neck cancer patients. **(a)** tSNE plot of HO-1 expressing classical monocyte subset, **(b)** tSNE plot of HO-1 expressing intermediate monocyte subset; **(c)** tSNE plot of HO-1 expressing non-classical monocyte subset **(d)** Box and Whisker plot representing gMFI of HO-1 in classical, intermediate and non-classical monocyte subsets With corresponding column statistics. P-values are represented as (ns:P > 0.05, * : P ≤ 0.05, ** : P ≤ 0.01 *** : P ≤ 0.001 ; **** : P ≤ 0.0001) . (H0-1; hemeoxigenase-1, gMFI; geometric mean fluorescent intensity, CM; classical Monocytes, N-CM; Non- classical Monocytes IM; Intermediate Monocytes).

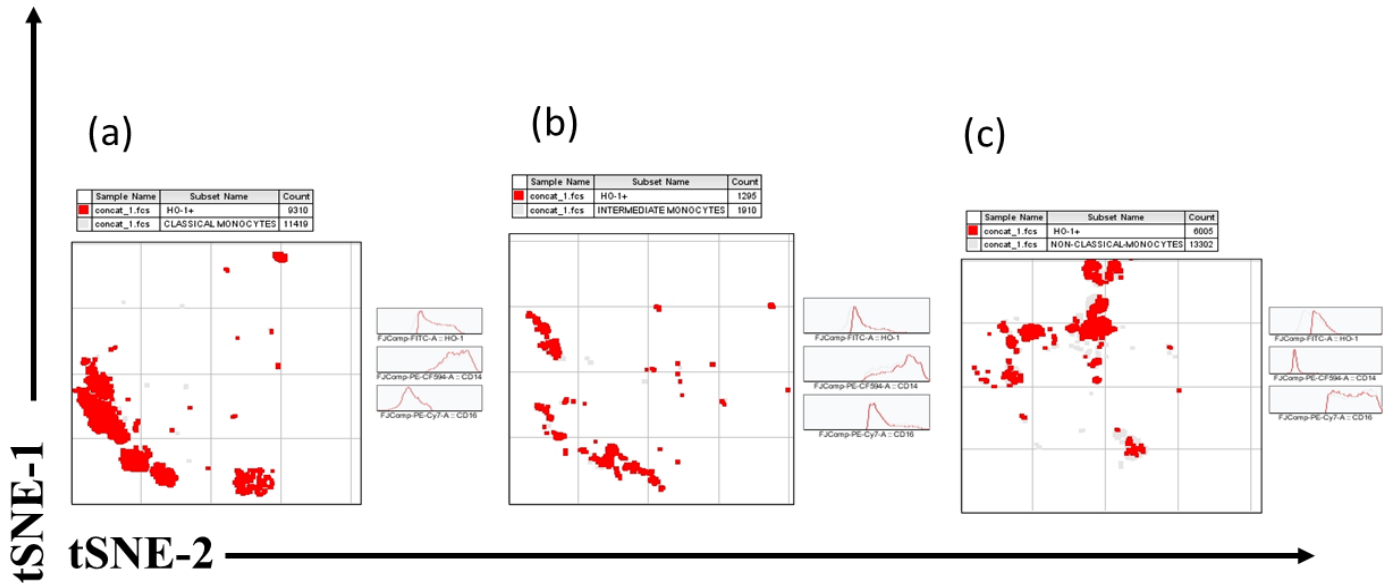

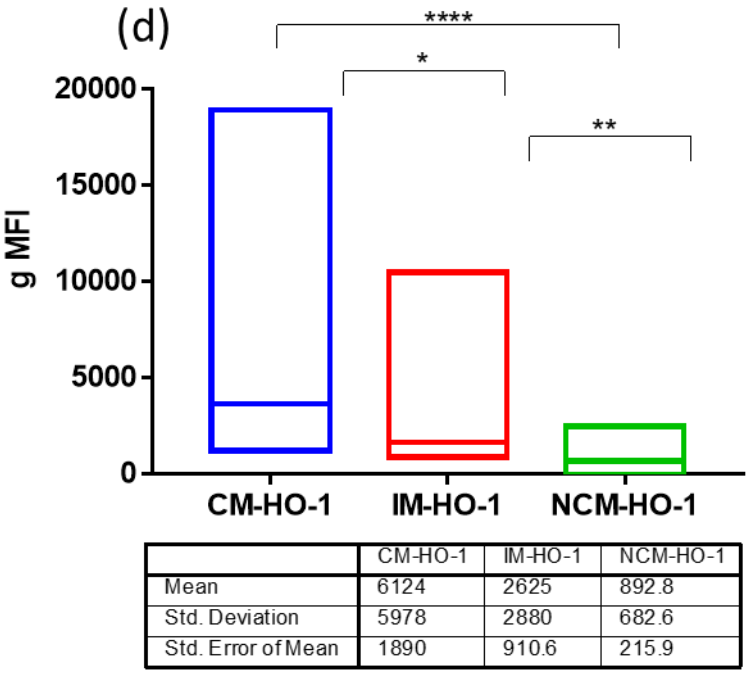

	CM-HO-1	IM-HO-1	NCM-HO-1
Mean	6124	2625	892.8
Std. Deviation	5978	2880	682.6
Std. Error of Mean	1890	910.6	215.9

Figure 32: Expression of HO-1 in three monocyte subsets in peripheral blood mononuclear cells of advanced renal cell carcinoma patients. (a) tSNE plot of HO-1 expressing classical monocyte subset, (b) tSNE plot of HO-1 expressing intermediate monocyte subset; (c) tSNE plot of HO-1 expressing non-classical monocyte subset (d) Box and Whisker plot representing gMFI of HO-1 in classical, intermediate and non-classical monocyte subsets With corresponding column statistics. P-values are represented as (ns:$P > 0.05$, *: $P \leq 0.05$, **: $P \leq 0.01$ ***: $P \leq 0.001$; ****: $P \leq 0.0001$). (H0-1; hemeoxigenase-1, gMFI; geometric mean fluorescent intensity, CM; classical Monocytes, N-CM; Non- classical Monocytes IM; Intermediate Monocytes).

3.10. Heme-oxygenase-1 in circulating monocyte subset and its association with therapy outcome in advanced cancer patients treated with ICIs:

The expression levels of HO-1 were correlated with the clinical outcome in terms of OS and PFS. Univariable Cox proportional hazard analysis was performed between the high-expression group and low-expression group, divided by a cutoff value (median value of gMFI) in each monocyte subset. In advanced lung cancer patients, higher expression of HO-1 in the classical monocyte subset(OS: HR = 1.29, 95% CI: 0.66-2.52, p = 0.4313 (PFS: HR = 1.07, 95% CI: 0.64-1.78, p = 0.7723)) and non-classical monocyte subset (OS: HR = 1.65, 95% CI: 0.84-3.21, p = 0.1322) (PFS: HR = 1.48, 95% CI: 0.89-2.47, p =0.1110) was associated with lower risk of progression or death .while the high expression of HO-1 in intermediate monocytes was associated with poor outcome in terms of both OS and PFS. (OS: HR = 0.87, 95% CI: 0.44-1.70, p = 0.6799) (PFS: HR = 0.73, 95% CI: 0.43-1.23, p =0.2165) **(Figure 33).**

The median OS was 13.7 months v/s 22.2 months for the low v/s high HO-1 expressing classical monocytes group and the median PFS was 7.3 months v/s 7.6 months low v/s high HO-1 expressing classical monocytes group. The median OS was 13.9 months v/s 22.2 months for the low v/s high HO-1 expressing non-classical monocytes group and the median PFS was 7.6 months v/s 11.3 months for low v/s high HO-1 expressing non-classical monocytes group. The median OS was 22.2 months v/s 16.2 months for the low v/s high HO-1 expressing intermediate monocytes group and the median PFS was 11.6 months v/s 7.1 months low v/s high HO-1 expressing non-classical monocytes group.

A similar trend was observed in melanoma, advanced head and neck cancer, and renal cell carcinoma, but the result remained inconclusive because of the lower sample size.

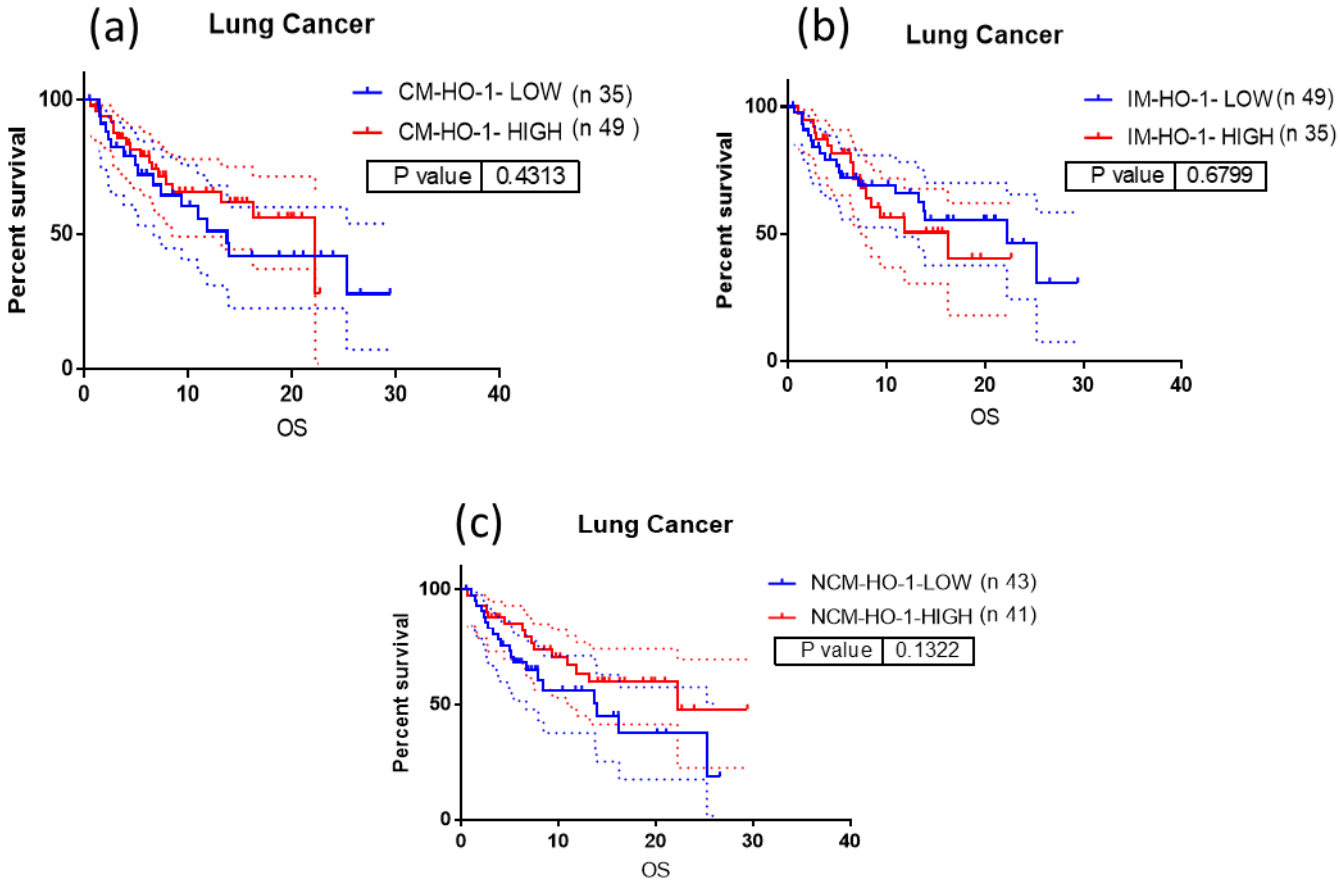

Figure 33 (a,b,c): Kaplan-Meier Survival Curves with 95% CI for Overall survival of advanced lung cancer Patients respectively treated With ICI's. Time is represented in months at baseline. (a) OS; CM-HO-1 high (red line) v/s CM-HO-1 Low (blue line), (b) OS; IM-HO-1 high (red line) v/s IM-HO-1 Low (blue line) (c) OS; N-CM-HO-1 high (red line) v/s N-CM-HO1 Low (blue line). Dotted lines represent upper and lower limit of 95% CI (Confidence Interval). Results are from univariable cox proportional Hazard model (OS; overall survival PFS; progression free survival CM; classical Monocytes, IM; Intermediate Monocytes, H0-1; hemeoxigenase-1).

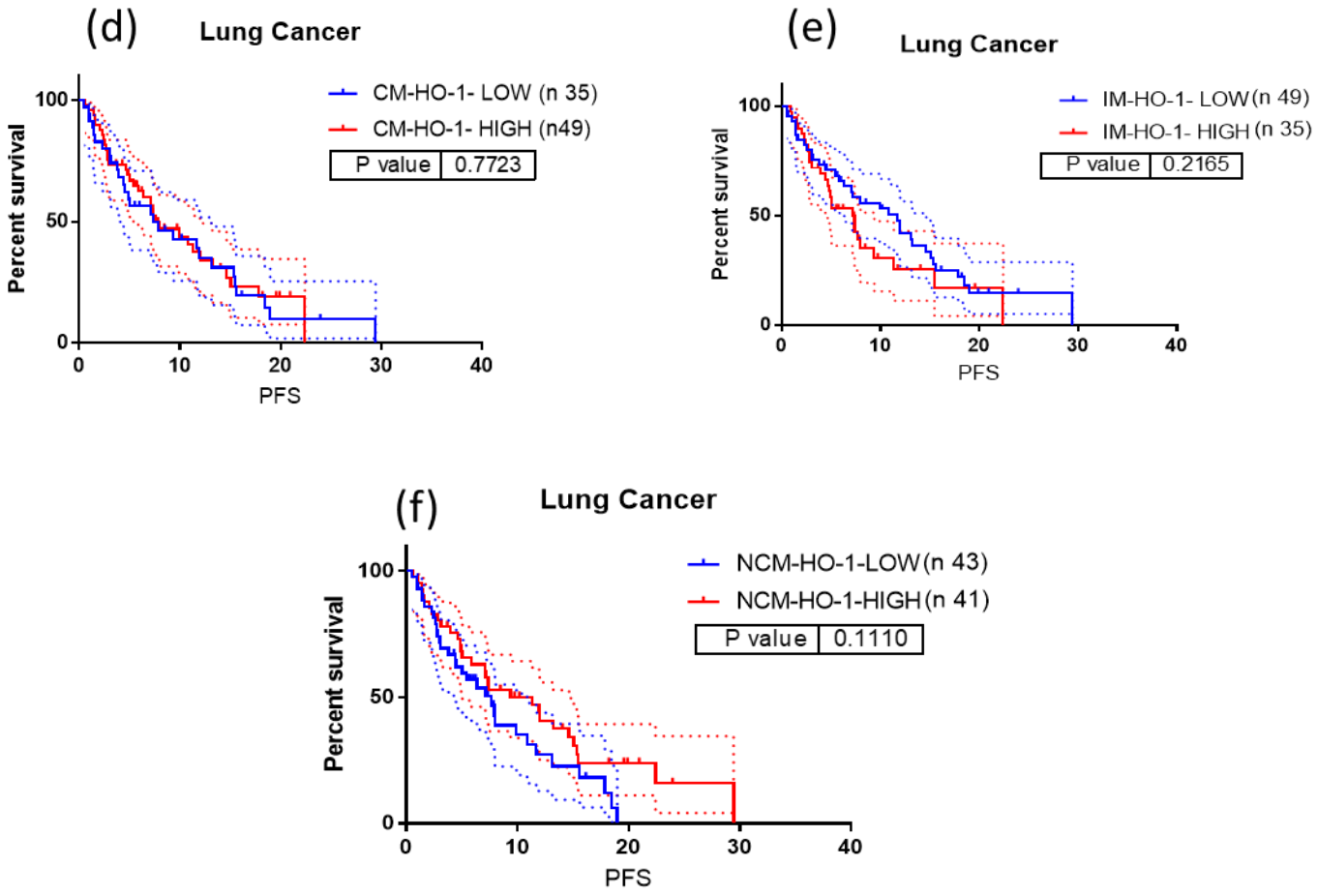

Figure 33 (d,e,f) : Kaplan-Meier Survival Curves with 95% CI for Progression-Free Survival of advanced lung cancer Patients respectively treated With ICI's. Time is represented in months at baseline (d) PFS; CM-HO-1 high (red line) v/s CM-HO-1 Low (blue line), (e) PFS; IM-HO-1 high (red line) v/s IM-HO-1 Low (blue line), (f) PFS; N-CM-HO-1 high (red line) v/s N-CM-HO1 Low (blue line). Dotted lines represent upper and lower limit of 95% CI (Confidence Interval). Results are from univariable cox proportional Hazard model (OS; overall survival PFS; progression free survival CM; classical Monocytes, IM; Intermediate Monocytes, H0-1; hemeoxigenase-1).

3.11. Heme-oxygenase-1 (HO-1) expression on monocyte subpopulation and its corelation with arterial Carboxy-haemoglobin (COHb).

Carbon-Monoxide (CO) is one of the byproducts of heme degradation by heme-oxygenase-1. We corelated the arterial Carboxy-hemoglobin percentage with the gMFI of HO-1 in all the three monocyte subsets. No statistically significant correlation was established in any of the advanced cancer type. **(Figure 34).**

a

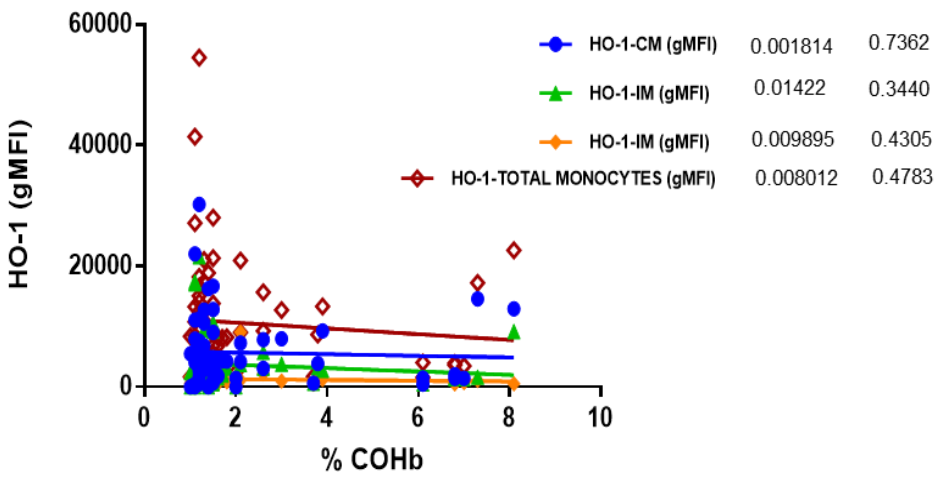
Lung Cancer
r²
P-value
HO-1-CM (gMFI) 0.001814 0.7362
HO-1-IM (gMFI) 0.01422 0.3440
HO-1-IM (gMFI) 0.009895 0.4305
HO-1-TOTAL MONOCYTES (gMFI) 0.008012 0.4783
HO-1 (gMFI)
60000
40000
20000
0
0 2 4 6 8 10
% COHb

b

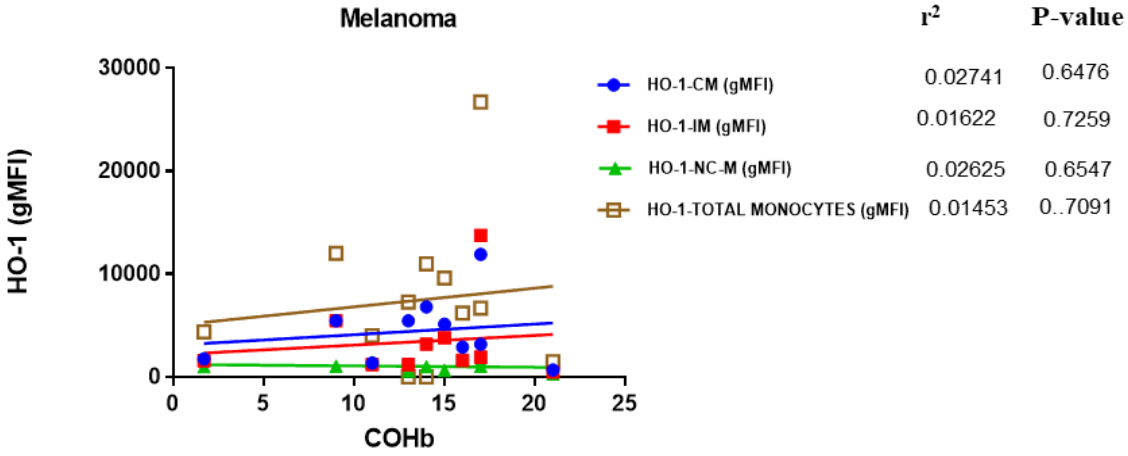
Melanoma
r²
P-value
HO-1-CM (gMFI) 0.02741 0.6476
HO-1-IM (gMFI) 0.01622 0.7259
HO-1-NC-M (gMFI) 0.02625 0.6547
HO-1-TOTAL MONOCYTES (gMFI) 0.01453 0..7091
HO-1 (gMFI)
30000
20000
10000
0
0 5 10 15 20 25
COHb

c

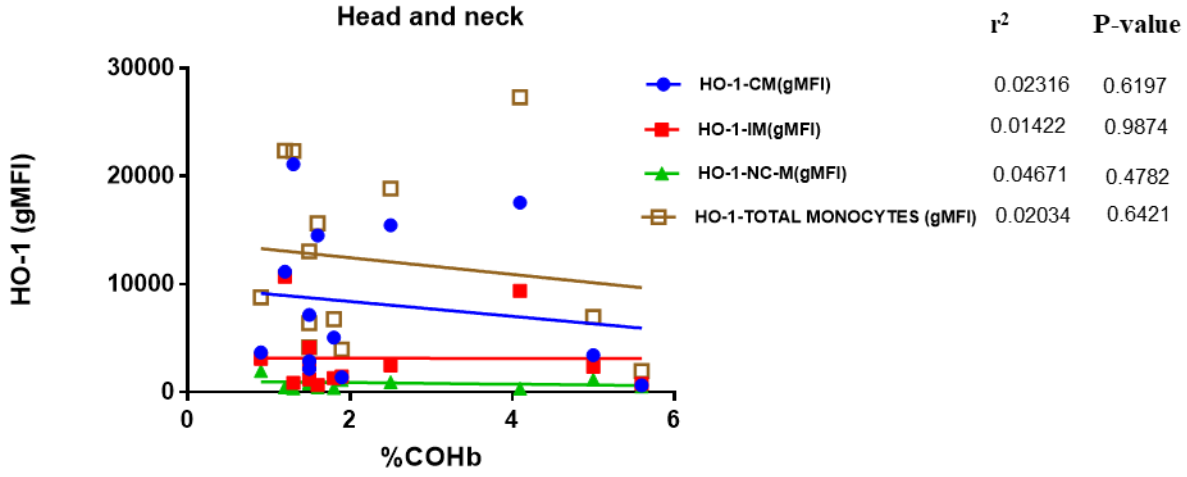
Head and neck
r²
P-value
HO-1-CM(gMFI) 0.02316 0.6197
HO-1-IM(gMFI) 0.01422 0.9874
HO-1-NC-M(gMFI) 0.04671 0.4782
HO-1-TOTAL MONOCYTES (gMFI) 0.02034 0.6421
HO-1 (gMFI)
30000
20000
10000
0
0 2 4 6
%COHb

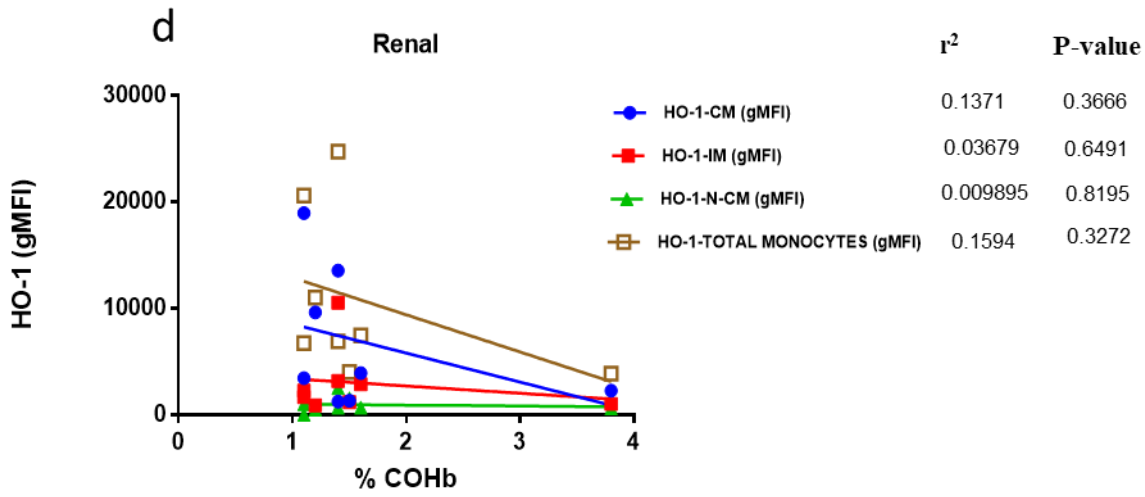

Figure 34: Correlation between %COHb on X-axis and HO-1(gMFI) on Y-axis, Pearson correlation coefficient were calculated and reported within the graphs (a) Advanced Lung Cancer, (b) Melanoma (c) Advanced Head and neck cancer (d) Advanced Renal cell Carcinoma. (COHb: Carboxy-hemoglobin; HO-1: Hemeoxygenase-1; CM; classical Monocytes, N-CM; Non- classical Monocytes IM; Intermediate Monocytes, gMFI; geometric mean fluorescent intensity.

3.12. Expression of C5aR1(CD88) on monocyte subset of advanced cancer patients treated with ICIs:

We evaluated the expression of C5aR1 (CD88) on the three-monocyte subset identified and reported as gMFI.

In advanced lung cancer patient samples, CD88 was expressed more on intermediate monocytes but was statistically insignificant compared to the expression on classical monocytes, non-classical monocytes had the least CD88 expression among the three subsets. In melanoma patient samples head and neck cancer patient samples and advanced renal cell carcinoma a similar trend was observed. **[Advanced lung cancer patients:** gMFI Mean±SD: classical monocytes 3290±3833; intermediate monocytes 4694±5257; non-classical monocytes 1120±2240. P= <0.0001 **Melanoma**: gMFI Mean±SD: classical monocytes 3039±2045; intermediate monocytes 4268±3263; non-classical monocytes 53.23±23.76. P= <0.0001. **Advanced head and neck cancer** gMFI Mean±SD: classical monocytes 3094±1882; intermediate monocytes 3505±2052; non-classical monocytes 100.2±159.1. P= <0.0001(Kruskal-Wallis test).**] (Figure 35 – Figure 38)**

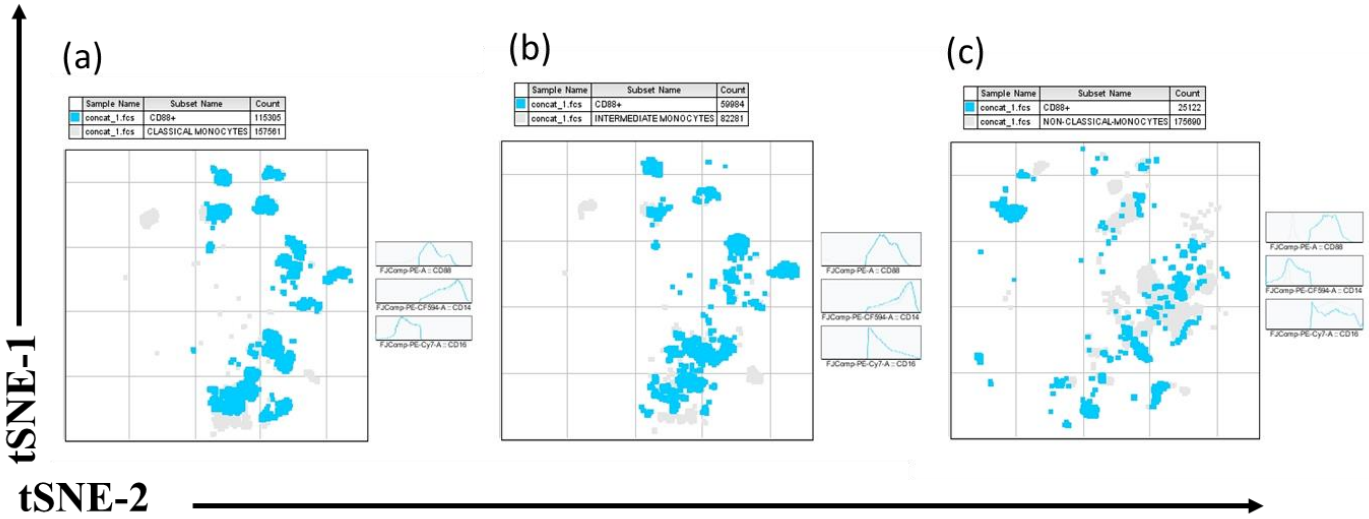

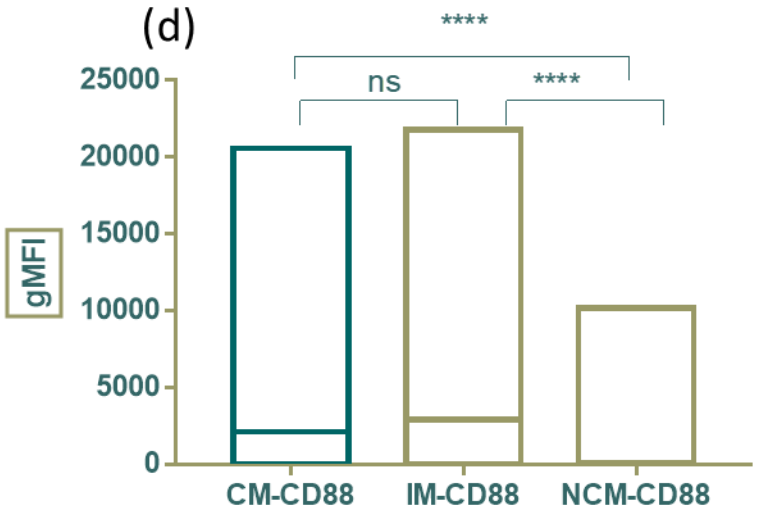

	CM-CD88	IM-CD88	NCM-CD88
Mean	3290	4694	1120
Std. Deviation	3833	5257	2240
Std. Error of Mean	418.2	577.1	244.4

Figure 35: Expression of CD88 on three monocyte subsets in peripheral blood mononuclear cells of advanced lung cancer patients. (a) tSNE plot of CD88 expressing classical monocyte subset, (b) tSNE plot of CD88 expressing intermediate monocyte subset; (c) tSNE plot of CD88 expressing non-classical monocyte subset (d) Box and Whisker plot representing gMFI of CD88 in classical, intermediate, and non-classical monocyte subsets with corresponding column statistics. P-values are represented as (ns:$P > 0.05$, *: $P \leq 0.05$, **: $P \leq 0.01$ *** : $P \leq 0.001$; **** : $P \leq 0.0001$) . (gMFI; geometric mean fluorescent intensity, CM; classical Monocytes, N-CM; Non- classical Monocytes IM; Intermediate Monocytes).

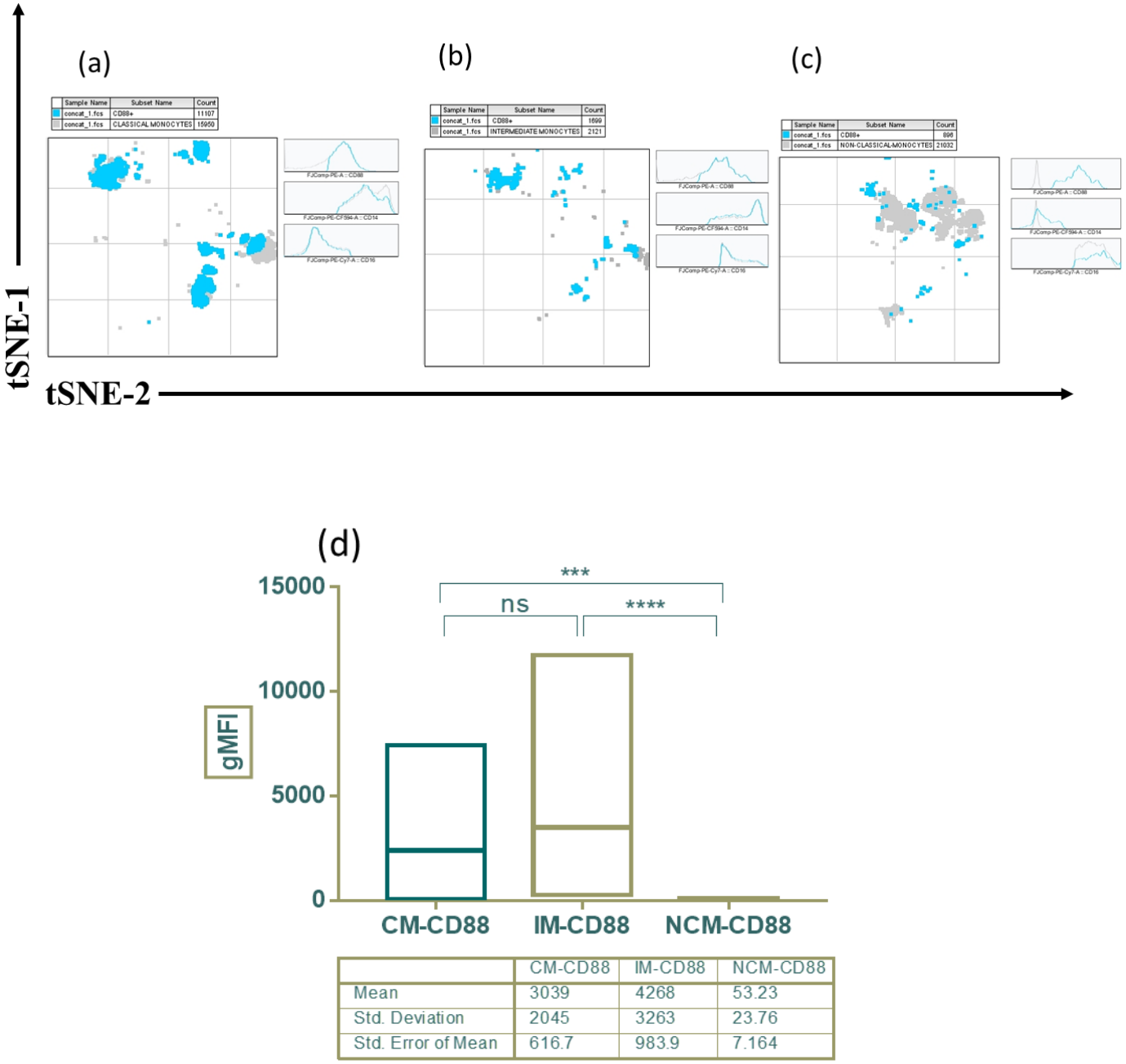

	CM-CD88	IM-CD88	NCM-CD88
Mean	3039	4268	53.23
Std. Deviation	2045	3263	23.76
Std. Error of Mean	616.7	983.9	7.164

Figure 36: Expression of CD88 on three monocyte subsets in peripheral blood mononuclear cells of melanoma patients. (a) tSNE plot of CD88 expressing classical monocyte subset, (b) tSNE plot of CD88 expressing intermediate monocyte subset; (c) tSNE plot of CD88 expressing non-classical monocyte subset (d) Box and Whisker plot representing gMFI of CD88 in classical, intermediate, and non-classical monocyte subsets with corresponding column statistics. P-values are represented as (ns:P > 0.05, *: P ≤ 0.05, **: P ≤ 0.01 ***: P ≤ 0.001; ****: P ≤ 0.0001). (gMFI; geometric mean fluorescent intensity, CM; classical Monocytes, N-CM; Non- classical Monocytes IM; Intermediate Monocytes).

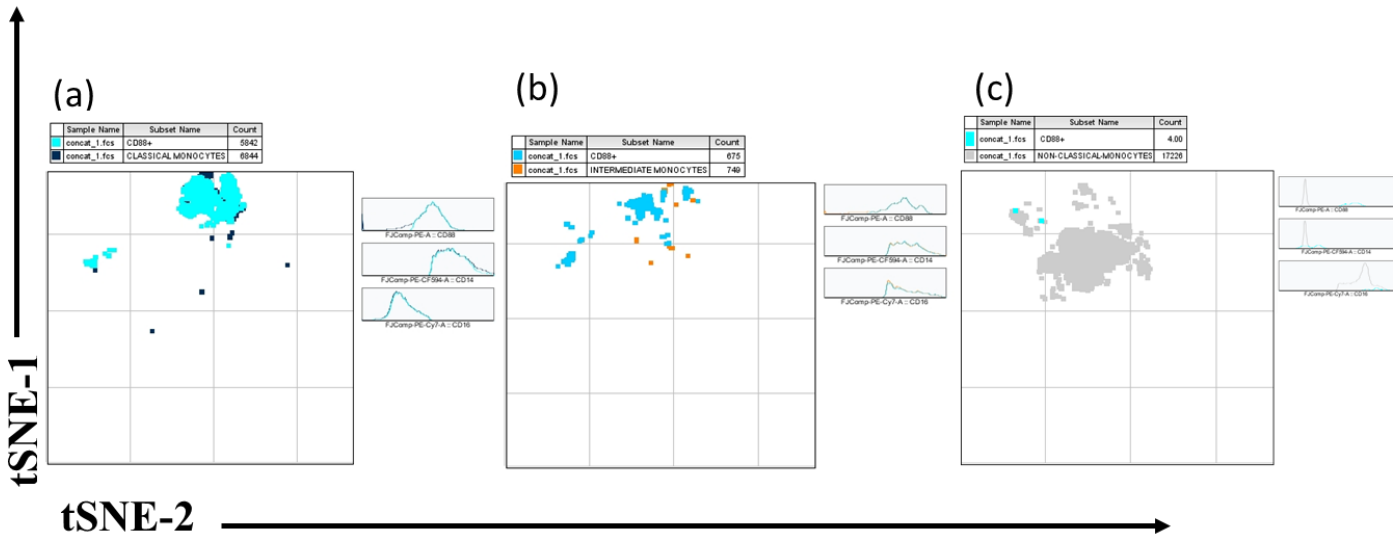

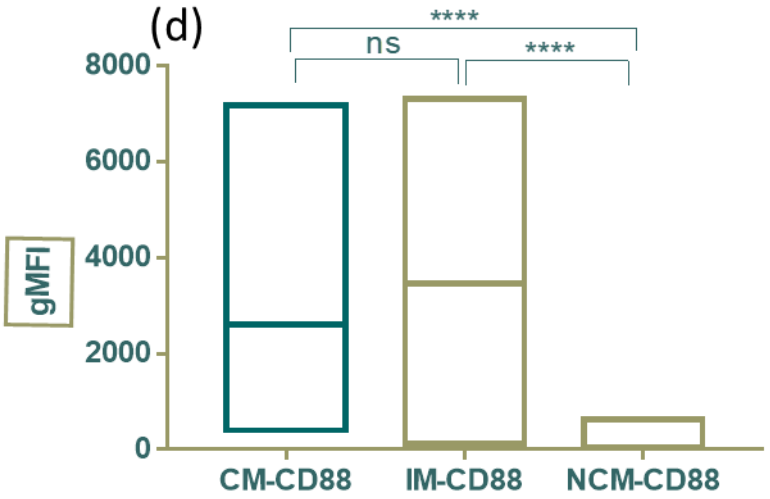

	CM-CD88	IM-CD88	NCM-CD88
Mean	3094	3505	100.2
Std. Deviation	1882	2052	159.1
Std. Error of Mean	503	592.4	44.12

Figure 37: Expression of CD88 on three monocyte subsets in peripheral blood mononuclear cells of advanced head and neck cancer patients. (a) tSNE plot of CD88 expressing classical monocyte subset, (b) tSNE plot of CD88 expressing intermediate monocyte subset; (c) tSNE plot of CD88 expressing non-classical monocyte subset (d) Box and Whisker plot representing gMFI of CD88 in classical, intermediate and non-classical monocyte subsets With corresponding column statistics. P-values are represented as (ns:$P > 0.05$, *: $P \leq 0.05$, ** : $P \leq 0.01$ *** : $P \leq 0.001$; **** : $P \leq 0.0001$) . (gMFI; geometric mean fluorescent intensity, CM; classical Monocytes, N-CM; Non- classical Monocytes IM; Intermediate Monocytes)**.**

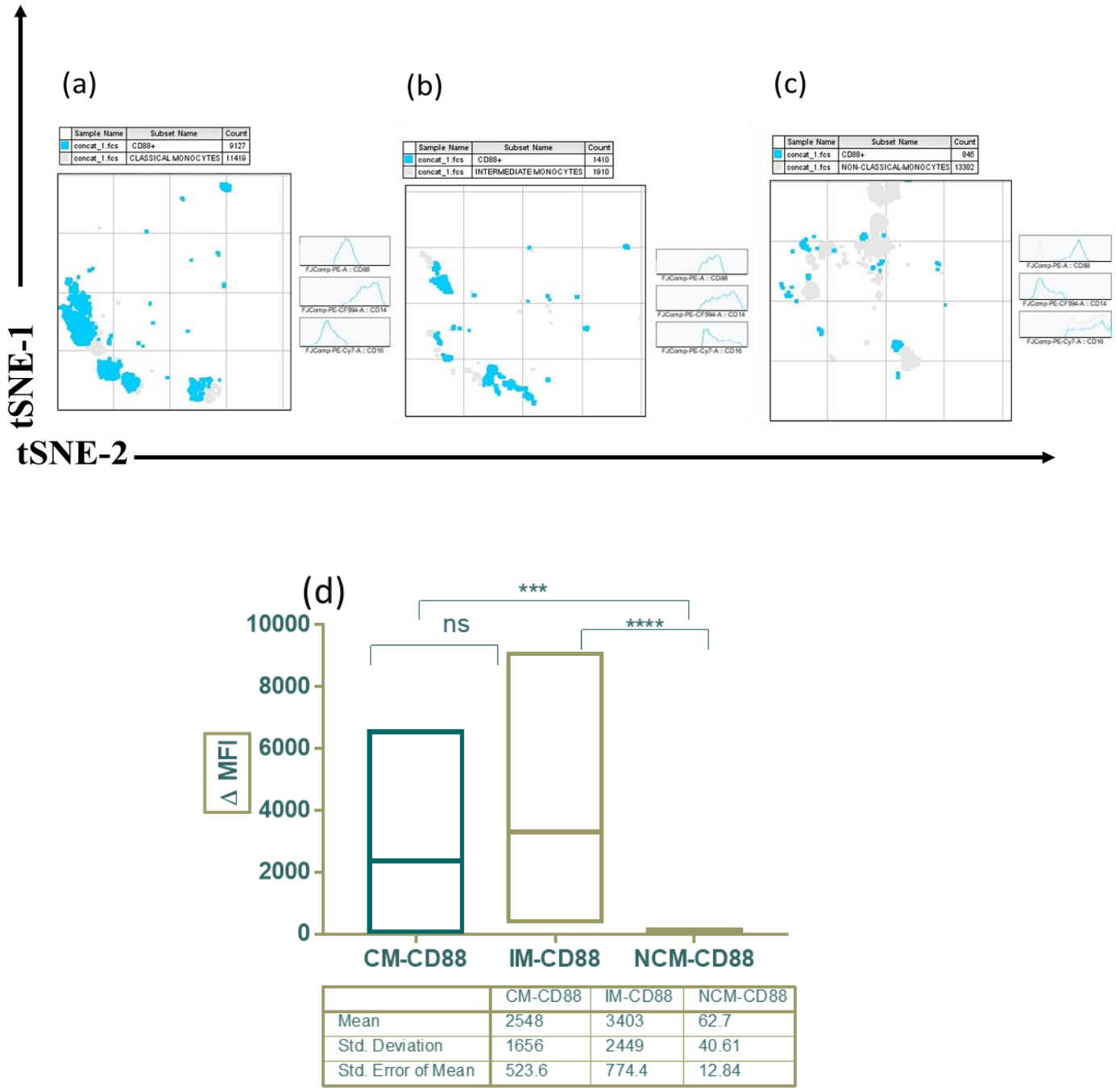

	CM-CD88	IM-CD88	NCM-CD88
Mean	2548	3403	62.7
Std. Deviation	1656	2449	40.61
Std. Error of Mean	523.6	774.4	12.84

Figure 38: Expression of CD88 on three monocyte subsets in peripheral blood mononuclear cells of advanced renal cell carcinoma patients. (a) tSNE plot of CD88 expressing classical monocyte subset, (b) tSNE plot of CD88 expressing intermediate monocyte subset; (c) tSNE plot of CD88 expressing non-classical monocyte subset (d) Box and Whisker plot representing gMFI of CD88 in classical, intermediate, and non-classical monocyte subsets with corresponding column statistics. P-values are represented as (ns:P > 0.05, *: P ≤ 0.05, **: P ≤ 0.01 ***: P ≤ 0.001; ****: P ≤ 0.0001). (gMFI; geometric mean fluorescent intensity, CM; classical Monocytes, N-CM; Non- classical Monocytes IM; Intermediate Monocytes).

3.13. C5aR1(CD88) on circulating monocyte subset and its association with therapy outcome in advanced cancer patients treated with ICIs:

The expression levels of CD88 were associated with the clinical outcome in terms of OS and PFS. univariable Cox proportional hazard analysis was performed between the high expression group and low expression group, divided by a cutoff value (median value of gMFI) in each monocyte subset. In advanced lung cancer patients' higher expression of CD88 on the classical monocyte subset (OS: HR = 1.26, 95% CI: 0.64-2.45, p = 0.4949 and non-classical monocyte subset (OS: HR = 1.65, 95% CI: 0.84-3.21, p = 0.1322) was associated with relatively lower risk of death. **(Figure 38).**

The median OS was 13.7 months v/s 25.2 months for the low v/s high CD88 expressing classical monocytes group the median OS was 16.2 months v/s 22.2 months for the low v/s high CD88 expressing non-classical monocytes group.

A similar trend was observed in melanoma, advanced head and neck cancer, and renal cell carcinoma, but the result remained inconclusive because of the lower sample size.

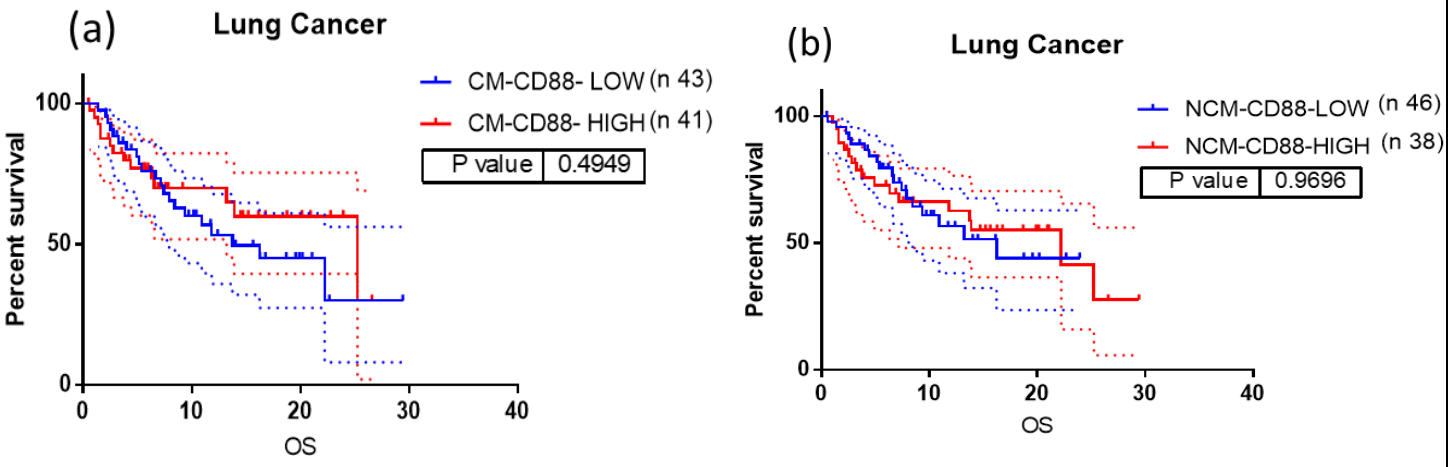

Figure 39: Kaplan-Meier Survival Curves with 95% CI for Overall survival (OS:**a,b**) of advanced lung cancer Patients respectively treated With ICI's. Time is represented in months at baseline. **(a)** OS; CM-CD88 high (red line) v/s CM-CD88 Low (blue line), **(b)** OS; N-CM-CD88 high (red line) v/s N-CM-CD88 Low (blue line) Dotted lines represent upper and lower limit of 95% CI (Confidence Interval) . Results are from univariable cox proportional Hazard model (OS; overall survival PFS; progression free survival CM; classical Monocytes, IM; Intermediate Monocytes).

4. Discussion

The immune system is the core defense against cancer development and progression. Failure of the immune system to recognize and eliminate malignant cells plays an important role in the pathogenesis of cancer. Tumor cells evade immune recognition, in part, due to the immunosuppressive features of the tumor microenvironment. Immunotherapy augments the host immune system to generate an antitumor effect. Immune checkpoints are pathways with inhibitory or stimulatory features that maintain self-tolerance and assist with immune response. The most well-described checkpoints are inhibitory in nature and include the cytotoxic T lymphocyte-associated molecule-4 (CTLA-4), programmed cell death receptor-1 (PD-1), and programmed cell death ligand-1 (PD-L1). Antibodies that block these pathways, also called Immune Checkpoint Inhibitors (ICIs), are developed to enhance the host immunologic activity against tumors and become standard of care in the treatment of many malignancies. However only a small percentage of patients have meaningful responses to these treatments.

The identification of blood-based biomarkers that can predict, at baseline of therapy, the benefits of outcome, remains a challenging task for clinicians. Several studies in literature suggest that peripheral blood based systemic inflammatory biomarkers such as NWR (Neutrophil to white blood cell ratio), PLR (Platelet to Lymphocyte Ratio), NLR (Neutrophil to lymphocyte ratio) , dNLR (derived Neutrophil to lymphocyte ratio),LMR (Lymphocyte to monocyte ratio) and SII (systemic inflammation Index) as good prognosticators (Li et al., 2019) (Zhou et al., 2014) (Ding et al., 2021). In this work we show that, NLR and dNLR had a significant impact on overall and progression free survival in advanced lung cancer, and in melanoma the higher NLR and dNLR was shown to have a poor overall and progression free survival, the mechanism by which NLR and dNLR relates to ICI activity and clinical outcome is unknown. An elevated LMR in advanced lung cancer has shown a better overall survival and longer progression free survival, LMR is believed to reflect the host immune status and the degree of tumor progression. Given that both a low lymphocyte count and high monocyte count reflect insufficient anti-tumor immunity and an elevated tumor burden (Goto et al., 2018). In melanoma a higher PLR was associated with poor progression free survival, the specific mechanism by which the PLR was associated with progression in cancer remains unknown. A higher value of NWR was associated with poor progression free survival in melanoma and advanced head and neck cancer. In advanced lung cancer patients, a higher

systemic inflammation index was associated with poor overall and progression free survival. Overall, these blood-based biomarkers at baseline could be interpreted by clinicians for low-cost and noninvasive prognostic marker for patients receiving ICI's.

Aberrant immune cells have been reported both in tumor microenvironment (TME) and in peripheral blood of cancer patients and these cells greatly influence the tumor progression and failure to ICIs through several immunosuppressive mechanisms (Mallick and Duttaroy, 2021). In this work we report the presence of immature immune suppressive myeloid cell population in peripheral blood by using multicolor flow cytometry and our results demonstrate that higher levels of Mo-MDSCs are associated with progression of the disease in advanced lung cancer and poor overall survival in head and neck cancer patients. These results highlight that only Mo-MDSCs achieve statistically significant prognostic effects. So, an insight in the mechanisms of immunosuppression by MDSCs should be considered. However, different levels of immune and T-cell suppression by these subsets of MDSCs are known: PMN-MDSCs induce antigen-specific T-cell tolerance through high levels of ROS and low levels of NO. Conversely, M-MDSCs impair both antigen-specific and neoantigen-specific T-cell responses through low ROS levels and high NO levels, and this inhibition appears to be continuous. This becomes relevant both for the detection of immunotherapy resistance biomarkers and for the definition of therapeutic strategies targeting MDSCs.

During cancer and inflammation, classical and intermediate monocytes are tethered and invade tissue. It is now widely accepted that classical monocytes can differentiate into monocyte derived macrophages or tumor associated macrophages and play an integral part in shaping inflammation and its resolution in tissues and tumor microenvironment (Robinson et al., 2021). Intermediate monocytes express the highest levels of antigen presentation-related molecules (Sakakura et al., 2021). Some studies shown that intermediate monocyte numbers are expanded in the blood of patients with cancer, implying that they must play an important role. However, their exact role in immunity remains elusive as it is reported that they are the main producers of IL-10. Whether these cells can produce pro- and anti-inflammatory mediators simultaneously or whether there are different kinetics of expression for these factors, especially in tumorigenesis requires further exploration (Prat et al., 2020). In this study we demonstrate that the frequency of occurrence of classical monocytes in advanced lung cancer is associated with higher risk of poor outcome in terms of OS and PFS, which adds to the existing evidence that classical monocytes migrate into tumor sites and then differentiate into TAMs. By contrast, non-classical monocytes have been documented to be

initially protective through the enhancement of NK cell activity (Cassetta and Pollard, 2016). However, in advanced cancers, the protumoral effect of classical monocytes appears to win. Moreover, classical monocytes can stimulate tumor cell transendothelial cell migration in a process mimicking extravasation((Strell and Entschladen, 2008). We observed a similar trend in the intermediate monocytes where the higher levels of this subset were associated with higher risk both in terms of OS and PFS, and this observation is consistent with previous studies showing that a high proportion of intermediate monocytes is positively correlated with decreased effector/regulatory T-cell ratio in tumor ascites(Prat et al., 2020). So, we can postulate tha, higher frequency of classical monocytes and intermediate monocytes in advanced lung cancer produce unfavorable outcome in patients treated with the ICI's

As classical monocyte remains the source of TAMs, and TAMs with high levels of hemeoxigenase-1 (HO-1+) seem to play a crucial defense mechanism through antioxidant, anti-inflammatory and anti-apoptotic properties (Krukowska and Magierowski, 2022). With these premises, we evaluated the prognostic role of HEME catabolism by the assessment of HO-1 expression level in monocytes subpopulations in peripheral blood samples of patients affected by advanced lung cancer. Our results suggest that in advanced lung cancer patients treated with ICIs higher levels of HO-1 in classical monocytes and in non-classical monocytes have a protective role and is associated with lower risk of progression or death, however we could not establish a statistical significance for this. The balance of HO-1 levels maintained in cancer and in normal cells is implicated in cancer prevalence, prognosis, or progression (Fang et al., 2021). Therefore, upregulation of HO-1 in neoplasm surrounding tissues could be considered as a defensive and protective response, this hypothesis is supported by the fact that therapeutic use of CO in various cancer types was already described, demonstrating a wide range of advantages exerted by CO (Tien Vo et al., 2021), however we could not establish a statistically significant correlation between the arterial CO levels and HO-1 expression , further robust analysis is needed to understand this complex phenomenon and role of both CO and HO-1 in TME In contrast to these higher levels of HO-1 in intermediate monocytes were found to be associated with poor outcome in advanced lung cancer, one possible explanation for this could be that in cancer patients there is a bias toward immature status in myeloid cells and expression of immunosuppressive surface molecules by intermediate monocytes may associate with poor outcome (Sakakura et al., 2021). This complex phenomenon within the different subsets of monocytes and this analysis raises a key question on how the signaling pathways that have been defined for the recruitment and

differentiation of monocytes interact with tumor microenvironment, tumor derived factors, and other immune cells, and how these interactions are overlaid with biological factors within the blood and tissue in cancer. This question is also relevant because it might be possible to derive interventions that can define a switch in cell fate or phenotype for therapeutic purposes. Thus, insights into intra- and inter-cellular crosstalk may better inform the roles of myeloid population especially monocyte subsets and macrophages in homeostasis, immunity, and cancer.

Imbalanced complement activation and the deposition of complement proteins have been demonstrated in many types of tumors. Plasma proteins, receptors, and regulators of complement activation regulate several biological functions of stromal and immune cells in the TME and promote the malignant biological properties of tumors. The main pathway involved in complement activation in the TME remains unclear (Afshar-Kharghan, 2017). With the premise that C5a generation in squamous cell carcinomas foster an immunosuppressive TME during carcinogenesis by activating $C5aR1^{+}$ macrophages and C5a mediated macrophage polarization by activation of the nuclear factor-κB (NF-κB) pathway and C5a receptor (C5aR1) expressed on TAMs exhibited a tumor-promoting functional profile (Piao et al., 2018), we evaluated the expression of CD88 (C5aR1) on monocyte subsets. Our results in advanced lung cancer showed CD88 was expressed more on intermediate monocytes but was statistically insignificant compared to the expression on classical monocytes. Non-classical monocytes had the least CD88 expression among the three subsets. In melanoma advanced head and neck cancer and advanced renal cell carcinoma a similar trend was observed but the observation remained inconclusive due to low sample size studied. In advanced lung cancer higher expression of CD88 on classical monocyte subset and non-classical monocyte subset was associated with relatively higher overall survival. However, our results were contrast to the other documented studies on role of complement in creating a immunosuppressive microenvironment it cannot be ruled out because C5a/C5aR is required of maturation of antigen presenting cells and their interactions with T-cells (Kemper and Atkinson, 2007) (Merle et al., 2015) , a scope and possibility is still open for better understanding of the mechanistic interaction between the complement system and TME which might provide a new understanding in cancer immunotherapy.

In conclusion to this study on advanced cancer patients, the clinical blood biomarkers can be postulated as a good prognostic and predictive biomarkers for therapeutic outcomes, as it falls in line with literature and various other independent studies. We were able to phenotype the

MDSCs in peripheral blood samples of advanced lung cancer. Melanoma, Head and neck cancer and Renal cell carcinoma patients, and our data show that Mo-MDSCs play a major role in unfavorable therapeutic outcome in advanced lung cancer and head and neck cancer patients, thus suggesting Mo-MDSCs (given its proven immunosuppressive role in cancer) as a potential target and biomarker for therapeutic intervention. Further we identified three major subsets of monocytes and report that higher frequencies of classical and intermediate, monocytes are associated with poor therapeutic outcomes in advanced lung cancer patients. HO-1 and C5aR1(CD88) expression in these three monocyte subsets were evaluated and our results suggest that both HO-1 and CD88 when expressed in higher levels in/on classical and non-classical monocytes are associated with better therapeutic outcome in advanced lung cancer patients treated with ICI's. At present we could not establish any therapeutic outcome association for MDSCs in melanoma and renal cell carcinoma, also we were not able to establish any therapeutic outcome association between HO-1 expression levels, CD88 expression levels on monocyte subsets in melanoma, head and neck cancer and renal cell carcinoma, this was due to the lower number of patients with this cancer included in the study. This is a set of preliminary findings further deep investigations on heterogeneity of monocyte subsets, myelopoiesis including emergency myelopoiesis, and TME on larger numbers of cancer patients can provide a better understanding on mechanism and factors involved for disease progression and poor therapeutic outcomes.

5. Bibliography

1. Abraham, N.G., 1991. Molecular regulation—Biological role of heme in hematopoiesis. Blood Reviews 5, 19–28. https://doi.org/10.1016/0268-960X(91)90004-V
2. Afshar-Kharghan, V., 2017. The role of the complement system in cancer. J Clin Invest 127, 780–789. https://doi.org/10.1172/JCI90962
3. Aghamajidi, A., Farhangnia, P., Pashangzadeh, S., Damavandi, A.R., Jafari, R., 2022. Tumor-promoting myeloid cells in the pathogenesis of human oncoviruses: potential targets for immunotherapy. Cancer Cell International 22, 327. https://doi.org/10.1186/s12935-022-02727-3
4. Ajona, D., Ortiz-Espinosa, S., Moreno, H., Lozano, T., Pajares, M.J., Agorreta, J., Bértolo, C., Lasarte, J.J., Vicent, S., Hoehlig, K., Vater, A., Lecanda, F., Montuenga, L.M., Pio, R., 2017. A Combined PD-1/C5a Blockade Synergistically Protects against Lung Cancer Growth and Metastasis. Cancer Discovery 7, 694–703. https://doi.org/10.1158/2159-8290.CD-16-1184
5. Alvarez, R., Oliver, L., Valdes, A., Mesa, C., 2018. Cancer-induced systemic myeloid dysfunction: Implications for treatment and a novel nanoparticle approach for its correction. Seminars in Oncology 45, 84–94. https://doi.org/10.1053/j.seminoncol.2018.05.001
6. Applegate, L.A., Luscher, P., Tyrrell, R.M., 1991. Induction of heme oxygenase: a general response to oxidant stress in cultured mammalian cells. Cancer Res 51, 974–978.
7. Arora, S., Velichinskii, R., Lesh, R.W., Ali, U., Kubiak, M., Bansal, P., Borghaei, H., Edelman, M.J., Boumber, Y., 2019. Existing and Emerging Biomarkers for Immune Checkpoint Immunotherapy in Solid Tumors. Adv Ther 36, 2638–2678. https://doi.org/10.1007/s12325-019-01051-z
8. Atkins, M.B., Curiel-Lewandrowski, C., Fisher, D.E., Swetter, S.M., Tsao, H., Aguirre-Ghiso, J.A., Soengas, M.S., Weeraratna, A.T., Flaherty, K.T., Herlyn, M., Sosman, J.A., Tawbi, H.A., Pavlick, A.C., Cassidy, P.B., Chandra, S., Chapman, P.B., Daud, A., Eroglu, Z., Ferris, L.K., Fox, B.A., Gershenwald, J.E., Gibney, G.T., Grossman, D., Hanks, B.A., Hanniford, D., Hernando, E., Jeter, J.M., Johnson, D.B., Khleif, S.N., Kirkwood, J.M., Leachman, S.A., Mays, D., Nelson, K.C., Sondak, V.K., Sullivan, R.J., Merlino, G., 2021. The State of Melanoma: Emergent Challenges and Opportunities. Clin Cancer Res 27, 2678–2697. https://doi.org/10.1158/1078-0432.CCR-20-4092
9. Balla, G., Jacob, H.S., Balla, J., Rosenberg, M., Nath, K., Apple, F., Eaton, J.W., Vercellotti, G.M., 1992. Ferritin: a cytoprotective antioxidant strategem of endothelium. Journal of Biological Chemistry 267, 18148–18153. https://doi.org/10.1016/S0021-9258(19)37165-0
10. Benjamin, D.J., Lyou, Y., 2021. Advances in Immunotherapy and the TGF-β Resistance Pathway in Metastatic Bladder Cancer. Cancers 13, 5724. https://doi.org/10.3390/cancers13225724
11. Bernardo, M., Tolstykh, T., Zhang, Y., Bangari, D.S., Cao, H., Heyl, K.A., Lee, J.S., Malkova, N.V., Malley, K., Marquez, E., Pollard, J., Qu, H., Roberts, E., Ryan, S., Singh, K., Sun, F., Wang, E., Bahjat, K., Wiederschain, D., Wagenaar, T.R., n.d. An experimental model of anti-PD-1 resistance exhibits activation of TGFß and Notch pathways and is sensitive to local mRNA immunotherapy. Oncoimmunology 10, 1881268. https://doi.org/10.1080/2162402X.2021.1881268

12. Blattner, C., Fleming, V., Weber, R., Himmelhan, B., Altevogt, P., Gebhardt, C., Schulze, T.J., Razon, H., Hawila, E., Wildbaum, G., Utikal, J., Karin, N., Umansky, V., 2018. CCR5+ Myeloid-Derived Suppressor Cells Are Enriched and Activated in Melanoma Lesions. Cancer Res 78, 157–167. https://doi.org/10.1158/0008-5472.CAN-17-0348
13. Bolton, K.L., Gillis, N.K., Coombs, C.C., Takahashi, K., Zehir, A., Bejar, R., Garcia-Manero, G., Futreal, A., Jensen, B.C., Diaz, L.A., Gupta, D., Mantha, S., Klimek, V., Papaemmanuil, E., Levine, R., Padron, E., 2019. Managing Clonal Hematopoiesis in Patients With Solid Tumors. JCO 37, 7–11. https://doi.org/10.1200/JCO.18.00331
14. Boscolo-Rizzo, P., Zorzi, M., Del Mistro, A., Da Mosto, M.C., Tirelli, G., Buzzoni, C., Rugge, M., Polesel, J., Guzzinati, S., 2018. The evolution of the epidemiological landscape of head and neck cancer in Italy: Is there evidence for an increase in the incidence of potentially HPV-related carcinomas? PLoS One 13, e0192621. https://doi.org/10.1371/journal.pone.0192621
15. Boyette, L.B., Macedo, C., Hadi, K., Elinoff, B.D., Walters, J.T., Ramaswami, B., Chalasani, G., Taboas, J.M., Lakkis, F.G., Metes, D.M., 2017. Phenotype, function, and differentiation potential of human monocyte subsets. PLOS ONE 12, e0176460. https://doi.org/10.1371/journal.pone.0176460
16. Bronte, V., Brandau, S., Chen, S.-H., Colombo, M.P., Frey, A.B., Greten, T.F., Mandruzzato, S., Murray, P.J., Ochoa, A., Ostrand-Rosenberg, S., Rodriguez, P.C., Sica, A., Umansky, V., Vonderheide, R.H., Gabrilovich, D.I., 2016. Recommendations for myeloid-derived suppressor cell nomenclature and characterization standards. Nat Commun 7, 12150. https://doi.org/10.1038/ncomms12150
17. Bukavina, L., Bensalah, K., Bray, F., Carlo, M., Challacombe, B., Karam, J.A., Kassouf, W., Mitchell, T., Montironi, R., O'Brien, T., Panebianco, V., Scelo, G., Shuch, B., van Poppel, H., Blosser, C.D., Psutka, S.P., 2022. Epidemiology of Renal Cell Carcinoma: 2022 Update. European Urology 82, 529–542. https://doi.org/10.1016/j.eururo.2022.08.019
18. C5a receptors C5aR1 and C5aR2 mediate opposing pathologies in a mouse model of melanoma, n.d. https://doi.org/10.1096/fj.201800980RR
19. Canè, S., Ugel, S., Trovato, R., Marigo, I., De Sanctis, F., Sartoris, S., Bronte, V., 2019. The Endless Saga of Monocyte Diversity. Frontiers in Immunology 10.
20. Cassetta, L., Pollard, J.W., 2016. Cancer immunosurveillance: role of patrolling monocytes. Cell Res 26, 3–4. https://doi.org/10.1038/cr.2015.144
21. Coffelt, S.B., Kersten, K., Doornebal, C.W., Weiden, J., Vrijland, K., Hau, C.-S., Verstegen, N.J.M., Ciampricotti, M., Hawinkels, L.J.A.C., Jonkers, J., de Visser, K.E., 2015. IL-17-producing γδ T cells and neutrophils conspire to promote breast cancer metastasis. Nature 522, 345–348. https://doi.org/10.1038/nature14282
22. Condamine, T., Gabrilovich, D.I., 2011. Molecular mechanisms regulating myeloid-derived suppressor cell differentiation and function. Trends Immunol 32, 19–25. https://doi.org/10.1016/j.it.2010.10.002
23. Consonni, F.M., Bleve, A., Totaro, M.G., Storto, M., Kunderfranco, P., Termanini, A., Pasqualini, F., Alì, C., Pandolfo, C., Sgambelluri, F., Grazia, G., Santinami, M., Maurichi, A., Milione, M., Erreni, M., Doni, A., Fabbri, M., Gribaldo, L., Rulli, E., Soares, M.P., Torri, V., Mortarini, R., Anichini, A., Sica, A., 2021. Heme catabolism by tumor-associated macrophages controls metastasis formation. Nat Immunol 22, 595–606. https://doi.org/10.1038/s41590-021-00921-5
24. Cormican, S., Griffin, M.D., 2020. Human Monocyte Subset Distinctions and Function: Insights From Gene Expression Analysis. Frontiers in Immunology 11.

25. Cramer, J.D., Burtness, B., Ferris, R.L., 2019. Immunotherapy for head and neck cancer: Recent advances and future directions. Oral Oncol 99, 104460. https://doi.org/10.1016/j.oraloncology.2019.104460
26. Cuitino, L., Obreque, J., Gajardo-Meneses, P., Villarroel, A., Crisóstomo, N., San Francisco, I.F., Valenzuela, R.A., Méndez, G.P., Llanos, C., 2019. Heme-Oxygenase-1 Is Decreased in Circulating Monocytes and Is Associated With Impaired Phagocytosis and ROS Production in Lupus Nephritis. Front Immunol 10, 2868. https://doi.org/10.3389/fimmu.2019.02868
27. Curti, B.D., Faries, M.B., 2021. Recent Advances in the Treatment of Melanoma. N Engl J Med 384, 2229–2240. https://doi.org/10.1056/NEJMra2034861
28. Debela, D.T., Muzazu, S.G., Heraro, K.D., Ndalama, M.T., Mesele, B.W., Haile, D.C., Kitui, S.K., Manyazewal, T., 2021. New approaches and procedures for cancer treatment: Current perspectives. SAGE Open Medicine 9, 20503121211034370. https://doi.org/10.1177/20503121211034366
29. Denis, M., Grasselly, C., Choffour, P.-A., Wierinckx, A., Mathé, D., Chettab, K., Tourette, A., Talhi, N., Bourguignon, A., Birzele, F., Kress, E., Jordheim, L.P., Klein, C., Matera, E.-L., Dumontet, C., 2022. In Vivo Syngeneic Tumor Models with Acquired Resistance to Anti–PD-1/PD-L1 Therapies. Cancer Immunology Research 10, 1013–1027. https://doi.org/10.1158/2326-6066.CIR-21-0802
30. Ding, M., Song, Y., Jing, J., Tian, M., Ding, L., Li, Q., Zhou, C., Dong, H., Ni, Y., Mou, Y., 2021. The Ratio of Preoperative Serum Biomarkers Predicts Prognosis in Patients With Oral Squamous Cell Carcinoma. Frontiers in Oncology 11.
31. Dominguez, C., McCampbell, K.K., David, J.M., Palena, C., n.d. Neutralization of IL-8 decreases tumor PMN-MDSCs and reduces mesenchymalization of claudin-low triple-negative breast cancer. JCI Insight 2, e94296. https://doi.org/10.1172/jci.insight.94296
32. Dyba, T., Randi, G., Bray, F., Martos, C., Giusti, F., Nicholson, N., Gavin, A., Flego, M., Neamtiu, L., Dimitrova, N., Carvalho, R.N., Ferlay, J., Bettio, M., 2021. The European cancer burden in 2020: Incidence and mortality estimates for 40 countries and 25 major cancers. European Journal of Cancer 157, 308–347. https://doi.org/10.1016/j.ejca.2021.07.039
33. Dyck, L., Prendeville, H., Raverdeau, M., Wilk, M.M., Loftus, R.M., Douglas, A., McCormack, J., Moran, B., Wilkinson, M., Mills, E.L., Doughty, M., Fabre, A., Heneghan, H., LeRoux, C., Hogan, A., Chouchani, E.T., O'Shea, D., Brennan, D., Lynch, L., 2022. Suppressive effects of the obese tumor microenvironment on CD8 T cell infiltration and effector function. J Exp Med 219, e20210042. https://doi.org/10.1084/jem.20210042
34. Dysthe, M., Parihar, R., 2020. Myeloid-Derived Suppressor Cells in the Tumor Microenvironment, in: Birbrair, A. (Ed.), Tumor Microenvironment: Hematopoietic Cells – Part A, Advances in Experimental Medicine and Biology. Springer International Publishing, Cham, pp. 117–140. https://doi.org/10.1007/978-3-030-35723-8_8
35. Esfahani, K., Roudaia, L., Buhlaiga, N., Del Rincon, S.V., Papneja, N., Miller, W.H., 2020. A review of cancer immunotherapy: from the past, to the present, to the future. Curr Oncol 27, S87–S97. https://doi.org/10.3747/co.27.5223
36. Fang, J., Islam, R., Gao, S., Zhang, C., Kunisaki, R., Sakaguchi, S., Honda, N., Zhou, J.-R., Yokomizo, K., 2021. Expression Dynamics of Heme Oxygenase-1 in Tumor Cells and the Host Contributes to the Progression of Tumors. Journal of Personalized Medicine 11, 1340. https://doi.org/10.3390/jpm11121340

37. Forkasiewicz, A., Dorociak, M., Stach, K., Szelachowski, P., Tabola, R., Augoff, K., 2020. The usefulness of lactate dehydrogenase measurements in current oncological practice. Cellular & Molecular Biology Letters 25, 35. https://doi.org/10.1186/s11658-020-00228-7
38. Forsea, A.-M., 2020. Melanoma Epidemiology and Early Detection in Europe: Diversity and Disparities. Dermatol Pract Concept 10, e2020033. https://doi.org/10.5826/dpc.1003a33
39. Fujimura, T., Kambayashi, Y., Aiba, S., 2012. Crosstalk between regulatory T cells (Tregs) and myeloid derived suppressor cells (MDSCs) during melanoma growth. Oncoimmunology 1, 1433–1434. https://doi.org/10.4161/onci.21176
40. Gabrilovich, D.I., Nagaraj, S., 2009. Myeloid-derived suppressor cells as regulators of the immune system. Nat Rev Immunol 9, 162–174. https://doi.org/10.1038/nri2506
41. Gabrilovich, D.I., Ostrand-Rosenberg, S., Bronte, V., 2012. Coordinated regulation of myeloid cells by tumours. Nat Rev Immunol 12, 253–268. https://doi.org/10.1038/nri3175
42. Galon, J., Bruni, D., 2020. Tumor Immunology and Tumor Evolution: Intertwined Histories. Immunity 52, 55–81. https://doi.org/10.1016/j.immuni.2019.12.018
43. Gao, J., Liu, W.-R., Tang, Z., Fan, J., Shi, Y.-H., 2022. Myeloid-derived suppressor cells in cancer. iLIVER 1, 81–89. https://doi.org/10.1016/j.iliver.2022.06.002
44. Giles, A.J., Chien, C.D., Reid, C.M., Fry, T.J., Park, D.M., Kaplan, R.N., Gilbert, M.R., 2016. The functional interplay between systemic cancer and the hematopoietic stem cell niche. Pharmacol Ther 168, 53–60. https://doi.org/10.1016/j.pharmthera.2016.09.006
45. Gimeno, R., Barquinero, J., 2011. Myeloid-derived suppressor cells (MDSC): Another player in the orchestra. Inmunologia 30, 45–53. https://doi.org/10.1016/S0213-9626(11)70015-4
46. Gordon, S., Plüddemann, A., 2019. The Mononuclear Phagocytic System. Generation of Diversity. Frontiers in Immunology 10.
47. Goto, W., Kashiwagi, S., Asano, Y., Takada, K., Takahashi, K., Hatano, T., Takashima, T., Tomita, S., Motomura, H., Hirakawa, K., Ohira, M., 2018. Predictive value of lymphocyte-to-monocyte ratio in the preoperative setting for progression of patients with breast cancer. BMC Cancer 18, 1137. https://doi.org/10.1186/s12885-018-5051-9
48. Greten, F.R., Grivennikov, S.I., 2019. Inflammation and Cancer: Triggers, Mechanisms, and Consequences. Immunity 51, 27–41. https://doi.org/10.1016/j.immuni.2019.06.025
49. Hagerling, C., Gonzalez, H., Salari, K., Wang, C.-Y., Lin, C., Robles, I., van Gogh, M., Dejmek, A., Jirström, K., Werb, Z., 2019. Immune effector monocyte–neutrophil cooperation induced by the primary tumor prevents metastatic progression of breast cancer. Proceedings of the National Academy of Sciences 116, 21704–21714. https://doi.org/10.1073/pnas.1907660116
50. Hanna, R.N., Cekic, C., Sag, D., Tacke, R., Thomas, G.D., Nowyhed, H., Herrley, E., Rasquinha, N., McArdle, S., Wu, R., Peluso, E., Metzger, D., Ichinose, H., Shaked, I., Chodaczek, G., Biswas, S.K., Hedrick, C.C., 2015. Patrolling monocytes control tumor metastasis to the lung. Science 350, 985–990. https://doi.org/10.1126/science.aac9407
51. Hiam-Galvez, K.J., Allen, B.M., Spitzer, M.H., 2021. Systemic immunity in cancer. Nat Rev Cancer 21, 345–359. https://doi.org/10.1038/s41568-021-00347-z
52. Hoechst, B., Voigtlaender, T., Ormandy, L., Gamrekelashvili, J., Zhao, F., Wedemeyer, H., Lehner, F., Manns, M.P., Greten, T.F., Korangy, F., 2009. Myeloid

Derived Suppressor Cells Inhibit Natural Killer Cells in Patients with Hepatocellular Carcinoma via the NKp30 Receptor. Hepatology 50, 799–807. https://doi.org/10.1002/hep.23054
53. Hofer, F., Di Sario, G., Musiu, C., Sartoris, S., De Sanctis, F., Ugel, S., 2021. A Complex Metabolic Network Confers Immunosuppressive Functions to Myeloid-Derived Suppressor Cells (MDSCs) within the Tumour Microenvironment. Cells 10, 2700. https://doi.org/10.3390/cells10102700
54. Hofmarcher, T., Lindgren, P., Wilking, N., Jönsson, B., 2020. The cost of cancer in Europe 2018. European Journal of Cancer 129, 41–49. https://doi.org/10.1016/j.ejca.2020.01.011
55. Infante, J., García-Gorostiaga, I., Sánchez-Juan, P., Sierra, M., Martín-Gurpegui, J.L., Terrazas, J., Mateo, I., Rodríguez-Rodríguez, E., Berciano, J., Combarros, O., 2010. Synergistic effect of two oxidative stress-related genes (heme oxygenase-1 and GSK3β) on the risk of Parkinson's disease. European Journal of Neurology 17, 760–762. https://doi.org/10.1111/j.1468-1331.2009.02908.x
56. Iranzo, P., Callejo, A., Assaf, J.D., Molina, G., Lopez, D.E., Garcia-Illescas, D., Pardo, N., Navarro, A., Martinez-Marti, A., Cedres, S., Carbonell, C., Frigola, J., Amat, R., Felip, E., 2022. Overview of Checkpoint Inhibitors Mechanism of Action: Role of Immune-Related Adverse Events and Their Treatment on Progression of Underlying Cancer. Frontiers in Medicine 9.
57. Jansen, T., Daiber, A., 2012. Direct Antioxidant Properties of Bilirubin and Biliverdin. Is there a Role for Biliverdin Reductase? Frontiers in Pharmacology 3.
58. Jayaraman, P., Parikh, F., Newton, J.M., Hanoteau, A., Rivas, C., Krupar, R., Rajapakshe, K., Pathak, R., Kanthaswamy, K., MacLaren, C., Huang, S., Coarfa, C., Spanos, C., Edwards, D.P., Parihar, R., Sikora, A.G., 2018. TGF-β1 programmed myeloid-derived suppressor cells (MDSC) acquire immune-stimulating and tumor killing activity capable of rejecting established tumors in combination with radiotherapy. Oncoimmunology 7, e1490853. https://doi.org/10.1080/2162402X.2018.1490853
59. Jeney, V., Balla, J., Yachie, A., Varga, Z., Vercellotti, G.M., Eaton, J.W., Balla, G., 2002. Pro-oxidant and cytotoxic effects of circulating heme. Blood 100, 879–887. https://doi.org/10.1182/blood.V100.3.879
60. Jin, J., Lin, J., Xu, A., Lou, J., Qian, C., Li, X., Wang, Y., Yu, W., Tao, H., 2021. CCL2: An Important Mediator Between Tumor Cells and Host Cells in Tumor Microenvironment. Front Oncol 11, 722916. https://doi.org/10.3389/fonc.2021.722916
61. Johnson, D.E., Burtness, B., Leemans, C.R., Lui, V.W.Y., Bauman, J.E., Grandis, J.R., 2020. Head and neck squamous cell carcinoma. Nat Rev Dis Primers 6, 1–22. https://doi.org/10.1038/s41572-020-00224-3
62. Kapellos, T.S., Bonaguro, L., Gemünd, I., Reusch, N., Saglam, A., Hinkley, E.R., Schultze, J.L., 2019. Human Monocyte Subsets and Phenotypes in Major Chronic Inflammatory Diseases. Front Immunol 10, 2035. https://doi.org/10.3389/fimmu.2019.02035
63. Kapturczak, M.H., Wasserfall, C., Brusko, T., Campbell-Thompson, M., Ellis, T.M., Atkinson, M.A., Agarwal, A., 2004. Heme Oxygenase-1 Modulates Early Inflammatory Responses: Evidence from the Heme Oxygenase-1-Deficient Mouse. The American Journal of Pathology 165, 1045–1053. https://doi.org/10.1016/S0002-9440(10)63365-2
64. Kemper, C., Atkinson, J.P., 2007. T-cell regulation: with complements from innate immunity. Nat Rev Immunol 7, 9–18. https://doi.org/10.1038/nri1994

65. Keyse, S.M., Tyrrell, R.M., 1989. Heme oxygenase is the major 32-kDa stress protein induced in human skin fibroblasts by UVA radiation, hydrogen peroxide, and sodium arsenite. Proc Natl Acad Sci U S A 86, 99–103.
66. Kietzmann, T., Samoylenko, A., Immenschuh, S., 2003. Transcriptional Regulation of Heme Oxygenase-1 Gene Expression by MAP Kinases of the JNK and p38 Pathways in Primary Cultures of Rat Hepatocytes*. Journal of Biological Chemistry 278, 17927–17936. https://doi.org/10.1074/jbc.M203929200
67. Krishnamoorthy, M., Gerhardt, L., Maleki Vareki, S., 2021. Immunosuppressive Effects of Myeloid-Derived Suppressor Cells in Cancer and Immunotherapy. Cells 10, 1170. https://doi.org/10.3390/cells10051170
68. Krukowska, K., Magierowski, M., 2022. Carbon monoxide (CO)/heme oxygenase (HO)-1 in gastrointestinal tumors pathophysiology and pharmacology - possible anti- and pro-cancer activities. Biochemical Pharmacology 201, 115058. https://doi.org/10.1016/j.bcp.2022.115058
69. Kwak, T., Wang, F., Deng, H., Condamine, T., Kumar, V., Perego, M., Kossenkov, A., Montaner, L.J., Xu, X., Xu, W., Zheng, C., Schuchter, L.M., Amaravadi, R.K., Mitchell, T.C., Karakousis, G.C., Mulligan, C., Nam, B., Masters, G., Hockstein, N., Bennett, J., Nefedova, Y., Gabrilovich, D.I., 2020. Distinct Populations of Immune-Suppressive Macrophages Differentiate from Monocytic Myeloid-Derived Suppressor Cells in Cancer. Cell Reports 33, 108571. https://doi.org/10.1016/j.celrep.2020.108571
70. Kwiecień, I., Rutkowska, E., Polubiec-Kownacka, M., Raniszewska, A., Rzepecki, P., Domagała-Kulawik, J., 2020a. Blood Monocyte Subsets with Activation Markers in Relation with Macrophages in Non-Small Cell Lung Cancer. Cancers (Basel) 12, 2513. https://doi.org/10.3390/cancers12092513
71. Kwiecień, I., Rutkowska, E., Polubiec-Kownacka, M., Rzepecki, P., Domagała-Kulawik, J., 2020b. Relationship between blood monocyte subsets with activation markers and macrophages in non-small cell lung cancer. European Respiratory Journal 56. https://doi.org/10.1183/13993003.congress-2020.1739
72. Lan, Y., Zhang, D., Xu, C., Hance, K.W., Marelli, B., Qi, J., Yu, H., Qin, G., Sircar, A., Hernández, V.M., Jenkins, M.H., Fontana, R.E., Deshpande, A., Locke, G., Sabzevari, H., Radvanyi, L., Lo, K.-M., 2018. Enhanced preclinical antitumor activity of M7824, a bifunctional fusion protein simultaneously targeting PD-L1 and TGF-β. Science Translational Medicine 10, eaan5488. https://doi.org/10.1126/scitranslmed.aan5488
73. Li, M., He, L., Zhu, J., Zhang, P., Liang, S., 2022. Targeting tumor-associated macrophages for cancer treatment. Cell & Bioscience 12, 85. https://doi.org/10.1186/s13578-022-00823-5
74. Li, M., Spakowicz, D., Burkart, J., Patel, S., Husain, M., He, K., Bertino, E.M., Shields, P.G., Carbone, D.P., Verschraegen, C.F., Presley, C.J., Otterson, G.A., Kendra, K., Owen, D.H., 2019. Change in neutrophil to lymphocyte ratio during immunotherapy treatment is a non-linear predictor of patient outcomes in advanced cancers. J Cancer Res Clin Oncol 145, 2541–2546. https://doi.org/10.1007/s00432-019-02982-4
75. Li, T., Liu, T., Zhu, W., Xie, S., Zhao, Z., Feng, B., Guo, H., Yang, R., 2021. Targeting MDSC for Immune-Checkpoint Blockade in Cancer Immunotherapy: Current Progress and New Prospects. Clin Med Insights Oncol 15, 11795549211035540. https://doi.org/10.1177/11795549211035540

76. Liu, C., Wang, M., Zhang, H., Li, C., Zhang, T., Liu, H., Zhu, S., Chen, J., 2022. Tumor microenvironment and immunotherapy of oral cancer. European Journal of Medical Research 27, 198. https://doi.org/10.1186/s40001-022-00835-4
77. Liu, X., Hogg, G.D., DeNardo, D.G., 2021. Rethinking immune checkpoint blockade: 'Beyond the T cell.' J Immunother Cancer 9, e001460. https://doi.org/10.1136/jitc-2020-001460
78. Mallick, R., Duttaroy, A.K., 2021. Can interruption of innate immune recognition-mediated emergency myelopoiesis impede tumor progression? Medical Hypotheses 155, 110663. https://doi.org/10.1016/j.mehy.2021.110663
79. Mantovani, A., Allavena, P., Marchesi, F., Garlanda, C., 2022. Macrophages as tools and targets in cancer therapy. Nat Rev Drug Discov 21, 799–820. https://doi.org/10.1038/s41573-022-00520-5
80. Mazzone, G.L., Rigato, I., Ostrow, J.D., Bossi, F., Bortoluzzi, A., Sukowati, C.H.C., Tedesco, F., Tiribelli, C., 2009. Bilirubin inhibits the TNFα-related induction of three endothelial adhesion molecules. Biochemical and Biophysical Research Communications 386, 338–344. https://doi.org/10.1016/j.bbrc.2009.06.029
81. Melero, I., Rouzaut, A., Motz, GregT., Coukos, G., 2014. T-Cell and NK-Cell Infiltration into Solid Tumors: A Key Limiting Factor for Efficacious Cancer Immunotherapy. Cancer Discov 4, 522–526. https://doi.org/10.1158/2159-8290.CD-13-0985
82. Merah-Mourah, F., Cohen, S.O., Charron, D., Mooney, N., Haziot, A., 2020. Identification of Novel Human Monocyte Subsets and Evidence for Phenotypic Groups Defined by Interindividual Variations of Expression of Adhesion Molecules. Sci Rep 10, 4397. https://doi.org/10.1038/s41598-020-61022-1
83. Merle, N.S., Noe, R., Halbwachs-Mecarelli, L., Fremeaux-Bacchi, V., Roumenina, L.T., 2015. Complement System Part II: Role in Immunity. Frontiers in Immunology 6.
84. Miao, P., Sheng, S., Sun, X., Liu, J., Huang, G., 2013. Lactate dehydrogenase a in cancer: A promising target for diagnosis and therapy. IUBMB Life 65, 904–910. https://doi.org/10.1002/iub.1216
85. Millrud, C.R., Bergenfelz, C., Leandersson, K., 2016. On the origin of myeloid-derived suppressor cells. Oncotarget 8, 3649–3665. https://doi.org/10.18632/oncotarget.12278
86. Morad, G., Helmink, B.A., Sharma, P., Wargo, J.A., 2021. Hallmarks of response, resistance, and toxicity to immune checkpoint blockade. Cell 184, 5309–5337. https://doi.org/10.1016/j.cell.2021.09.020
87. Murciano-Goroff, Y.R., Warner, A.B., Wolchok, J.D., 2020. The future of cancer immunotherapy: microenvironment-targeting combinations. Cell Res 30, 507–519. https://doi.org/10.1038/s41422-020-0337-2
88. Murdoch, C., Muthana, M., Coffelt, S.B., Lewis, C.E., 2008. The role of myeloid cells in the promotion of tumour angiogenesis. Nat Rev Cancer 8, 618–631. https://doi.org/10.1038/nrc2444
89. Olingy, C.E., Dinh, H.Q., Hedrick, C.C., 2019. Monocyte heterogeneity and functions in cancer. J Leukoc Biol 106, 309–322. https://doi.org/10.1002/JLB.4RI0818-311R
90. Otterbein, L.E., Bach, F.H., Alam, J., Soares, M., Tao Lu, H., Wysk, M., Davis, R.J., Flavell, R.A., Choi, A.M.K., 2000. Carbon monoxide has anti-inflammatory effects involving the mitogen-activated protein kinase pathway. Nat Med 6, 422–428. https://doi.org/10.1038/74680

91. Ożańska, A., Szymczak, D., Rybka, J., 2020. Pattern of human monocyte subpopulations in health and disease. Scandinavian Journal of Immunology 92, e12883. https://doi.org/10.1111/sji.12883
92. Petitprez, F., Meylan, M., de Reyniès, A., Sautès-Fridman, C., Fridman, W.H., 2020. The Tumor Microenvironment in the Response to Immune Checkpoint Blockade Therapies. Frontiers in Immunology 11.
93. Petrache, I., Otterbein, L.E., Alam, J., Wiegand, G.W., Choi, A.M., 2000. Heme oxygenase-1 inhibits TNF-alpha-induced apoptosis in cultured fibroblasts. Am J Physiol Lung Cell Mol Physiol 278, L312-319. https://doi.org/10.1152/ajplung.2000.278.2.L312
94. Piao, C., Zhang, W.-M., Li, T.-T., Zhang, C., Qiu, S., Liu, Y., Liu, S., Jin, M., Jia, L.-X., Song, W.-C., Du, J., 2018. Complement 5a stimulates macrophage polarization and contributes to tumor metastases of colon cancer. Experimental Cell Research 366, 127–138. https://doi.org/10.1016/j.yexcr.2018.03.009
95. Porta, C., Sica, A., Riboldi, E., 2018. Tumor-associated myeloid cells: new understandings on their metabolic regulation and their influence in cancer immunotherapy. The FEBS Journal 285, 717–733. https://doi.org/10.1111/febs.14288
96. Prat, M., Naour, A.L., Coulson, K., Lemée, F., Leray, H., Jacquemin, G., Rahabi, M.C., Lemaitre, L., Authier, H., Ferron, G., Barret, J.-M., Martinez, A., Ayyoub, M., Delord, J.-P., Gladieff, L., Tabah-Fisch, I., Prost, J.-F., Couderc, B., Coste, A., 2020. Circulating CD14high CD16low intermediate blood monocytes as a biomarker of ascites immune status and ovarian cancer progression. J Immunother Cancer 8, e000472. https://doi.org/10.1136/jitc-2019-000472
97. Reis-Sobreiro, M., Teixeira da Mota, A., Jardim, C., Serre, K., 2021. Bringing Macrophages to the Frontline against Cancer: Current Immunotherapies Targeting Macrophages. Cells 10, 2364. https://doi.org/10.3390/cells10092364
98. Robinson, A., Han, C.Z., Glass, C.K., Pollard, J.W., 2021. Monocyte Regulation in Homeostasis and Malignancy. Trends in Immunology 42, 104–119. https://doi.org/10.1016/j.it.2020.12.001
99. Sakakura, K., Takahashi, H., Motegi, S.-I., Yokobori-Kuwabara, Y., Oyama, T., Chikamatsu, K., 2021. Immunological features of circulating monocyte subsets in patients with squamous cell carcinoma of the head and neck. Clinical Immunology 225, 108677. https://doi.org/10.1016/j.clim.2021.108677
100. Sanaei, M.-J., Salimzadeh, L., Bagheri, N., 2020. Crosstalk between myeloid-derived suppressor cells and the immune system in prostate cancer. Journal of Leukocyte Biology 107, 43–56. https://doi.org/10.1002/JLB.4RU0819-150RR
101. Sankar, K., Ye, J.C., Li, Z., Zheng, L., Song, W., Hu-Lieskovan, S., 2022. The role of biomarkers in personalized immunotherapy. Biomarker Research 10, 32. https://doi.org/10.1186/s40364-022-00378-0
102. Scalea, J.R., Lee, Y., Davila, E., Bromberg, J.S., 2018. Myeloid-Derived Suppressor Cells and their Potential Application in Transplantation. Transplantation 102, 359–367. https://doi.org/10.1097/TP.0000000000002022
103. Schauer, D., Starlinger, P., Reiter, C., Jahn, N., Zajc, P., Buchberger, E., Bachleitner-Hofmann, T., Bergmann, M., Stift, A., Gruenberger, T., Brostjan, C., 2012. Intermediate Monocytes but Not TIE2-Expressing Monocytes Are a Sensitive Diagnostic Indicator for Colorectal Cancer. PLOS ONE 7, e44450. https://doi.org/10.1371/journal.pone.0044450
104. Senent, Y., Tavira, B., Pio, R., Ajona, D., 2022. The complement system as a regulator of tumor-promoting activities mediated by myeloid-derived suppressor cells. Cancer Letters 549, 215900. https://doi.org/10.1016/j.canlet.2022.215900

105. Sharma, P., Allison, J.P., 2015. Immune Checkpoint Targeting in Cancer Therapy: Toward Combination Strategies with Curative Potential. Cell 161, 205–214. https://doi.org/10.1016/j.cell.2015.03.030
106. Sica, A., Guarneri, V., Gennari, A., n.d. Myelopoiesis, metabolism and therapy: a crucial crossroads in cancer progression. Cell Stress 3, 284–294. https://doi.org/10.15698/cst2019.09.197
107. Siddiqui, F., Vaqar, S., Siddiqui, A.H., 2022. Lung Cancer, in: StatPearls. StatPearls Publishing, Treasure Island (FL).
108. Song, B.-N., Kim, S.-K., Mun, J.-Y., Choi, Y.-D., Leem, S.-H., Chu, I.-S., 2019. Identification of an immunotherapy-responsive molecular subtype of bladder cancer. EBioMedicine 50, 238–245. https://doi.org/10.1016/j.ebiom.2019.10.058
109. Stewart, T.J., Smyth, M.J., 2011. Improving cancer immunotherapy by targeting tumor-induced immune suppression. Cancer Metastasis Rev 30, 125–140. https://doi.org/10.1007/s10555-011-9280-5
110. Strell, C., Entschladen, F., 2008. Extravasation of leukocytes in comparison to tumor cells. Cell Communication and Signaling 6, 10. https://doi.org/10.1186/1478-811X-6-10
111. Tang, H., Qiao, J., Fu, Y.-X., 2016. Immunotherapy and tumor microenvironment. Cancer Letters 370, 85–90. https://doi.org/10.1016/j.canlet.2015.10.009
112. Tang, T., Huang, X., Zhang, G., Hong, Z., Bai, X., Liang, T., 2021. Advantages of targeting the tumor immune microenvironment over blocking immune checkpoint in cancer immunotherapy. Sig Transduct Target Ther 6, 1–13. https://doi.org/10.1038/s41392-020-00449-4
113. Tecchio, C., Huber, V., Scapini, P., Calzetti, F., Margotto, D., Todeschini, G., Pilla, L., Martinelli, G., Pizzolo, G., Rivoltini, L., Cassatella, M.A., 2004. IFNα-stimulated neutrophils and monocytes release a soluble form of TNF-related apoptosis-inducing ligand (TRAIL/Apo-2 ligand) displaying apoptotic activity on leukemic cells. Blood 103, 3837–3844. https://doi.org/10.1182/blood-2003-08-2806
114. Tenhunen, R., Marver, H.S., Schmid, R., 1968. The enzymatic conversion of heme to bilirubin by microsomal heme oxygenase. Proc Natl Acad Sci U S A 61, 748–755. https://doi.org/10.1073/pnas.61.2.748
115. Thurman, J.M., Laskowski, J., Nemenoff, R.A., 2020. Complement and Cancer—A Dysfunctional Relationship? Antibodies 9, 61. https://doi.org/10.3390/antib9040061
116. Tien Vo, T.T., Vo, Q.C., Tuan, V.P., Wee, Y., Cheng, H.-C., Lee, I.-T., 2021. The potentials of carbon monoxide-releasing molecules in cancer treatment: An outlook from ROS biology and medicine. Redox Biology 46, 102124. https://doi.org/10.1016/j.redox.2021.102124
117. Tiwari, A., Trivedi, R., Lin, S.-Y., 2022. Tumor microenvironment: barrier or opportunity towards effective cancer therapy. Journal of Biomedical Science 29, 83. https://doi.org/10.1186/s12929-022-00866-3
118. Todoric, J., Antonucci, L., Karin, M., 2016. Targeting Inflammation in Cancer Prevention and Therapy. Cancer Prev Res (Phila) 9, 895–905. https://doi.org/10.1158/1940-6207.CAPR-16-0209
119. Ugolini, A., Tyurin, V.A., Tyurina, Y.Y., Tcyganov, E.N., Donthireddy, L., Kagan, V.E., Gabrilovich, D.I., Veglia, F., n.d. Polymorphonuclear myeloid-derived suppressor cells limit antigen cross-presentation by dendritic cells in cancer. JCI Insight 5, e138581. https://doi.org/10.1172/jci.insight.138581

120. Vadrevu, S.K., Chintala, N.K., Sharma, S.K., Sharma, P., Cleveland, C., Riediger, L., Manne, S., Fairlie, D.P., Gorczyca, W., Almanza, O., Karbowniczek, M., Markiewski, M.M., 2014. Complement C5a Receptor Facilitates Cancer Metastasis by Altering T-Cell Responses in the Metastatic Niche. Cancer Research 74, 3454–3465. https://doi.org/10.1158/0008-5472.CAN-14-0157

121. Van der Mude, A., 2022. A proposed Information–Based modality for the treatment of cancer. Biosystems 211, 104587. https://doi.org/10.1016/j.biosystems.2021.104587

122. Veglia, F., Sanseviero, E., Gabrilovich, D.I., 2021. Myeloid-derived suppressor cells in the era of increasing myeloid cell diversity. Nat Rev Immunol 21, 485–498. https://doi.org/10.1038/s41577-020-00490-y

123. Waldman, A.D., Fritz, J.M., Lenardo, M.J., 2020. A guide to cancer immunotherapy: from T cell basic science to clinical practice. Nat Rev Immunol 20, 651–668. https://doi.org/10.1038/s41577-020-0306-5

124. Walter-Nuno, A.B., Taracena, M.L., Mesquita, R.D., Oliveira, P.L., Paiva-Silva, G.O., 2018. Silencing of iron and heme-related genes revealed a paramount role of iron in the physiology of the hematophagous vector Rhodnius prolixus. Frontiers in Genetics 9, undefined-undefined. https://doi.org/10.3389/fgene.2018.00019

125. Wang, Y., Schafer, C.C., Hough, K.P., Tousif, S., Duncan, S.R., Kearney, J.F., Ponnazhagan, S., Hsu, H.-C., Deshane, J.S., 2018. Myeloid-Derived Suppressor Cells Impair B Cell Responses in Lung Cancer through IL-7 and STAT5. J Immunol 201, 278–295. https://doi.org/10.4049/jimmunol.1701069

126. Wang, Y., Zhang, H., He, Y.-W., 2019. The Complement Receptors C3aR and C5aR Are a New Class of Immune Checkpoint Receptor in Cancer Immunotherapy. Frontiers in Immunology 10.

127. Weber, R., Fleming, V., Hu, X., Nagibin, V., Groth, C., Altevogt, P., Utikal, J., Umansky, V., 2018. Myeloid-Derived Suppressor Cells Hinder the Anti-Cancer Activity of Immune Checkpoint Inhibitors. Front Immunol 9, 1310. https://doi.org/10.3389/fimmu.2018.01310

128. Wegiel, B., Hedblom, A., Li, M., Gallo, D., Csizmadia, E., Harris, C., Nemeth, Z., Zuckerbraun, B.S., Soares, M., Persson, J.L., Otterbein, L.E., 2014. Heme oxygenase-1 derived carbon monoxide permits maturation of myeloid cells. Cell Death Dis 5, e1139. https://doi.org/10.1038/cddis.2014.97

129. Wellenstein, M.D., Coffelt, S.B., Duits, D.E.M., van Miltenburg, M.H., Slagter, M., de Rink, I., Henneman, L., Kas, S.M., Prekovic, S., Hau, C.-S., Vrijland, K., Drenth, A.P., de Korte-Grimmerink, R., Schut, E., van der Heijden, I., Zwart, W., Wessels, L.F.A., Schumacher, T.N., Jonkers, J., de Visser, K.E., 2019. Loss of p53 triggers WNT-dependent systemic inflammation to drive breast cancer metastasis. Nature 572, 538–542. https://doi.org/10.1038/s41586-019-1450-6

130. Wildes, T.J., DiVita Dean, B., Flores, C.T., 2021. Myelopoiesis during Solid Cancers and Strategies for Immunotherapy. Cells 10, 968. https://doi.org/10.3390/cells10050968

131. Wildgruber, M., Aschenbrenner, T., Wendorff, H., Czubba, M., Glinzer, A., Haller, B., Schiemann, M., Zimmermann, A., Berger, H., Eckstein, H.-H., Meier, R., Wohlgemuth, W.A., Libby, P., Zernecke, A., 2016. The "Intermediate" CD14++CD16+ monocyte subset increases in severe peripheral artery disease in humans. Sci Rep 6, 39483. https://doi.org/10.1038/srep39483

132. Wolf, A.A., Yáñez, A., Barman, P.K., Goodridge, H.S., 2019. The Ontogeny of Monocyte Subsets. Frontiers in Immunology 10.

133. Wu, W.-C., Sun, H.-W., Chen, H.-T., Liang, J., Yu, X.-J., Wu, C., Wang, Z., Zheng, L., 2014. Circulating hematopoietic stem and progenitor cells are myeloid-biased in cancer patients. Proc Natl Acad Sci U S A 111, 4221–4226. https://doi.org/10.1073/pnas.1320753111

134. Wu, Y., Lu, C., Pan, N., Zhang, M., An, Y., Xu, M., Zhang, L., Guo, Y., Tan, L., 2021. Serum lactate dehydrogenase activities as systems biomarkers for 48 types of human diseases. Sci Rep 11, 12997. https://doi.org/10.1038/s41598-021-92430-6

135. Wu, Y., Yi, M., Niu, M., Mei, Q., Wu, K., 2022. Myeloid-derived suppressor cells: an emerging target for anticancer immunotherapy. Molecular Cancer 21, 184. https://doi.org/10.1186/s12943-022-01657-y

136. Xu, X., Meng, Q., Erben, U., Wang, P., Glauben, R., Kühl, A.A., Wu, H., Ma, C.W., Hu, M., Wang, Y., Sun, W., Jia, J., Wu, X., Chen, W., Siegmund, B., Qin, Z., 2017. Myeloid-derived suppressor cells promote B-cell production of IgA in a TNFR2-dependent manner. Cell Mol Immunol 14, 597–606. https://doi.org/10.1038/cmi.2015.103

137. Yap, T.A., Parkes, E.E., Peng, W., Moyers, J.T., Curran, M.A., Tawbi, H.A., 2021. Development of Immunotherapy Combination Strategies in Cancer. Cancer Discovery 11, 1368–1397. https://doi.org/10.1158/2159-8290.CD-20-1209

138. Yu, S., Wang, Y., He, P., Shao, B., Liu, F., Xiang, Z., Yang, T., Zeng, Y., He, T., Ma, J., Wang, X., Liu, L., 2022. Effective Combinations of Immunotherapy and Radiotherapy for Cancer Treatment. Frontiers in Oncology 12.

139. Zalfa, C., Paust, S., 2021. Natural Killer Cell Interactions With Myeloid Derived Suppressor Cells in the Tumor Microenvironment and Implications for Cancer Immunotherapy. Front Immunol 12, 633205. https://doi.org/10.3389/fimmu.2021.633205

140. Zhang, R., Liu, Q., Li, T., Liao, Q., Zhao, Y., 2019. Role of the complement system in the tumor microenvironment. Cancer Cell International 19, 300. https://doi.org/10.1186/s12935-019-1027-3

141. Zhao, H., Wu, L., Yan, G., Chen, Y., Zhou, M., Wu, Y., Li, Y., 2021. Inflammation and tumor progression: signaling pathways and targeted intervention. Sig Transduct Target Ther 6, 1–46. https://doi.org/10.1038/s41392-021-00658-5

142. Zhou, X., Du, Y., Huang, Z., Xu, J., Qiu, T., Wang, J., Wang, T., Zhu, W., Liu, P., 2014. Prognostic Value of PLR in Various Cancers: A Meta-Analysis. PLoS One 9, e101119. https://doi.org/10.1371/journal.pone.0101119

Other Research and teaching activities:

During this period of PhD program, I was also involved in other projects studying host immunology in perspective of cancer. The study of T-cell senescence in breast cancer patients and Geriatric hematological and solid tumors patients can be mentioned.

As teaching activities for bachelor's and master's students has been a part of PhD curriculum at Professor Alassandra Gennari's laboratory, I took part in teaching and assisting several students during my PhD. The major role was to teach laboratory techniques, research methodologies and assisting with thesis writing.

Skills and techniques learned and used during PhD course:

1. Handling, processing, and banking of biological samples.
2. Peripheral Blood separation.
3. Multicolor Flow cytometry.
4. PCR techniques (RT- PCR; nanodrop PCR).
5. Managing clinical data.
6. Research Methodologies (Clinical and biological)
7. Literature, databases search, data analysis and statistics.
8. Data presentation.

List of seminars, congress and webinars attended.

1. 04/11/2019: Prof. A Goris "Novel DNA and RNA "omics" technologies"

2. 06/11/2019: Prof. A Goris "A lecture on MS genetics: "The genetics of the immune system in health and disease"

25/11/2019: Dr. Mandar Bawadekar "Citrullination and the Peptidylarginine Deiminases in Immunity, Inflammation, and Arthritis"

4. 10/12/2019: Dr. Massimo Tommasino "Novel mechanisms of HPV-driven carcinogenesis"

5. 11/12/2019: Prof. M. Falasca "Targeting the endocannabinoid system in pancreatic cancer"

6. 16/12/2019: Prof. M. Falasca “Lipidomic and proteomic analysis of exosomes”

7. 16/01/2020: Prof. Francesco Peri "Small molecules targeting Toll-Like Receptor 4: towards a new generation of therapeutics"

8. 18/02/2020: Prof. Cristina Meini, Dr. Emiliano Loria “Aging and attachment. Early caregiving relationships and Aging”

9. 05/05/2020: Prof. Davide Porporato “Gastronomy of longevity: the memory of food, a trajectory of well-being”

10. 03/06/2020: Prof. Bianca Gardella Tedeschi "The elderly: a new legal entity?"

11. 30/07/22020: Dr. Elisa Francone “The role of gut microbiota in colorectal cancer”

12. 31/07/2020: Dr. Davide Susta “Intermittent Hypoxia-Hyperoxia Conditioning and Cardiorespiratory Fitness in Older Comorbid Cardiac Outpatients.”

13. 02/09/2020: Whole Genome Genotyping with Infinium Assay.

14. 30/08/2021- 03/09/2021 Conferma iscrizione "International Summer School on Immuno-Oncology: emerging targets and combination therapies"

15. 08/06/2021 Dr ANSELMO:"Flow cytometry analysis of extracellular vesicles in cardiovascular diseases; from bench to bedside”

16. 26/10/2021 “The Molecular Underpinnings of mRNA Vaccines” Prof. Steven R. Ellis Department of Biochemistry and Molecular Genetics University of Louisville, Louisville KY, USA

17. 16/02/2022 “Peculiar aspects of pediatric multiple sclerosis” Dott. Angelo Ghezzi.

18. 09/05/2022 Development of 3D cell culture models for tumor engineering, Prof Dr. Bojana Obradović.

19. 06/06/2022 Diamond Blackfan Anemia and Cancer Predisposition: More Questions than Answers” Prof. Steven R. Ellis Department of Biochemistry and Molecular Genetics University of Louisville, Louisville KY, USA.

20. 12/07/2022 Prevention and Prediction of Type 1 Diabetes Prof. Francesco Chiarelli.

21. 14/09/2022-17/09/2022 – International summer school on immuno oncology.

22. 30/07/2021-03/08/2022– International summer school on immuno oncology.

List of publication:

1) Breast Cancer Survivorship, Quality of Life, and Late Toxicities: Simone Nardin, Edoardo Mora, Feba Mariam Varughese, Francesca D'Avanzo, **Ajay Ram Vachanaram**, Valentina Rossi, Chiara Saggia, Sara Rubinelli and Alessandra Gennari* (Frontiers in oncology 2020 June 16; 10: 864. doi: 10.3389/fonc.2020.00864, PMID: 32612947).

2) Psychotropic drugs show anticancer activity by distrupting mitochondrial and lysosomal function: Marco Varalda, Annamaria Antona, Valentina Bettio, Konkonika Roy, **Ajay Ram Vachanaram,** Vaibhav Yellenki, Alberto Massarotti, Gianluca Baldanzi, Daniela Capello* (Frontiers in oncology 2020 Oct 19;10:562196. doi: 10.3389/fonc.2020.562196. PMID: 33194631).

3) A randomized clinical study on the impact of Comprehensive Geriatric Assessment (CGA) based interventions on the quality of life of elderly, frail, onco-hematologic patients candidate to anticancer therapy: protocol of the ONCO-Aging study : Abdurraouf Mokhtar Mahmoud, Federica Biello, Paola Maria Maggiora, Riccardo Bruna, Giovanni Burrafato, Miriam Cappelli, Feba Varughese, Veronica Martini, Francesca Platini, Clara Deambrogi, Andrea Patriarca, Maura Nicolosi, **Ajay ram Vachanaram**, Carla Pisani, Eleonora Ferrara, Elvira Catania, Danila Azzolina, Francesco Barone-Adesi, Marco Krengli, Gianluca Gaidano & Alessandra Gennari *.(BMC geriatrics 2021 May 19;21(1):320. doi: 10.1186/s12877-021-02237-3. PMID: 34011271).

LIST OF ABSTRACTS

1) PD-L1 status and efficacy of immune check-point inhibitors (ICIs) in advanced cancer patients: Federica Biello, David James Pinato, Gloria Borra, Silvia Genestroni, Guido Siffredi, Ilaria Repetti, Veronica Martini, Feba mariam Varughese, **Ajay Ram Vachanaram**, Edoardo Mora, Simone Nardin, Paolo Bruzzi, Antonio Sica, Alessandra Gennari *. (American society of clinical oncology annual meeting I, 29-31 May 2020, DOI: 10.1200/JCO.2020.38.15_suppl.e15263).

2) HEME catabolism in peripheral monocytes and response to immune checkpoint inhibitors in advanced lung cancer**.** Authors: F Biello, V Martini, C Branni, G Borra, S Genestroni, A Mennitto, C Cattrini, AP Sponghini, A Gatti, F Platini, A Rua, PM Maggiora, M Cavalleri, **AR Vachanaram**, FM Varughese, D Ferrante, DJ Pinato, A Sica, A Gennari*.(European Society for Medical Oncology, 16-21 September 2021, DOI: https://doi.org/10.1016/j.annonc.2021.08.1721).

3) Peripheral T-lymphocytes senescence and response to neoadjuvant therapy (NAT) in operable breast cancer (BC): Authors F D'Avanzo, V Rossi, C Saggia, F Platini, G Borra, V Martini, A Rua, E Gioffi, C Branni, PM Maggiora, A Tassone, FM Varughese, **A Ram Vachanaram**, R Ben Ayed, C Angelillo, A Barcellini, R Boldorini, I Dodaro, D Ferrante, A Gennari *. (European Society for Medical Oncology, 9-13 September, 2022, DOI:https://doi.org/10.1016/j.annonc.2022.07.194)